PAOLO CHIGGIATO CERN TE-VSC JUAS-2012

VACUUM TECHNOLOGY FOR

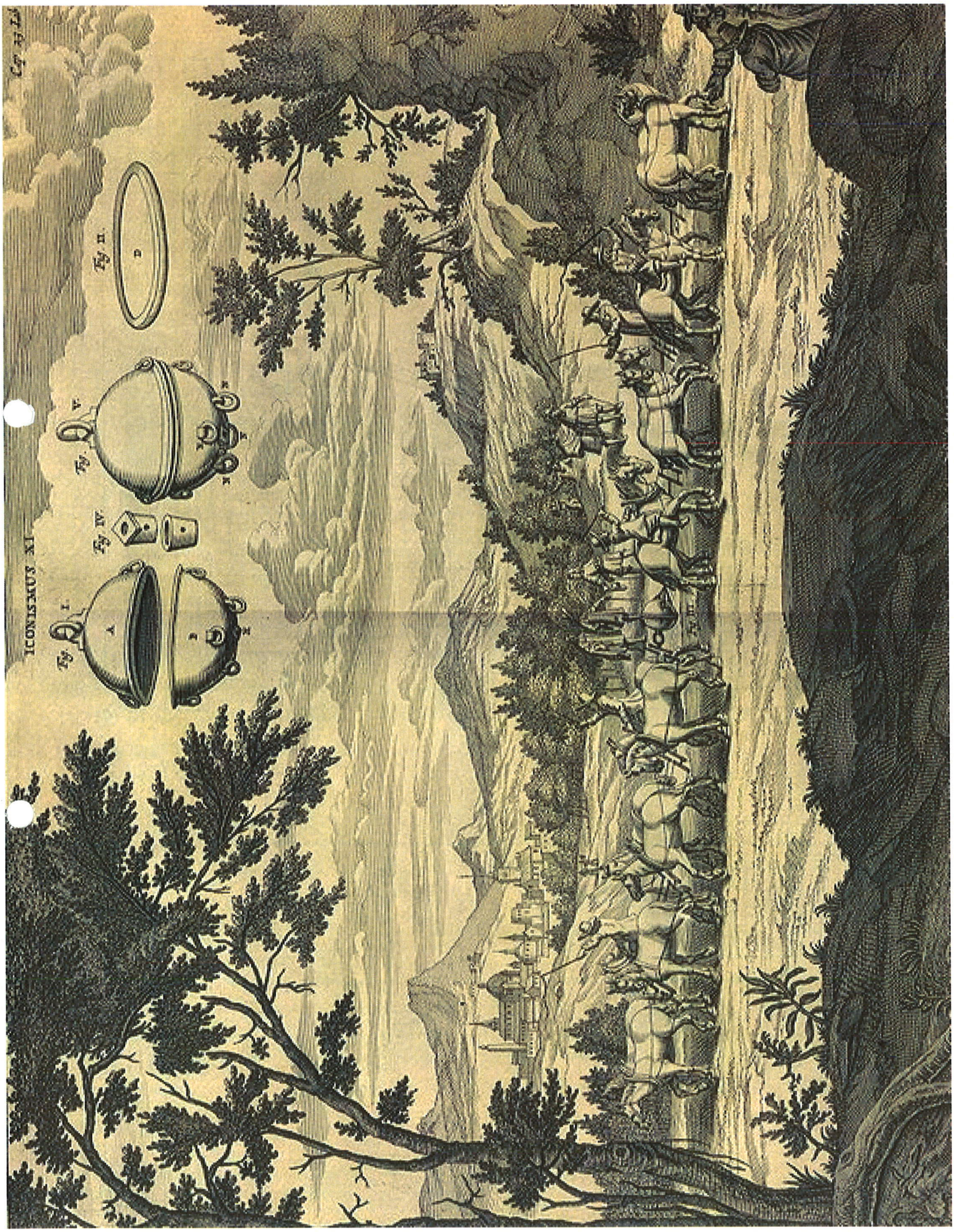

PARTICLE ACCELERATORS

UNIT 1 — INTRODUCTION

① WHY VACUUM IS NEEDED IN PARTICLE ACCELERATORS ?

Beams interact with gas molecules and are deviated from their paths. The interaction results in particle losses either by

→ particle – molecule scattering

or

→ beam instabilities

The gas-beam interaction is more critical in storage ring than in linear accelerators or transfer lines. In the former, the same beams have to circulate for many hours without excessive losses; instabilities can accumulate and spoil the desired beam performance. In the transfer lines, beams pass only once.

② HOW DO BEAM PARTICLES AND GAS MOLECULES INTERACT ?

a) Definition of cross-section / mean free path / beam lifetime

$I \begin{cases} \text{particles} \\ \text{per unit area} \\ \text{per unit time} \end{cases}$

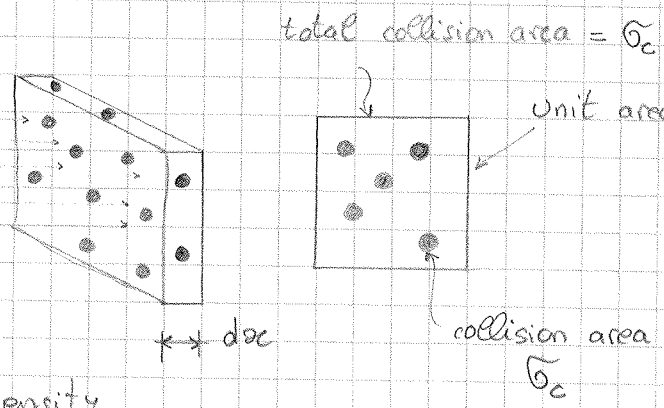

n → gas molecule density

The beam particle losses while passing through dx are

$$dI = -I \sigma_c \cdot n \, dx$$

$$\rightarrow \frac{dI}{I} = -\sigma_c \, n \, dx \rightarrow I = I_0 \cdot e^{-x \cdot \sigma_c \cdot n}$$

$$I = I_0 \cdot e^{-\frac{x}{l}} \quad \text{where} \quad l = \frac{1}{\sigma_c \cdot n}$$

ℓ is the mean free path of the beam particles in the gas phase.

$$I = I_0 \cdot e^{-x \cdot \sigma_c \cdot n} = I_0 \cdot e^{-\frac{v}{v} \cdot x \sigma_c n} = I_0 \cdot e^{-\frac{t}{\tau}}$$

beam speed

$$\tau = \frac{1}{v \cdot \sigma_c \cdot n}$$

τ is called the "beam lifetime".

In case of more than one particle interaction, the cross sections are added: $\sigma_{TOT} = \sigma_1 + \sigma_2 + \dots$

As a consequence: $\frac{1}{\ell_{TOT}} = \frac{1}{\ell_1} + \frac{1}{\ell_2} + \dots$ and $\frac{1}{\tau_{TOT}} = \frac{1}{\tau_1} + \frac{1}{\tau_2} + \dots$

As a first approximation, the order of magnitude of σ_c is that of the geometrical cross section for the relevant process:

$\sigma_c \approx r^2$

- atomic interactions: $(10^{-8})^2 = 10^{-16}\ cm^2$
- nuclear interactions: $(10^{-12})^2 = 10^{-24}\ cm^2 = 1\ b$

$[1\ b = 1\ barn = 10^{-24}\ cm^2]$

$\Rightarrow$ Nuclear reactions can be, in general, neglected

b) Processes of beam-gas interaction.

- ELASTIC → SINGLE AND MULTIPLE COULOMB SCATTERING (*)
  increase betatron amplitude
- INELASTIC →
  - BREMSSTRAHLUNG (*)
  - IONIZATION ENERGY LOSS
  - ELECTRON CAPTURE AND ELECTRON LOSS
  - NUCLEAR REACTION

  particles lost at the RF acceptance limit or momentum dynamic aperture

ELASTIC SCATTERING :

The process is described by the classical Rutherford scattering. It can be shown that for Coulomb scattering :

$$\frac{1}{\tau} \propto Z^2 \cdot P$$

where Z is the atomic number of the gas molecule.
P is the residual gas pressure

INELASTIC SCATTERING :

Charged particles passing through matter become deflected by strong electrical fields from the atomic nuclei. This deflection is associated to a particle acceleration $\rightarrow$ the particle loses energy through emission of radiation $\Rightarrow$ <u>bremsstrahlung</u>.
Excessive losses of particle energy move the particle out of accelerator energy acceptance. $\Rightarrow$ particle loss.
This process is much more important for $\bar{e}$ than p^+.
Here again :

$$\frac{1}{\tau} \propto Z^2 \cdot P$$

<u>IMPORTANT CONSEQUENCE</u> $\Rightarrow$ In addition to gas molecule density, the number of proton per molecule plays a crucial role in beam-gas interactions.
As an example, the same pressure of hydrogen and CO has not the same effect on beam lifetime.

③ WHAT IS THE VACUUM LEVEL NEEDED IN PARTICLE ACCELERATORS.

The beam lifetime defined by the residual gas should be longer than those imposed by other losses, for example beam collisions or limited aperture offered by collimators and scrapers.

Example: LHC (from www.lhc-closer.es)

Beam lifetime due to collisions at the interaction points

$$N = \mathcal{L} \cdot \sigma_c \ \frac{\text{collisions}}{s}$$

$\mathcal{L}$ = luminosity $\simeq 10^{34}\ cm^{-2} \cdot s^{-1}$

σ_c = cross section for p^+-p^+ collision at 7 TeV $\overset{!}{=} 110 \times 10^{-3}\ b$

$$= 10^{34} \cdot 110 \times 10^{-27} \cong 10^{9}\ \frac{\text{collisions}}{s}$$

for a fully-filled LHC (2808 bunches):

$$N = 3.6 \times 10^{5}\ \frac{\text{collision}}{\text{bunch} \cdot s} \rightarrow 2 \text{ points of collision}: 7.2 \times 10^{5}$$

the initial number of protons per bunch is 1.15×10^{11}

$$\Rightarrow \frac{1}{\tau_{pp}} = \frac{7.2 \times 10^{5}}{1.15 \times 10^{11}} \cong 6 \times 10^{-6}\ s^{-1}$$ probability of collision per second and per proton

beam lifetime due to p-p collisions $\tau_{pp} = 1.5 \times 10^{5}\ s = 40\ h$

It comes out that the beam lifetime due to collisions with the residual gas should be of the same order or, preferably, longer. For the LHC, the design value for beam-gas interactions is

$$\tau_{gas} \approx 100\ h$$

this corresponds to a gas density of about $10^{15}\ \frac{\text{molecules } H_2}{m^3}$ →

beam lifetime $= 100\,h \times 3600\,\frac{s}{h} = \tau$

$$\frac{1}{\tau} = \frac{\text{nr of protons lost in 1 second}}{\text{initial nr of proton in a bunch}} = \frac{N_e}{N_0}$$

$N_0 = 1{,}15 \times 10^{11}$

$$\frac{1}{\tau} = \underbrace{\sigma}_{\approx 50\,mb} \cdot \overbrace{\rho}^{\#\text{ density}} \times \overbrace{\ell_{LHC}}^{27\,km} \times \underbrace{f}_{\text{lap per } s = \frac{c}{\ell_{LHC}}}$$

$N_e = \sigma \times \rho_H \times \ell_{LHC} \times N_0 \times f$

$$\Rightarrow \rho_H = \frac{10^{-2}}{3600} \times \frac{1}{(\underbrace{50\times10^{-3}}_{\sigma\,[m^{-2}]} \times 10^{-28}) \cdot 27\times10^{3} \cdot 11111} \approx 2 \times 10^{15}\ \frac{H\ \text{nucleous}}{m^3}$$

$$\Rightarrow \rho_{H_2} \approx 10^{15}\ \frac{H_2\ \text{molecules}}{m^3} = 10^{9}\ \frac{H_2\ \text{molecules}}{cm^3}$$

In the experimental areas, the gas density requirement is two orders of magnitude lower:

$$\Rightarrow (\rho_{H_2})_{exp.} \approx 10^{13}\ \frac{H_2\ \text{molecules}}{m^3}$$

to minimize the detectors' background.

<u>What is the gas density in air ?</u>

$$PV = nRT \Rightarrow PV = N_{atm} \cdot K_B \cdot T \Rightarrow \rho_{atm} = \frac{\overbrace{P}^{1\,atm \approx 10^5\,Pa}}{\underbrace{K_B}_{1{,}38\times10^{-23}\,\frac{J}{K}} \cdot \underbrace{T}_{292\,K}} \cong 2{,}5\times10^{25}\ \frac{\text{molecules}}{m^3}$$

with the beam circulating

from 2.5×10^{25} to 10^{13} $\Rightarrow$ 12 to 13 orders of magnitude lower !

$\Rightarrow$ A) How can we achive this low density ?

$\Rightarrow$ B) Where is the gas coming from ?

A) This low density can be achieved by adsorbing the residual gas onto dedicated surfaces in the beam pipe vacuum.

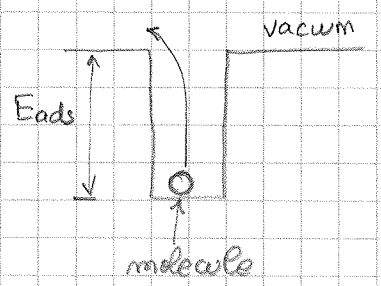

Probability of excaping from the surface $\propto e^{-\frac{E_{ads}}{kT}}$

$\Rightarrow$ average time of sojourn $\propto e^{\frac{E_{ads}}{kT}}$

$e^{\frac{E_{ads}}{kT}} \gg$ typical time of accelerator running

$\Rightarrow$ Two possibilities

$e^{\frac{E_{ads}}{kT}}$ → E_{ads} large $\Rightarrow$ chemical pumping (getter)

→ T small $\Rightarrow$ cryogenic pumping

B) Once the atmospheric gas is extracted, the main source of gas is the material of the beam pipes, in particular its surface. In many accelerators, the gas desorption is stimulated by the beam by particle impingement and induced heating.

- → electron
- → proton
- → ion
- → photons

UNIT 2

THE GAS SOURCES IN BEAM VACUUM

① SOME DEFINITIONS

Outgassing : is the spontaneous evolution of gas from solid or liquid

Degassing : is the deliberate removal of gas from a solid or liquid

Desorption : is the release of adsorbed chemical species from the surface of a solid or liquid

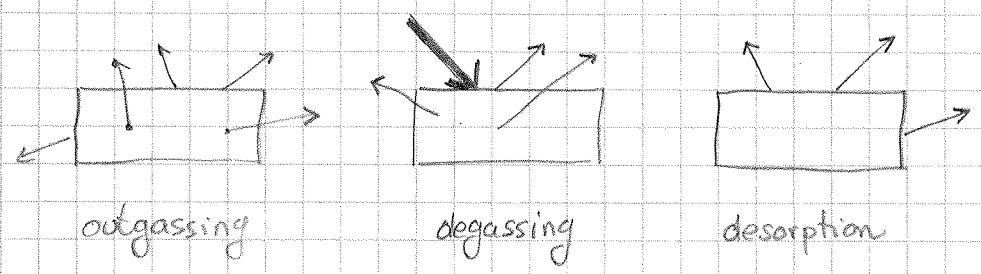

Intrinsic outgassing rate : is the quantity of gas leaving a material per unit of time and unit of exposed geometric surface (or unit of mass) at a specific time after the start of the evacuation.

Geometric surface : is the visible surface without correction for roughness or open porosity.

Measured outgassing rate : is the difference between the intrinsic outgassing and the rate of readsorption in the test chamber.

② UNITS OF MEASUREMENT

The rate of gas release is expressed in term of number of molecules or pressure-volume units at a specific temperature T:

$$N \Longleftrightarrow P \cdot V$$

The two values are correlated by the ideal gas equation:

pressure — Boltzmann constant

$$P \cdot V = n R T = N \cdot k_B \cdot T$$

volume — nr of moles — gas constant — number of molecules

$$k_B = 1{,}38 \times 10^{-23} \frac{Pa\,m^3}{K} = 1{,}04 \times 10^{-22} \frac{Torr \cdot \ell}{K} = 1{,}38 \times 10^{-22} \frac{mbar \cdot \ell}{K}$$

To convert PV quantities in number of molecules, we have to divide by $k_B T$.

WARNING: a quantity of gas expressed in PV units consists of a different number of molecules at different temperatures.

CONVERSION TABLE AT 20°C

↱	Pa m	Torr l / s cm²	mbar l / s cm²	molec / s cm²	mol / s cm²
Pa m / s		7.5×10^{-4}	10^{-3}	2.5×10^{16}	4.1×10^{-8}
Torr l / s cm²	1330		1.33	3.3×10^{19}	5.5×10^{-5}
mbar l / s cm²	10^{-3}	0.75		2.5×10^{19}	4.1×10^{-5}
molec / s cm²	4×10^{-17}	3×10^{-20}	4×10^{-20}		1.7×10^{-24}
mol / s cm²	2.4×10^{7}	1.8×10^{4}	2.4×10^{4}	6.02×10^{23}	

③ ORDER OF MAGNITUDE FOR OUTGASSING RATES

MATERIAL	$\frac{Torr \cdot l}{s \cdot cm^2}$ (20°C)	$\frac{molecules}{s \cdot cm^2}$	main gas
NEOPRENE, NOT BAKED AFTER 10h PUMPING	10^{-5}	$3{,}3 \times 10^{14}$	H_2O
VITON, NOT BAKED AFTER 10 h PUMPING	10^{-7}	$3{,}3 \times 10^{12}$	H_2O
AUSTENITIC ST. STEEL NOT BAKED, 10 h PUMPING	2×10^{-10}	6.6×10^{9}	H_2O
AUSTENITIC ST. STEEL BAKED IN SITU 150°C x 24h	2×10^{-12}	6.6×10^{7}	H_2
OFS COPPER BAKED IN SITU 200°C x 24h	$\approx 10^{-14}$	6.6×10^{5}	H_2
Ti Zr V NEG coating activated at 180° x 24h	$< 10^{-16}$	$< 3.3 \times 10^{3}$	CH_4
	$\approx 10^{18}$	≈ 30	Kr

⇒ The outgassing rates can span more than 10 orders of magnitude. The choice of materials and their treatments is crucial. A small piece of bad material can spoil the performance of the vacuum system as a whole.

It is important to underline that even the vacuum instruments are source of gas. They can release molecules in the range $10^{+9} \div 10^{11}$ molecules/s. Vacuum instruments will be considered in unit 4.

④ MEASUREMENT OF OUTGASSING RATE.

The aim of the measurement is to evaluate the number of molecules leaving a piece of material. In general the procedure implies the installation of the sample in a dedicate vacuum system and the recording of the gas density or pressure ($P = nRT$).

a) Pressure rise measurement

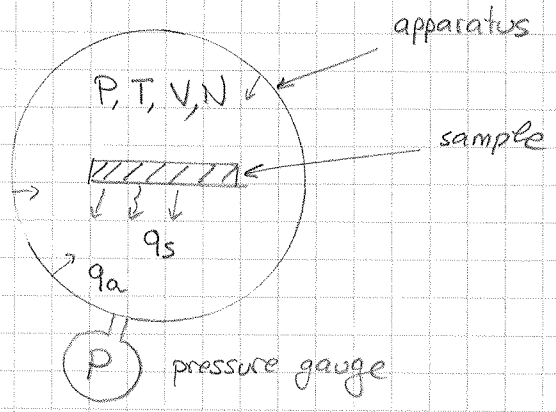

The sample is installed in a vacuum system which is pumped, treated as for specification and then isolated.

In the gas phase the number N of gas molecules increases. The variation is equal to number of molecules released from the sample ($q_s \cdot A_s$) and the system itself ($q_a A_a$):

$$\frac{dN}{dt} = q_s A_s + q_a A_a$$

molecules $/(s \cdot cm^2)$

$$PV = N k_B T \Rightarrow \frac{dP}{dt} = \frac{k_B T}{V} \cdot \frac{dN}{dt} = \frac{k_B T}{V} \cdot (q_s A_s + q_a A_a)$$

$$\Rightarrow \Delta P = \frac{k_B T}{V} \cdot (q_s A_s + q_a A_a)\, \Delta t$$

the pressure increases linearly if there is no repumping in the system.

$$L = \frac{q_s A_s + q_a A_a}{V} \cdot \Delta t$$

in PV units ($Torr \cdot \ell / s \cdot cm^2$)

$\Rightarrow$ The sensitivity of the system is limited by the outgassing rate of the system: $q_s A_s$ versus $q_a A_a$.

The pressure rise method is used only:

- for the measurement of upper limit
- when the sample is the system itself
- when the sample surface area is very large ($A_s \gg A_a$)

Another major inconvenient is the interference between the pressure gauge and the gas.

b) <u>The throughput method</u>

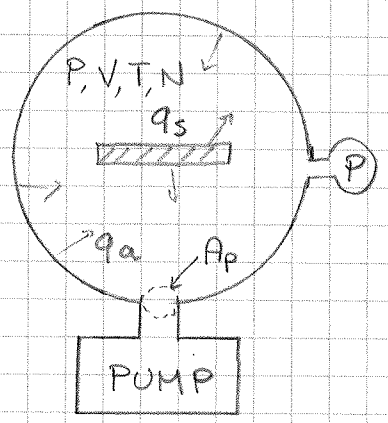

In this case a continuous pumping is applied to the test system. In a stationary regime, the outgassing rate of the system is equal to the flux of gas definitely removed from the volume by the pump.

$$Q = q_a A_a + q_s A_s$$

$$\frac{dN}{dt} = Q - \sigma_c \cdot A_p \cdot \Gamma$$

σ_c = probability of pumping for a molecule entering A_p

$$\rightarrow \frac{dP}{dt} = \frac{k_B T}{V} Q - \frac{k_B T}{V} \cdot \left(\frac{1}{4} \frac{N}{V} \overline{v}_{th} \right) \cdot \sigma_c A_p$$

since $PV = N k_B T$:

$$V \frac{dP}{dt} = (k_B T) Q - (k_B T) \cdot \sigma_c P \cdot \underbrace{\left(A_p \cdot \frac{\overline{v}_{th}}{4} \right)}_{\text{conductance of the pump aperture } C_a}$$

conversion factor

<u>Remember</u>:

For a maxwellian gas, the rate of impingment Γ onto a surface is

$$\Gamma = \frac{1}{4} n \overline{v}_{th}$$

gas density

average speed

$$\overline{v}_{th}^2 = \frac{\sum_i^N v_i^2}{N}$$

$$\frac{1}{2} m \overline{v}_{th}^2 = \frac{3}{2} kT$$

$$\Rightarrow V \frac{dP}{dt} = Q - \sigma_c P C_a \rightarrow \left[\frac{\text{volume}}{\text{time}} \right]$$

$$\Rightarrow \Delta P = \frac{Q}{\sigma_c \cdot C_a} \left(1 - e^{-\frac{t}{\tau_p}} \right) \qquad \tau_p = \frac{V}{S_{eff}}$$

$\sigma_c \cdot C_a$ = effective pumping speed of a given pump = S_{eff}

τ_p is in general much smaller than the time of measurement;

$$\Delta P = \frac{Q}{S_{eff}} = \frac{A_a q_a + A_s q_s}{S_{eff}}$$

Here again the main limitation is the outgassing of the test system. The gauge interference is not so important as for the pressure rise method.

c) Coupled method

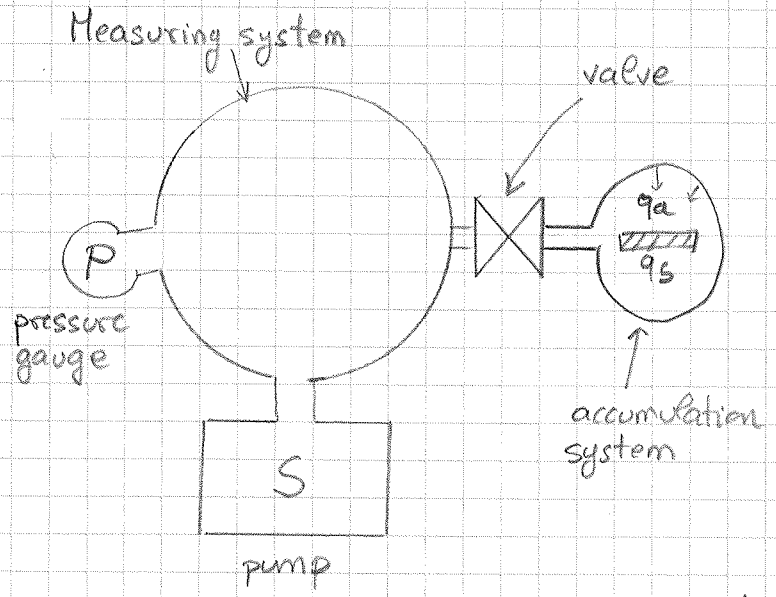

The sample can be separated from the rest of the system by a valve. The gas evolving from the sample is accumulated for a time t_a. Then the valve is opened slowly and the accumulated gas expands toward the test system where it can be quantified.

$$Q = S_{eff} \cdot \int_{t_a}^{t_a+\Delta t} \Delta P(t)\, dt$$

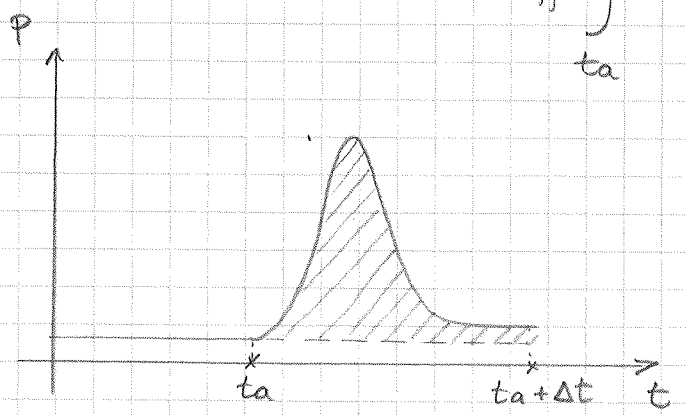

→ The limitation of this system is given by the outgassing rate of the accumulation vessel, however this can be minimized.

→ There is no more effect of the pressure gauge on the accumulated gas.

→ This method works only for gas molecules that are not repumped by the system.

d) Weight loss

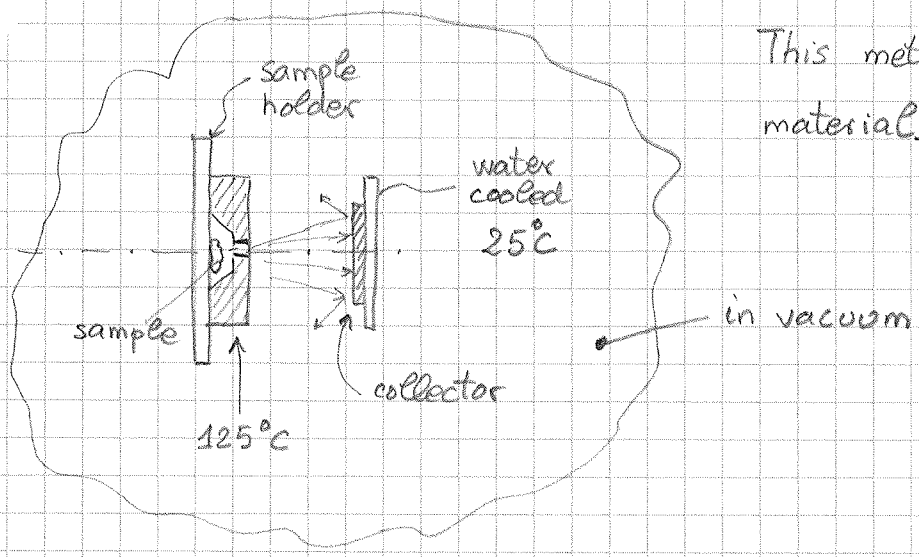

This method is used only for organic materials.

The material (a few grams) is stored for one day in a room where humidity and temperature are controlled. Then it is quickly weighted and installed in a sample holder made of copper. The gas can escape from the sample through a small aperture placed in front of a Cr plated collector of known weight.

The system is evacuated to at least 10^{-6} mbar; the sample holder is heated at 125 °C while the collector is kept at 25 °C.

24 h later, the system is cooled down to room temperature; sample holder and collector are weighted again.

Two important quantities are obtained: - the total mass loss (TML)
- the collected volatile condensable material (CVCM)

This method is largely used in the space research and industry. A very useful database is available in the NASA website!

outgassing.nasa.gov

(5) THE OUTGASSING RATE OF METALS

In general, both surface and bulk of materials are source of gas. The gas molecules can be chemisorbed onto the surfaces or dissolved in the bulk.

The molecules bound to the surface can be released if enough energy is given to the molecule to break the chemical bonding with the surface. In addition the gas atoms dissolved in the material have to diffuse toward the surface, where they can be released.

Organic materials (polymers) and metals behaves differently in term of outgassing:

Polymers
- can dissolve entire molecules (for ex. H_2O, C_2H_5OH, ...) even very heavy.
- the solubility is very large (for ex. for H_2O up to a few %)
- the gas mobility is very high

Metals
- only atoms can be dissolved in the bulk (H, O, C..)
- in general the solubility is small ($\approx 10^{-3}$ at. fraction)
- only H has a significant mobility at room temperature

⇒ In one day, H atoms travel in average 4 μm in austenitic stainless steels. O atoms travel the same distance in about 1000 years!
In the same time, H_2O moves about 20 μm away in PEEK, a high-tech polymer.

⇒ IN METALS, among the gas dissolved in the bulk, only hydrogen can be released and participate to the outgassing phenomena at room temperature. As a consequence, the reduction of H content in metals is a crucial step in the preliminary treatments for vacuum applications

When a material is not in vacuum, its surface is in direct contact with atmospheric gas and its contaminants.

In addition metals are machined, welded, extruded, laminated and manipulated. The result is a surface covered by hydrocarbons, moisture, hydroxides and oxides over thicknesses in the range between a few to hundreds of nanometers.

These contaminations are incompatible with the vacuum system of accelerators: surface treatments are mandatory.

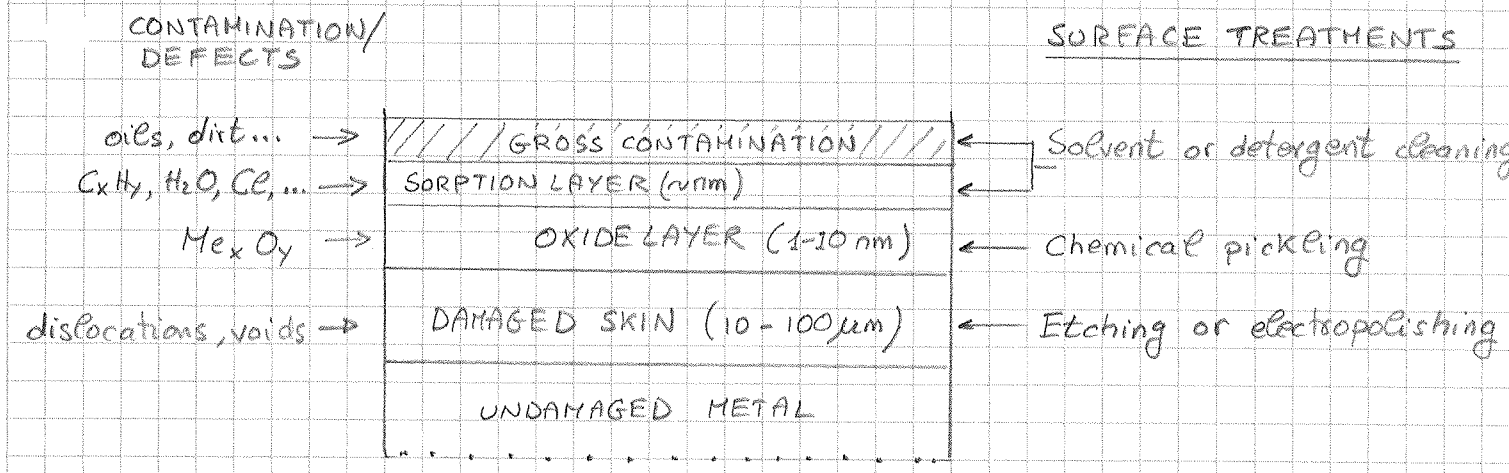

SOLVENTS: their molecules interact and transport away contaminants by diffusion in the liquid (dilution) → quite selective!

DETERGENTS IN WATER: allows organic molecules and water to combine by forming micelle (surfactants: surface acting agents) Their are based on molecules with hydrophilic heads and lipophilic tail ⇒ less selective than solvents.

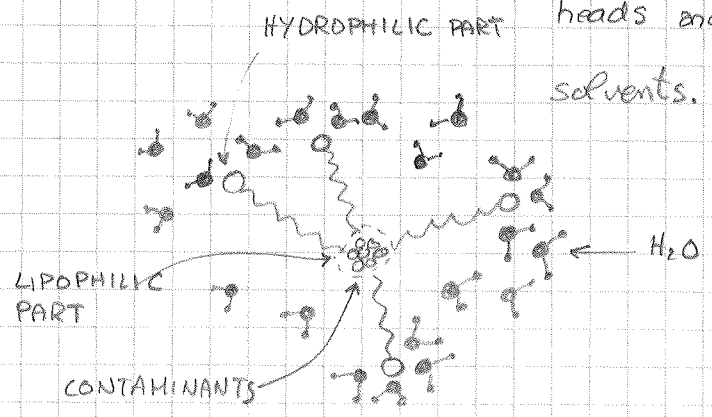

After surface treatment, in general a metallic surface is covered by a thin oxide layer with, on top, water vapour in equilibrium with atmospheric moisture (about 10 Torr in air).

Water vapour dominates the outgassing process of metals unless the whole vacuum system is heated in situ (bake-out).

Heating the vacuum chambers to reduce the outgassing rate of water vapour has a strong impact on cost, design and operation of vacuum systems for particle accelerators.

5.1 OUTGASSING OF WATER VAPOUR FROM METALLIC SURFACES.

This is one of the most puzzling subjects still open in vacuum technology:

"After evacuation, the outgassing rate of water molecules for typical metals (st. steel, copper, Al alloys, Ti, Be, ...) varies approximately inversely as the first power of pumping time"

$$\boxed{q_{H_2O} \propto \frac{1}{t_p^{\alpha}}} \longleftarrow \text{FOR METALS } \alpha \simeq 1$$

For "technically smooth surfaces" after 1 h of pumping:

$$\boxed{q_{H_2O} \approx 2 \times 10^{-9} \frac{\text{Torr} \cdot \ell}{\text{s} \cdot \text{cm}^2}}$$ FOR ANY METAL USED IN VACUUM SYSTEMS

$$\Rightarrow \quad q_{H_2O} \approx \frac{2 \times 10^{-9}}{t_p[h]} \quad \frac{\text{Torr} \cdot \ell}{\text{s} \cdot \text{cm}^2}$$

The water vapour outgassing rate depends on pumping time!!

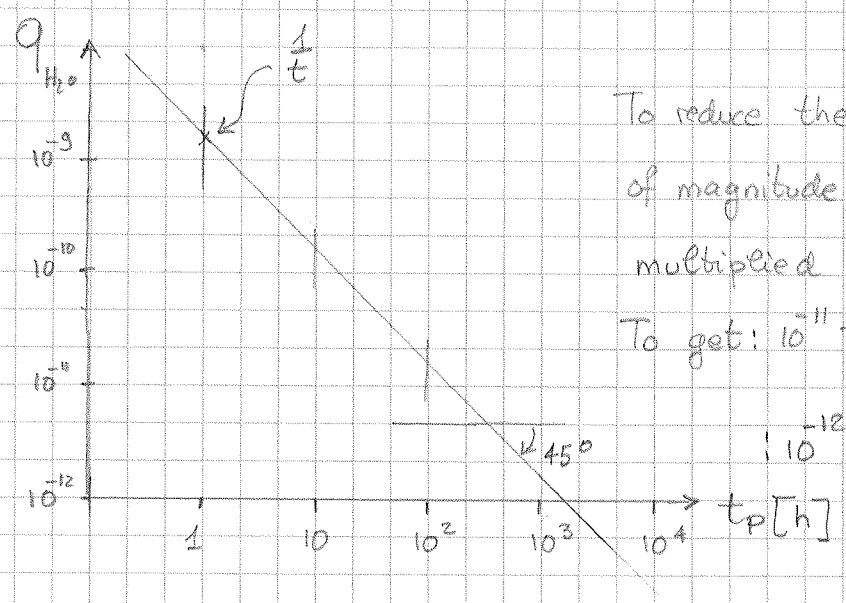

To reduce the outgassing rate by one order of magnitude, the pumping time has to be multiplied by a factor of 10.

To get: $10^{-11}\ \frac{\text{Torr}\ \ell}{s \cdot cm^2} \rightarrow$ week(s) of pumping

$10^{-12}\ \frac{\text{Torr}\ \ell}{s \cdot cm^2} \rightarrow$ months of pumping

The total quantity of water molecules released during pumping is

$$N \propto \int_0^\infty \frac{1}{t_p}\, dp \rightarrow \infty,$$ of course this is not true.

There is experimental evidence that N tends to about 1 to 2 monolayers.

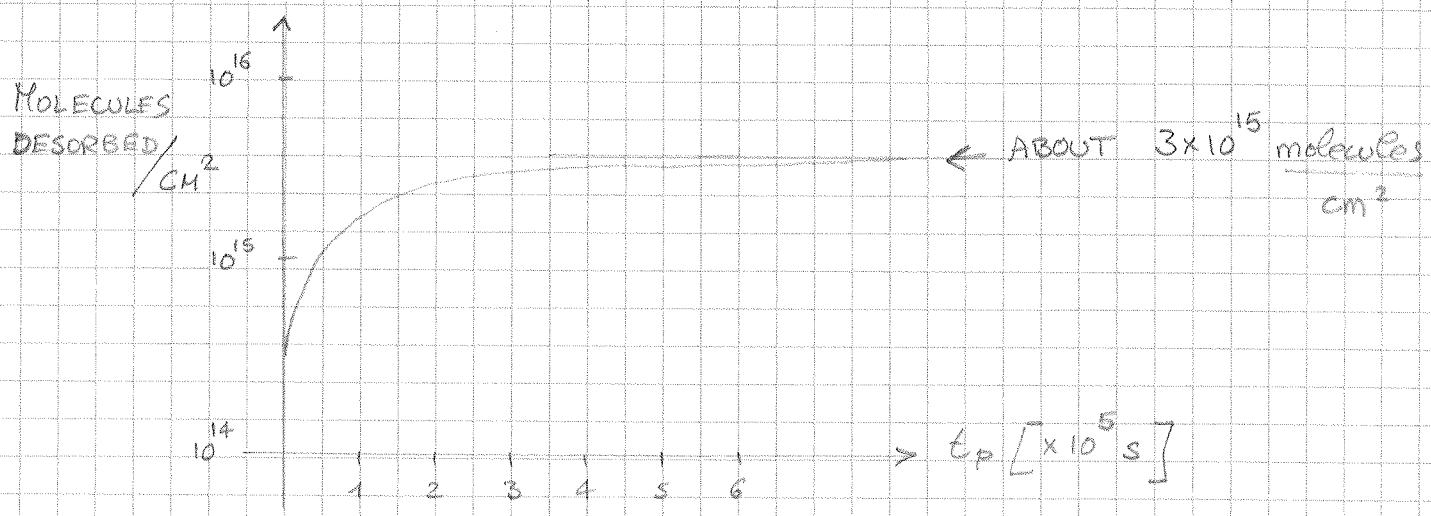

(see D. Edwards Jr, Journal of Vacuum Science and Tech, 14 (1977) 606 and 14 (1977) 1030)

Can the 1/t outgassing rate trend be obtained by simple mathematical model? ⇒

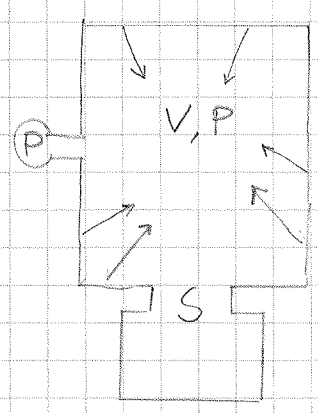

Θ = fraction of sites occupied

The total number of site for a molecule on the surfaces is limited and assumed to be roughly

$$N_S \approx 10^{15} \frac{\text{molecules}}{cm^2} = 3\times10^{-5} \frac{\text{Torr}\,\ell}{s\cdot cm^2}$$

variation of the quantity of gas

$$\begin{cases} V\dfrac{dP}{dt_p} = -SP + \dfrac{N_S\,\Theta}{\tau_d} \\[2ex] \dfrac{d\Theta}{dt} = -\dfrac{\Theta}{\tau_d} \end{cases}$$

$\dfrac{N_S\,\Theta}{\tau_d}$ → quantity of gas leaving the surface

$-SP$ → quantity of gas removed by the pump

$$\tau_d = \tau_0 \cdot \exp\left(\frac{E_d}{k_B T}\right)$$

$$\tau_0 \approx \frac{h}{k_B T} \approx 10^{-13}\,s$$

$$\Rightarrow P(t) \cong \frac{N_S}{S\cdot\tau_d}\cdot e^{-\frac{t_p}{\tau_d}} \Rightarrow q_{H_2O} \cong \frac{N_S}{\tau_d}\cdot e^{-\frac{t_p}{\tau_d}} \quad \text{for } t_p > \tau_d$$

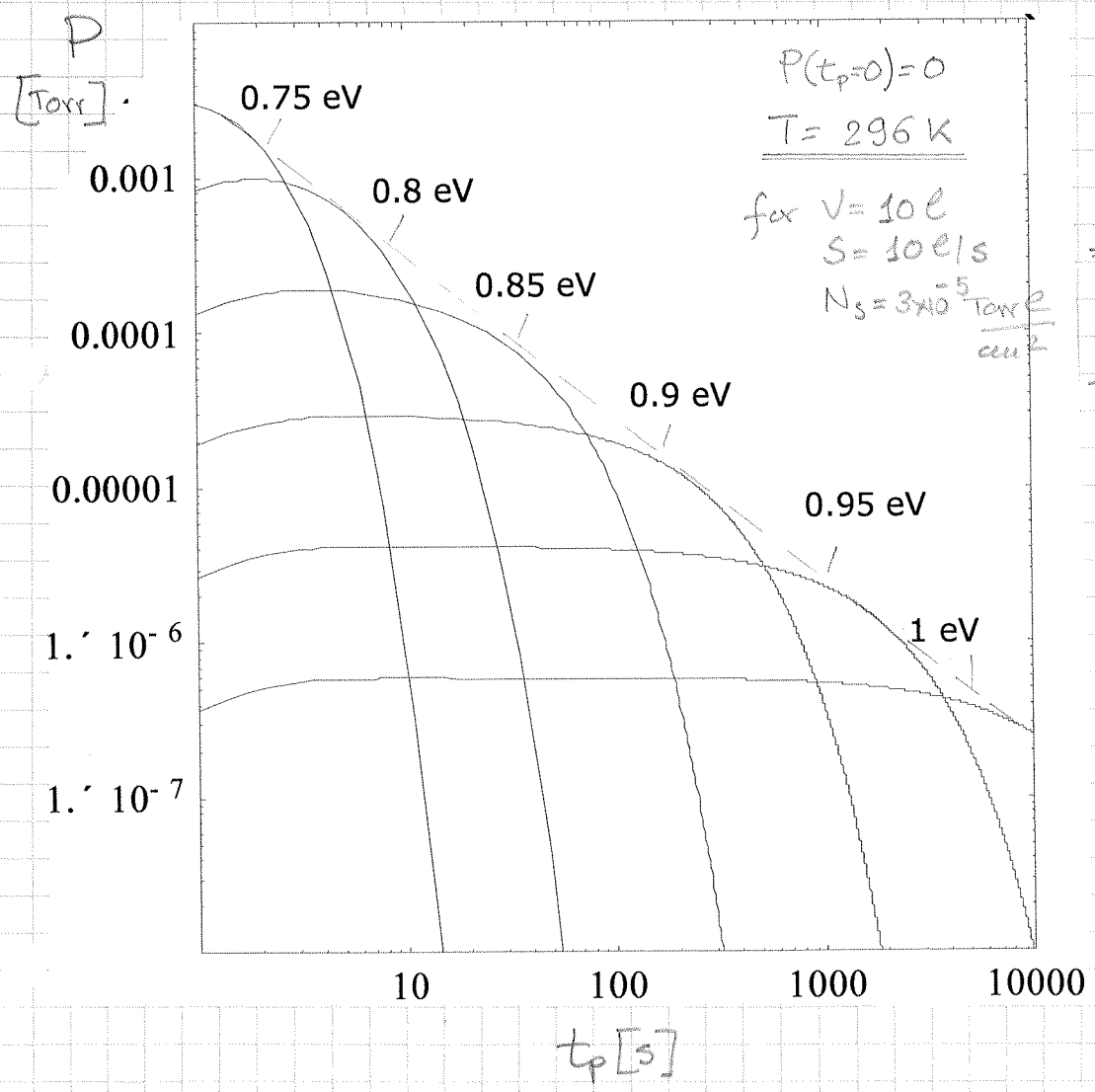

The resulting function is an exponential

⇒ far to be $1/t$

Two oversimplifications have been introduced:

① Only 1 adsorption energy.

② No readsorption on the system walls.

It can be shown that many adsorption energies are necessary to model the 1/t behaviour. The 1/t curve is seen as the convolution of many exponential decays.

For a given pumping time "$\bar{t}_p$", the adsorption sites of low energy does not contribute anymore to the pumpdown process because their are emptied in a time much lower than "t_p":

$$\tau_d = \tau_0 \cdot e^{+\frac{E_d}{kT}}$$

The adsorption sites of high energy do not contribute neither, because the molecules are too tightly bounded and are desorbed only after longer times. In other words, for every "$\bar{t}_p$" there are adsorption sites which have a dominant role in the outgassing process.

$$q = \frac{N_s}{\tau_d} \cdot e^{-\bar{t}_p/\tau_d} \Rightarrow \frac{dq}{d\tau_d} = -\frac{N_s}{\tau_d^2} \cdot e^{-\frac{\bar{t}_p}{\tau_d}} + \frac{N_s}{\tau_d} e^{-\bar{t}_p/\tau_d} \cdot \frac{\bar{t}_p}{\tau_d^2} = 0$$

$\Rightarrow \tau_d = t_d$ In this condition: $q_{MAX} = \frac{N_s}{t_p} \cdot e^{-1} = \frac{N_s}{e} \cdot \frac{1}{t_p}$

$$\frac{N_s}{e} = 1{,}1 \times 10^{-5} \Rightarrow \underbrace{q_{MAX} = \frac{1{,}1 \times 10^{-5}}{t_p[s]} = \frac{3 \times 10^{-9}}{t_p[h]}}_{\text{Edwards' upper limit}} \left[\frac{Torr \cdot \ell}{s \cdot cm^2}\right]$$

Compare: experimental $\sim \frac{2 \times 10^{-9}}{t_p[h]}$

Edwards' upper limit $\frac{3 \times 10^{-9}}{t_p[h]}$

$\Rightarrow$ Water molecule are at any pumping time adsorbed in the worst possible energetic state!

The Edwards' upper limit is a very good estimation of the water outgassing rate for "technically" smooth surfaces made of Cu, Al, ..., stainless steel. For normal steel the outgassing rate can be up to 2 orders of magnitude higher depending on the roughness of the oxide layer.

Water desorption could be accelerated, and lower pressures obtained more rapidly, by:

smooth surf. → a) Reducing the number of adsorption sites.

cooling or heating → b) Reducing or increasing the sejour time

- The reduction of q by smoothing is limited because, for "technically" smooth surfaces, the effective surface area is not far from minimun that can be achieved. Maybe a reduction of a factor 3 can be obtained for mirror like surfaces.
- The total number of sites could be reduced by changing the nature of the surface: coatings, special chemical treatments ⇒ work for te future!

- Cooling and heating are widely used in particle accelerators. The first is in most of the cases a bonus of cryogenic system installed for other purposes (superconductivity) ⇒ LHC arcs. The second is intentionally applied. The whole vacuum system is equiped with heating elements or an oven is installed around the vacuum chamber. Cold spots must be avoided.

The insitu heating is very effective if the heating temperature is higher than 100°C. A typical duration is about 24 h. This is <u>BAKEOUT</u> in the vacuum technology jargon.

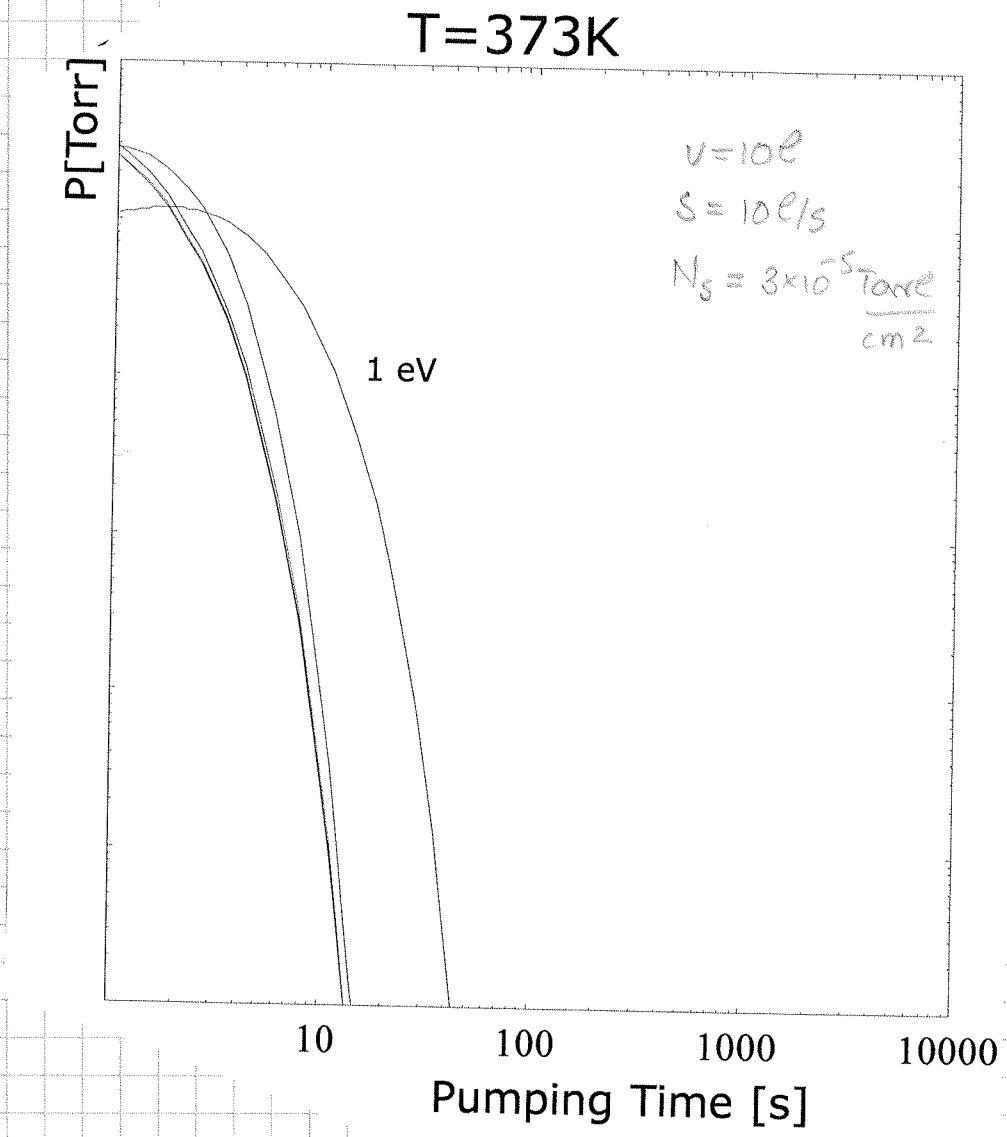

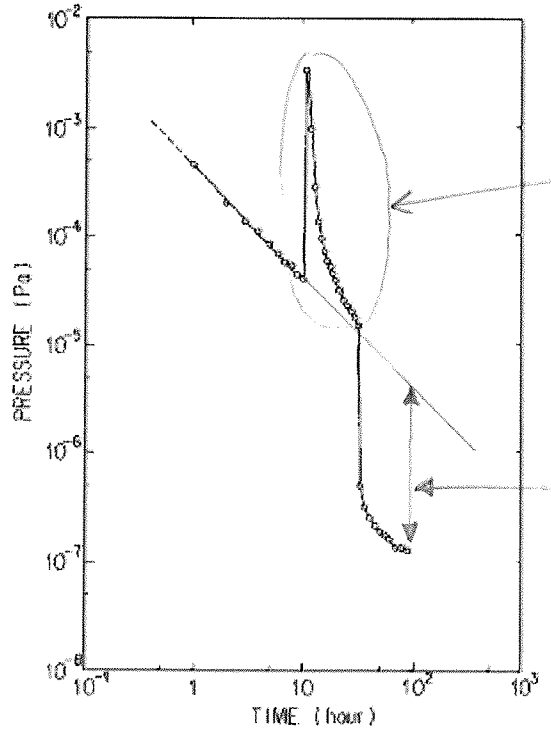

K. Kanazawa, J. Vac. Sci. Technol. A 7 (6), 1989

5.2 OUTGASSING OF H_2 FROM METALS

Whenever water vapour outgassing is strongly reduced, either by long pumping or bakeout, H_2 becomes the gas molecule with the highest outgassing rate.

Hydrogen is dissolved in metals as a single atom (H). Its diffusion is relatively fast and, after recombination onto the surface, it can be released as a molecule.

Most of the H atoms are dissolved in metals at the liquid state during the production process. The liquid metal reacts easily with hydrogenated molecules and the transport and solubility of H are facilitated.

Source of H_2 :
- the metal ores
- the tools needed for fusion
- the refractory materials of the furnace
- the combustion gas; the treatment gas
- water vapour.

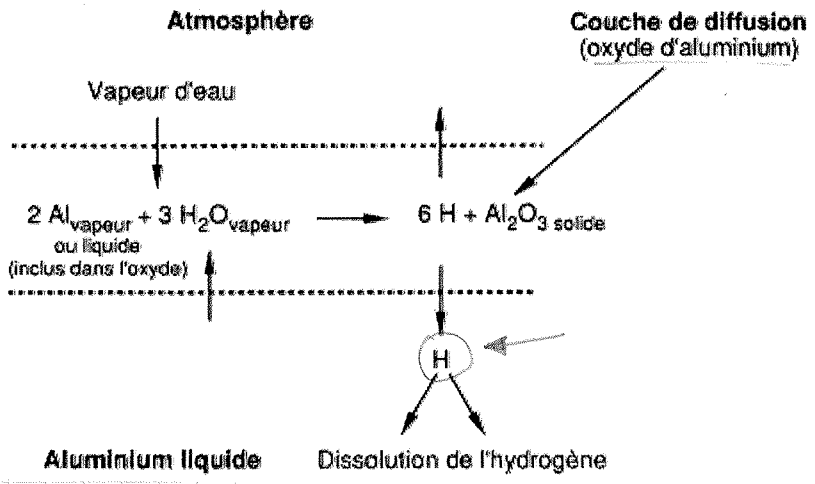

For most of the metals used in vacuum technology, the solubility of hydrogen in the liquid state is much higher than in the solid state.

If the cooling is too fast, H atoms are blocked in the solid at a concentration far above the expected equilibrium value.

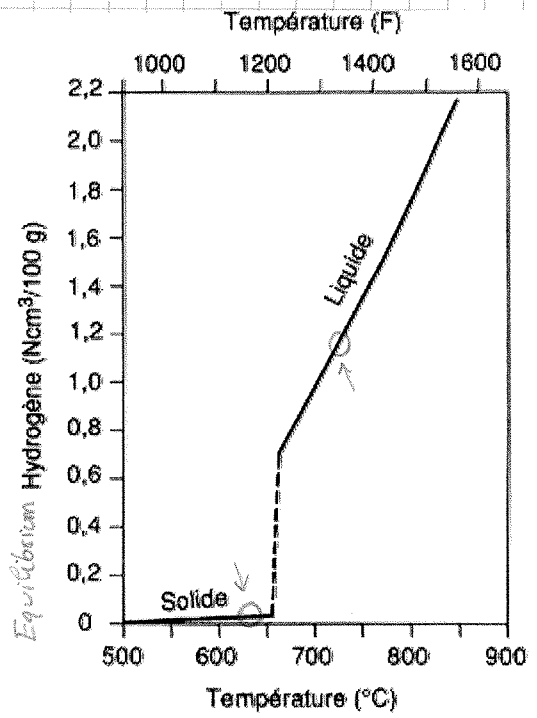

Al

1 Ncm³ correspond à 1 cm³ de gaz mesuré dans les conditions normales de température (°C) et de pression (10^5 Pa).

Example of H source:

→ some austenitic stainless steel are hyperquenched from 1100°C to RT in water, air or oil !!

After solidifications, the metals used in vacuum technology have a residual content of hydrogen lower than 10 ppm (wt.), except for very reactive metals (Ti, Nb, Zr).

For austenitic stainless steels typical values are around 1 ppm (wt.), namely ≈ 50 ppm at. For Al, values 10 times lower are reported.

Typical H_2 outgassing rates are reported here below:

Metals	Bakeout	q [Torr l/s cm²]	q [molecules/s.cm²]
Austenitic St. Steel	150°C × 24 h	3×10^{-12}	$1\times10^{+8}$
Austenitic St. Steel	200°C × 24h	2×10^{-12}	7×10^{7}
Austenitic St. Steel	300°C × 24 h	4×10^{-13}	$1{,}3\times10^{7}$
Copper Silver added (OFS)	150°C × 24h	2×10^{-12}	7×10^{7}
Copper Silver added (OFS)	200°C × 24h	$\approx 10^{-14}$	3×10^{5}
Beryllium	150°C × 24h	$< 10^{-14}$	$< 3\times10^{5}$
Al alloys	150°C × 24h	$\approx 10^{-13}$	$\approx 3\times10^{6}$

As for water vapour, hydrogen outgassing can be reduced by heating the vacuum components. Increasing the temperature the H mobility is higher and the metal is emptied faster. Then, cooling the vacuum component at room temperature, a lower outgassing rate is measured.

However, there is a crucial difference: water molecules are recharged any time the vacuum system is vented to air, while H_2 is not.
H_2 recharging is hindered by the dissociation of the molecule on the oxide layer and by the low solubility at room temperature of most of the metals used in vacuum technology. The H solubilities fix the content of H in equilibrium with a defined pressure of H_2. For example, IN STAINLESS STEEL to recharge 1 wt. ppm at room temperature, 7 atm of H_2 are needed if the H_2 molecules could dissociate without limitation.

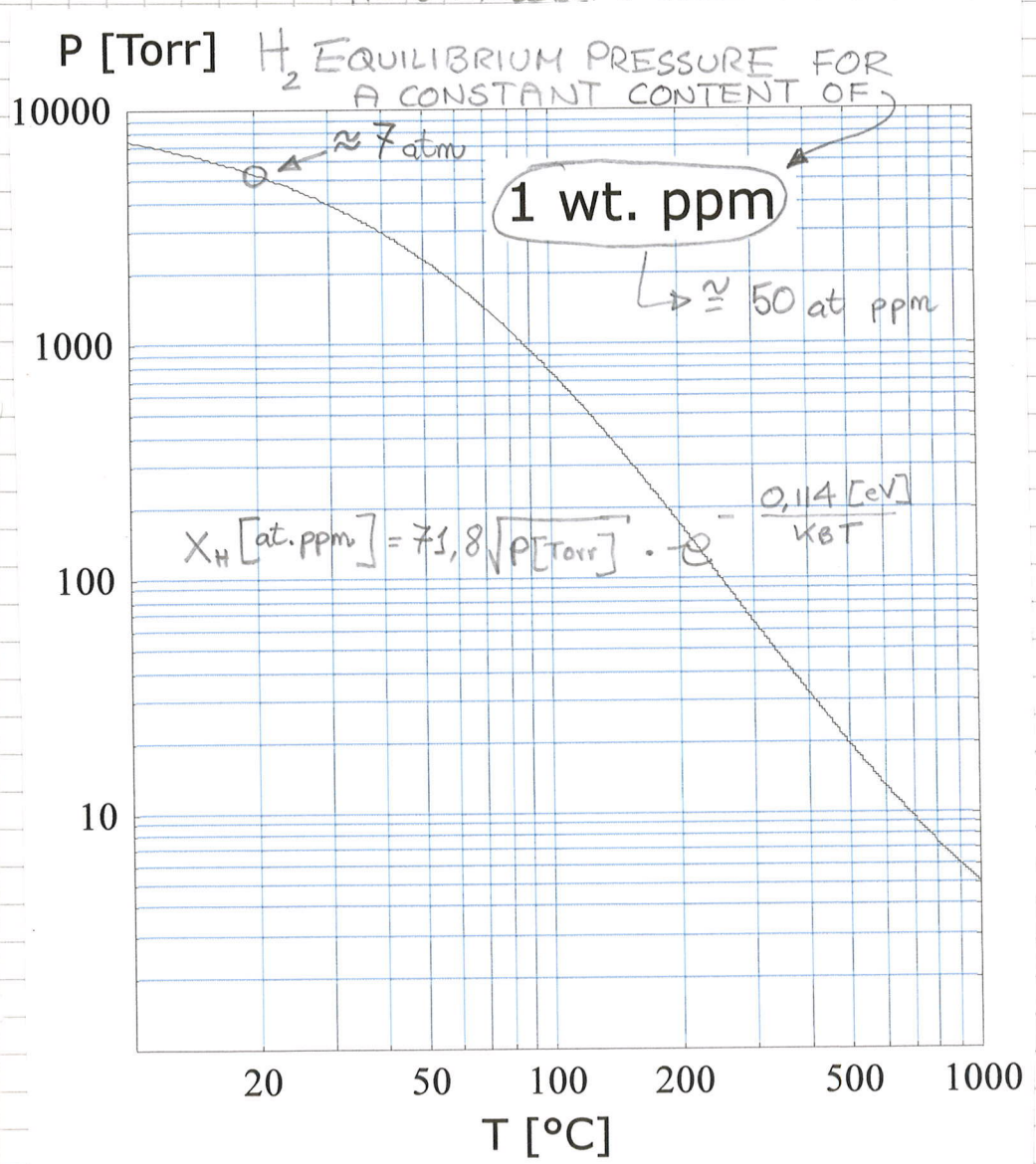

The H_2 pressure in air is 10^{-4} Torr;
⇒ maximum recharging $\approx 2\times10^{-4}$ wt. ppm

CONSEQUENCE

Vacuum materials keep memory of previous thermal treatments
⇓
Thermal treatment can be done ex-situ.

In general, for Cu and Al alloys a few bakeout at 150 ÷ 200°C (24h) are sufficient to reduce the outgassing rate of H_2 to less than 10^{-13} Torr ℓ/(s·cm²).

Austenitic stainless steels are less prone to release H_2 and so low temperature bakeouts have a limited efficiency ⇒ higher temperatures are needed. To avoid excessive surface oxidation, the vacuum materials are then inserted in a vacuum furnace ⇒ in vacuum jargon this is a "VACUUM FIRING".

- The effect of repeated bakeout and vacuum firing are shown here below:

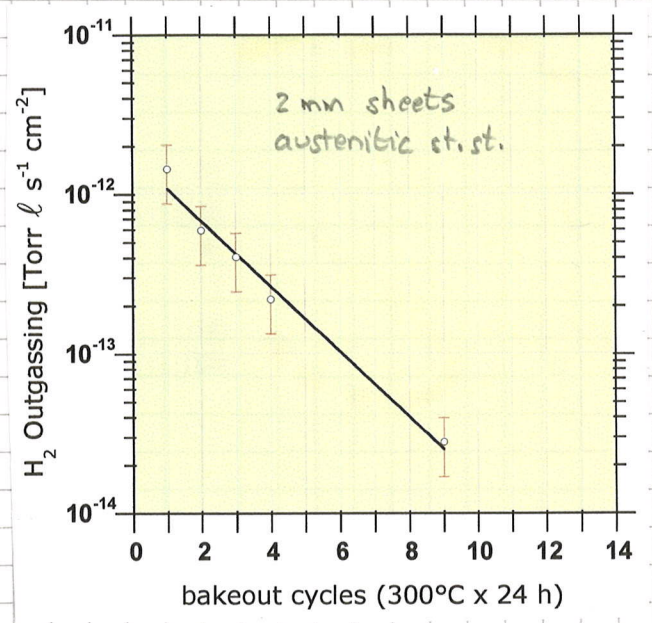

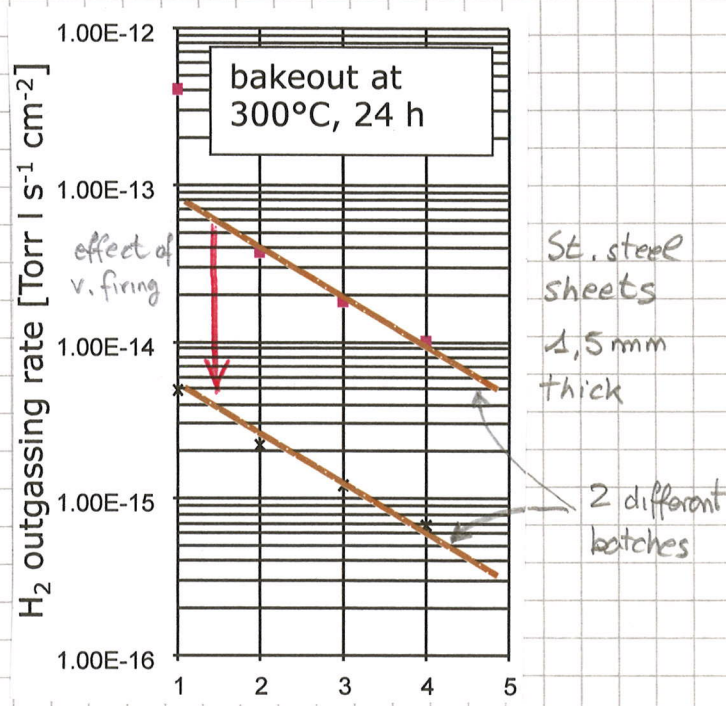

Experiment result: $\frac{q_{n+1}}{q_n}$ = constant for a given temperature cycle and material.

n = number of bakeout cycles

- The H_2 outgassing rate of most of the vacuum materials has a typical variation with temperature:

$$q = q_0 \cdot e^{-E/k_B T} \Rightarrow \ln \frac{q}{q_0} = -\frac{E}{k_B T}$$

Examples:

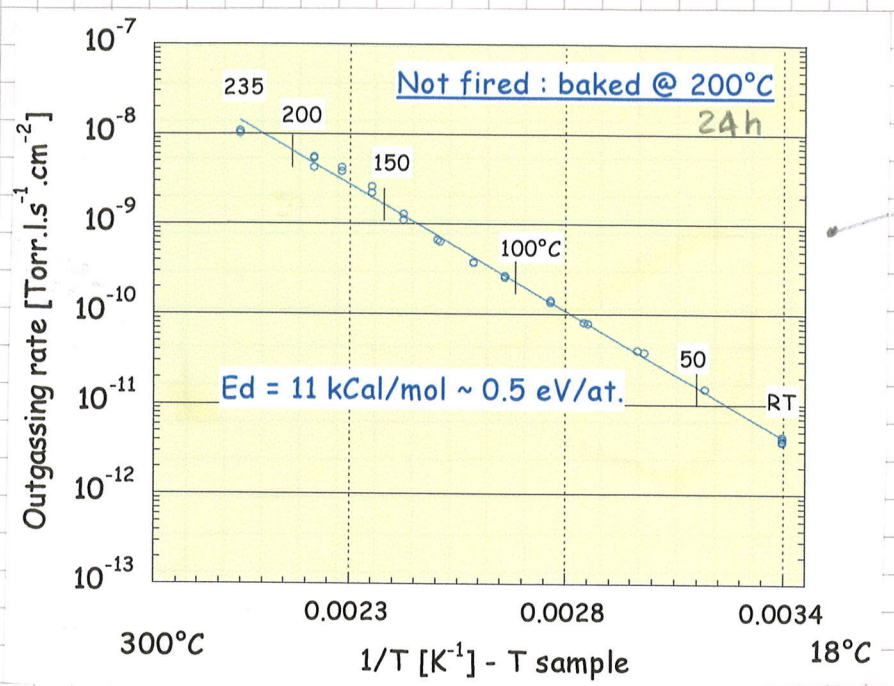

Austenitic st. steel

Wall thickness 2 mm

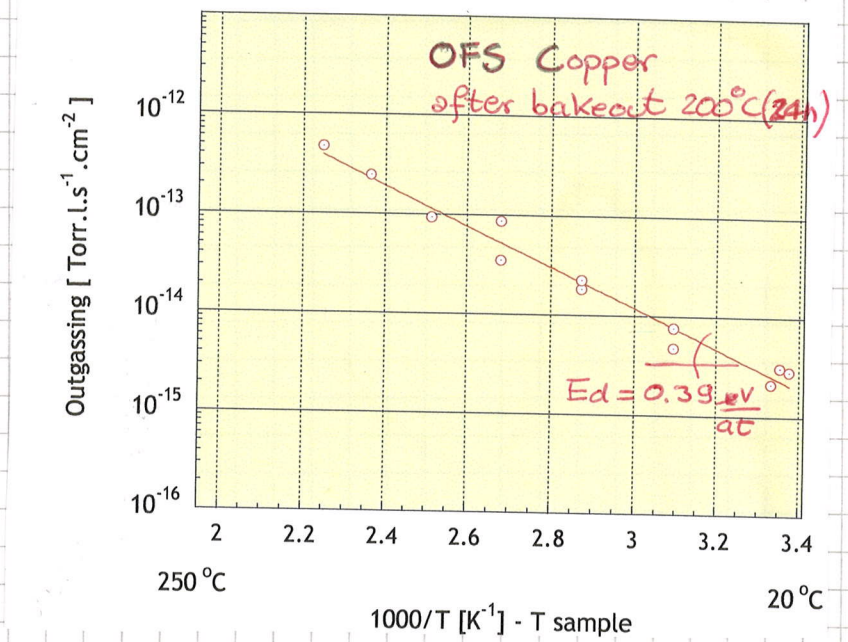

5.3 THE DIFFUSION LIMITED MODEL OF H_2 OUTGASSING

H_2 outgassing can be estimated by means of a simple diffusion model. This implies that the bottleneck of the outgassing process is the diffusion of H atoms to the surface. The recombination of two H atoms to form a molecule is neglected.

The diffusion model predicts quantitatively the measured values for most of the metals used in vacuum (endothermal metals: st. steel, copper, Al...)

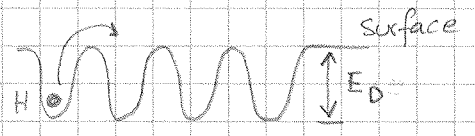

$$D(T) = D_0 \cdot \exp\left(-\frac{E_D}{k_B T}\right)$$

Fick's equations
$$\begin{cases} \Gamma(x,t) = -D \dfrac{\partial c(x,t)}{\partial x} \\ \dfrac{\partial c(x,t)}{\partial t} = D \cdot \dfrac{\partial^2 c(x,t)}{\partial x^2} \end{cases}$$

$c(x,t)$ = H concentration

$$q(t) = -D \left.\frac{\partial c(x,t)}{\partial x}\right|_{x = \text{SURFACE}}$$

SEMI-INFINITE SOLID APPROXIMATION:

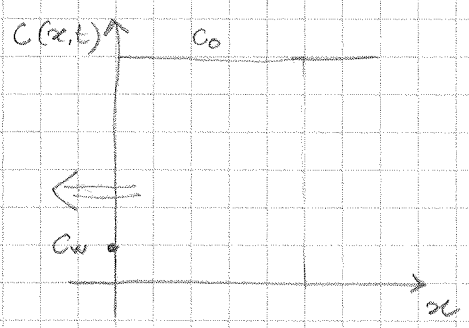

$$D \frac{\partial^2 c}{\partial x^2} = \frac{\partial c}{\partial t}$$

I.C. $c(x,0) = c_0$

B.C. $c(0,t) = c_w$

$$c(x,t) = (c_0 - c_w) \cdot \operatorname{erf} \frac{x}{2\sqrt{Dt}}$$

$$q(t) = \frac{D(c_0 - c_w)}{\sqrt{\pi D t}} \propto t^{-0,5}$$

In general, the $t^{-0,5}$ behaviour is valid even for a finite slab when its thickness L is much larger than $\sqrt{Dt}$ (the diffusion length).

$$L \gg \sqrt{Dt}$$

SLAB APPROXIMATION

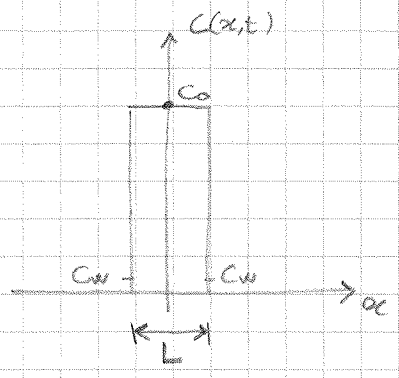

$$\left.\begin{array}{l} D\dfrac{\partial^2 c}{\partial x^2} = \dfrac{\partial c}{\partial t} \\ \text{I.C.} \quad c(x,0) = C_0 \\ \text{B.C.} \quad c\left(\pm\dfrac{L}{2}, t\right) = C_w \end{array}\right\} \quad q(t) = \frac{4(C_0 - C_w)}{L} D \cdot \sum_{0}^{\infty}{}_{n}\, e^{-(2n+1)^2 \pi^2 \cdot \frac{Dt}{L^2}}$$

For $Dt > 0{,}05\,L^2$ only the first term of the series is relevant:

$$\underline{\underline{q(t) \simeq \frac{4(C_0 - C_w)D}{L} \cdot e^{-\pi^2 \cdot \frac{Dt}{L^2}}}}$$

C_w can be calculated in the hypothesis of equilibrium between H_2 in gas and solid phase:

$$C_w = \underset{\text{solubility}}{K_s} \cdot \sqrt{P} \longrightarrow \underline{\text{Sievert's law}}$$

THERMAL MEMORY

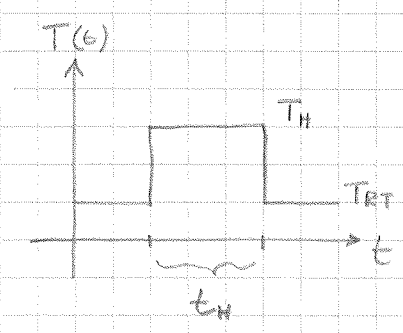

The diffusion equations can be used to calculate the outgassing rate of slabs after an arbitrary thermal cycle.

In the simplest case, namely heating at a constant temperature T_H for a duration t_H, the solution is:

$$q \approx \frac{4(C_0 - C_w)}{L} D(T_{RT}) \exp\left[-\pi^2 \frac{D(T_H) \cdot t_H}{L^2}\right]$$

For an arbitrary temperature profile:

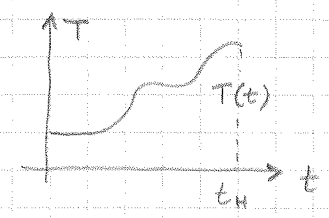

$$q \approx \frac{4(C_0 - C_w)}{L} \cdot D(T_{RT}) \cdot \exp\left[-\pi^2 \cdot \frac{\int_0^{t_H} D(T(t)) \cdot dt}{L^2}\right]$$

The dimentionless number:

$$F_o = \frac{\int_0^{t_H} D(T)\,dt}{L^2}$$

(diffusion length^2 = average distance of the random atomic movement^2)

(thickness of the vacuum chamber wall)^2

is called Fourier number (for the analogy with thermal transmission).

F_o records the thermal history of the material and determines how much the initial concentration is depleted

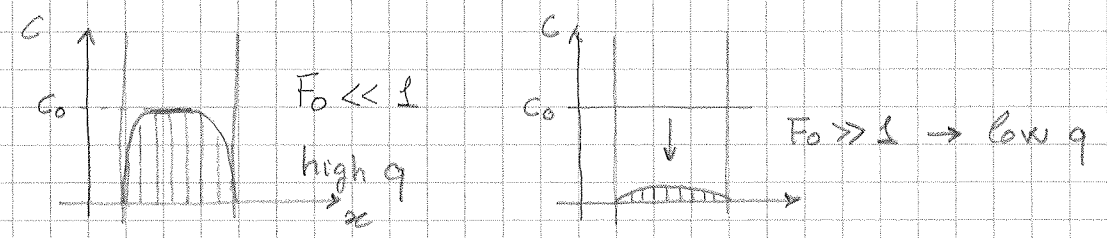

If $F_o > 3$ the material can be considered as emptied or in equilibrium with the surrounding gas phase.

For multiple bakeout at T_h for t_h $\Rightarrow$

$$\underbrace{\frac{q_{n+1}(t)}{q_n(t)} = \exp\left[\pi^2 \cdot \frac{D(T_{bo}) \cdot t_{bo}}{L^2}\right]}$$

Each bakeout reduces the outgassing rate by the same factor as shown experimentally.

DIFFUSION MODEL OF VACUUM FIRING

As already written, vacuum firing aims at removing as much as possible H from the bulk of austenitic stainless steels components before their installation in vacuum systems.

The temperature of heating is higher than that of in situ bakeouts.

To be effective the thermal treatment should result in a diffusion length longer than the slab thickness.

$$\sqrt{D(T_F)\cdot t_F} > L$$

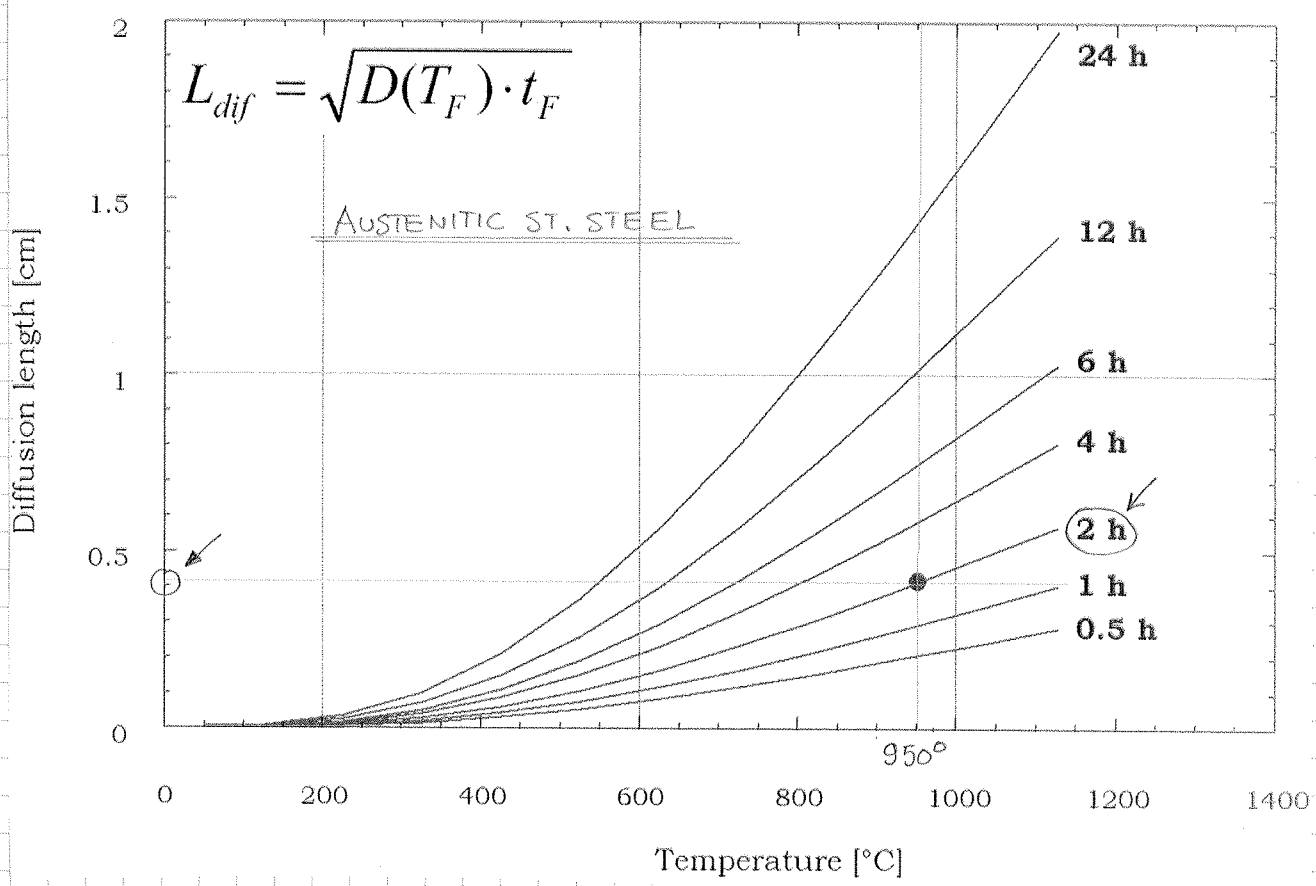

At CERN, 950°C × 2h is considered as a standard treatment.

- The diffusion model can predict the H_2 outgassing rate of stainless steel components of different wall thickness.

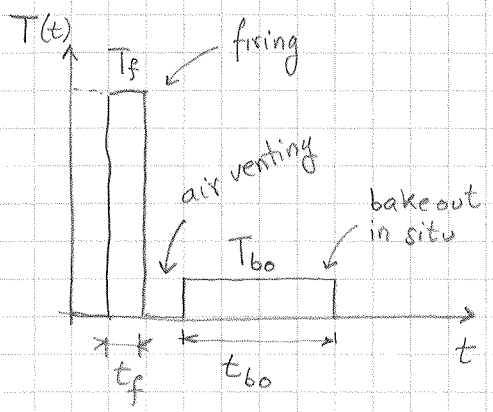

For thick slab ($L \gg \sqrt{D_F t_F}$) the results should converge to the semi-infinite solid approximation. In this case the pressure in the furnace is not relevant if $P_F \ll 1$ Torr (equilibrium pressure of H at 950°C for $C_0 \approx 1$ wt. ppm)

For thin slab ($F_0 > 3$), the initial residual hydrogen is completely removed during vacuum firing. The slab reaches equilibrium with the H_2 pressure in the furnace. For a typical vacuum of 10^{-5} Torr during the thermal treatment a concentration of 6×10^{15} H atoms / cm^3 is attained.

In both limits the outgassing rate does not depend on the slab thickness.

A detailed calculation is shown in the following curve:

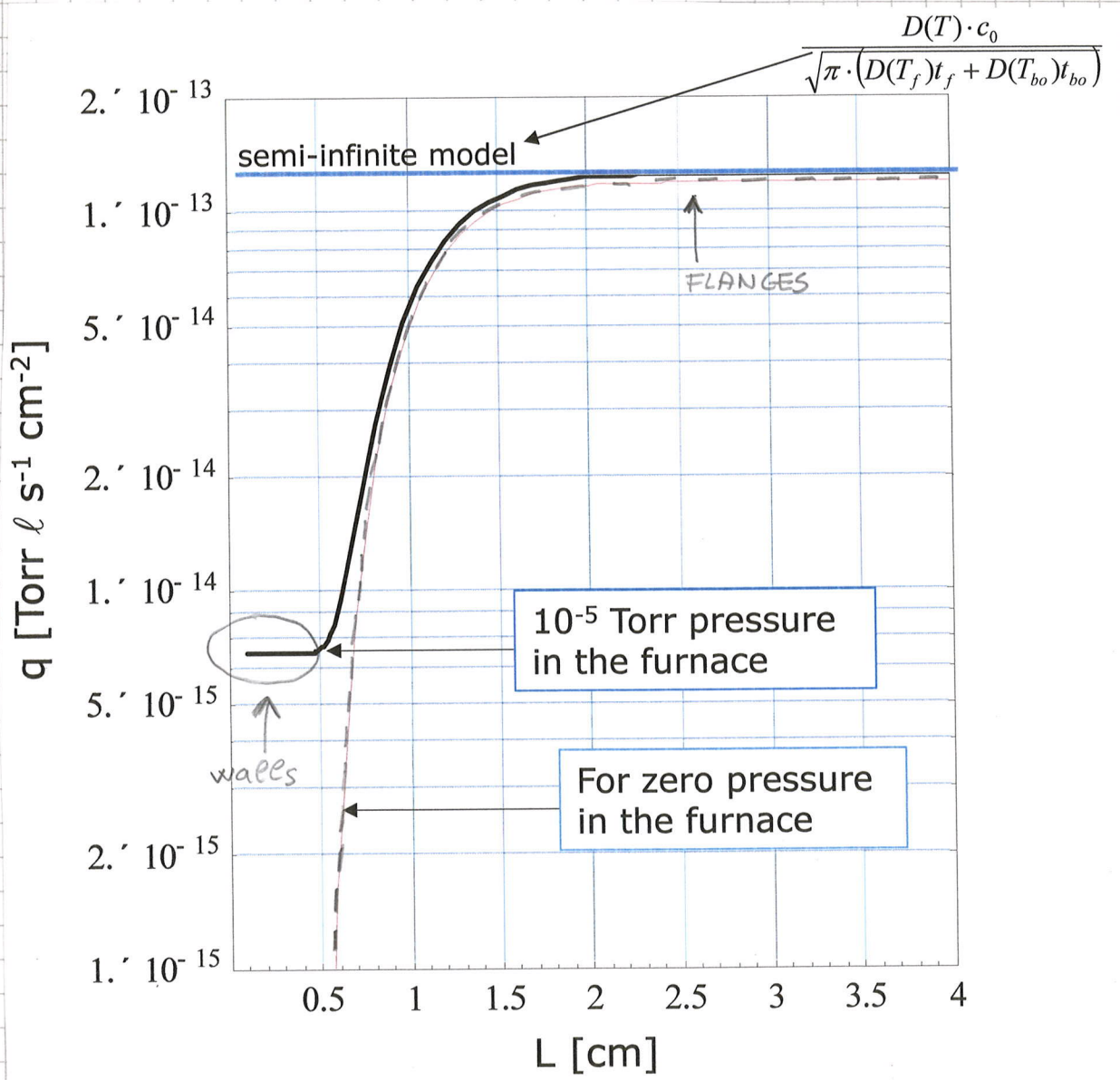

Outgassing rates in the 10^{-15} Torr ℓ/s·cm^2 are obtained for typical vacuum chambers; 20 times more for flanges $\Longrightarrow$ experimentally verified !!

6. AIR BAKEOUT

The methods for the reduction of H outgassing presented in the previous pages rely on heating in vacuum.
However other methods based on heating in air or in pure oxygen are also very effective.

- The air bakeout of austenitic stainless steels was proposed in the sixties. Such processing is reported to decrease the outgassing rate at room temperature by 3 orders of magnitude. Typical heating temperatures are 400°C ÷ 450°C for tens of hours.

- During the air heating an oxide layer 10 times thicker than the native oxide is formed. The oxide is essentially iron oxide (99%).

This treatment is rarely used in particle accelerators.

7. DEGASSING INDUCED BY PARTICLE BEAMS.

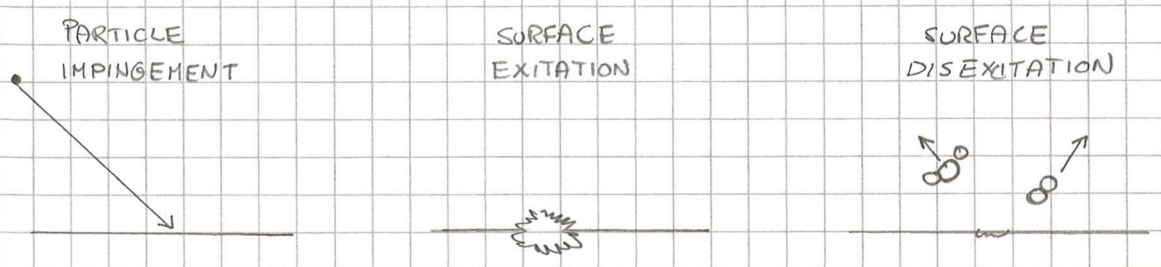

The impingement of particles (electrons, ions, photons) of energy higher than a few eV results in gas molecules desorption from solid surfaces.
The first observations of particle induced desorption were underlined at the beginning of the XX century in parallel with the first growth of vacuum technology.

In 1918, Dempster observed ion desorption from electron bombarded salts (Phys. Rev. 11, 323).

POSITIVE IONS FROM ELECTRON BOMBARDMENT.

It was thought that the bombardment of salts by electrons might break up the chemical compounds and give rise to many positive ions. At first a Wehnelt cathode was used; the ions formed passed beside the cathode (Fig. 1) and were then accelerated by a large potential difference. Aluminium phosphate on a piece of platinum foil was first bombarded. The intensity of the rays increased very rapidly with a slight increase in the amount or energy of the bombarding electrons, indicating that the salt needs to be heated to a certain degree before the ions are separated. Although the aluminium phosphate was chemically pure, the rays obtained under the bombardment of 128 volt electrons were very complex; the following ions were observed besides a couple of unresolved groups; H_1, H_2, Li (weak), O_1 (strong), Na (strong), O_3 (?) (weak), $M = 62$ (weak, possibly Na_2O), $M = 67$ (strong, possibly $H_3PO_2 = 66$), $M = 76$ (strong), $M = 86$ (weak, possibly Rb = 85.5), $M = 112$ (strong, possibly $P_2O_3 = 110$).

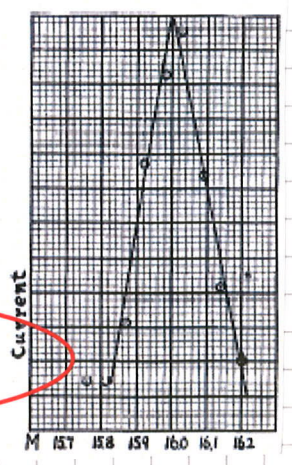

The experiments indicated the convenience of the method of obtaining positive rays and opened up an interesting field for investigation.

The experiments were however first directed

Millikan reported the first evidence of photon induced desorption in 1909, during the measurement of the photoelectric current of metallic surfaces exposed to ultraviolet radiation. The first interpretation of the phenomenon is attributed to Winch in 1930 (Phys. Rev. 36, 601). He was the first to understand the implication of photoelectrons in the photon induced desorption.

specimen to ultraviolet fatigue curves, taken by leaving the specimen in a vacuum of 10^{-7} mm of Hg unexposed, showed during the first stages a rapid decrease in photo-current with time of standing, but, after 360 hours of exposure for the film and 160 hours for the solid gold, the photo-current from the former held constant for 3 hours, and from the latter 1½ hours. This seemed to indicate that a fairly stable equilibrium had been reached, and the subsequent fatigue was consistent with the idea that it was due to return of gas to the surface.

The experiment was repeated, using a silver filament approximately 0.025 mm thick, and an increase in emission comparable to that for the gold film was obtained.

The probable explanation is that photo-electrons, both when ejected and returned to the surface by a reverse field, remove ad-sorbed gas from the surface.

Millikan[1] noted an increase in photoelectric emission on exposure of certain metals to ultraviolet, but did not note the corresponding change in long wave-length limit or that the photoelectrons themselves apparently play an important part in the outgassing.

Work is being carried forward testing this explanation and obtaining more data on photoelectric properties of thin films.

RALPH P. WINCH
Laboratory of Physics,
University of Wisconsin,
Madison, Wisconsin,
July 15, 1930.

Millikan, Phys. Rev. 29, 85 (1909).

In modern accelerators, most of the gas source is ascribed to particle induced desorption. The thermal outgassing is still the main gas source for low energy proton accelerators, LINACs and antimater facilities.

7.1 ELECTRON STIMULATED DESORPTION (ESD)

7.1.1 General experimental observations

The most relevant parameter in ESD is the desorption yield η :

$$\eta = \frac{\text{number of molecules desorbed}}{\text{number of electrons bombarding the surface}}$$

(1) η is a function of the electron energy and depends on the nature of the gas molecule and of the metallic surface.
For typical metals of vacuum technology :

$$\eta_{H_2} > \eta_{CO} > \eta_{CO_2} > \eta_{CH_4}$$

For electron energies of about 500 eV, typical values for η are

$$\eta_{H_2} \approx 10^{-1} \qquad \eta_{CH_4} \approx 10^{-3}$$

η depends strongly on electron energy in the range $0 \div 500$ eV; for energy in the $2 \div 15$ keV, η can be considered as constant.

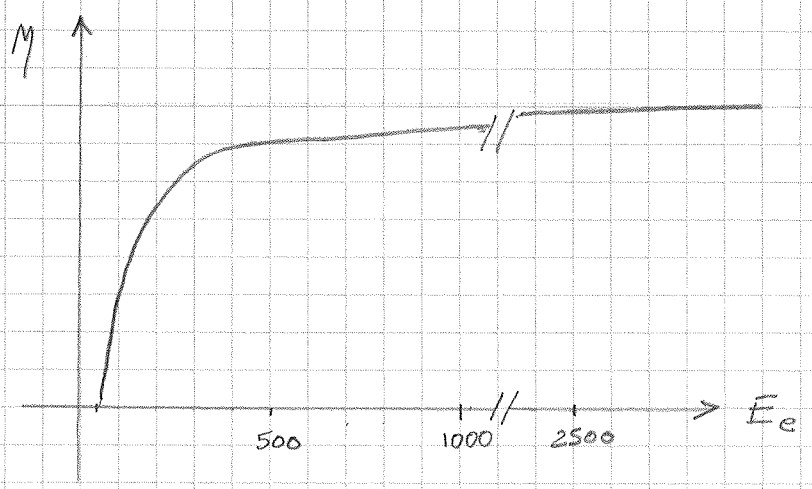

Most of the desorbed molecules are neutral, but ions are also present to a much lower extent (100 times less).

(2) The molecules desorbed by electrons acquire a kinetic energy of a few eV, up to 10 eV.

(3) η depends on dose of electrons that have bombarded the unit surface

$$D \left[\frac{\text{electrons}}{cm^2} \right]$$

This is easily understood; the previous electrons have removed gas from the surface → the surface is cleaner.

Except for H_2O, the measured η has a power law dependence on the dose D:

$$\eta = \eta_0 D^{-\alpha}$$

where $0,6 < \alpha < 1$.

α=0.62

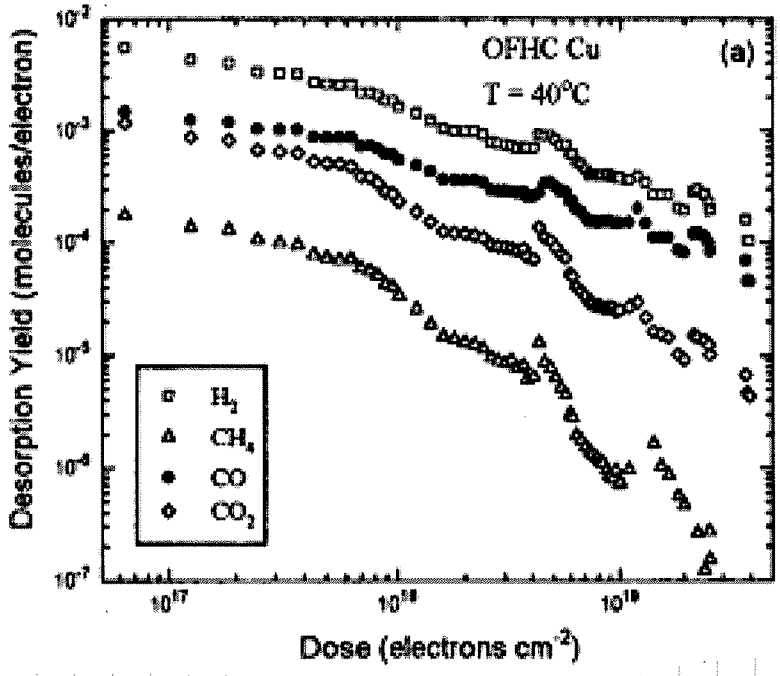

E_e = 300 eV

Samples baked at 150°C for 24 h and 300°C for 2 h

α=0.68

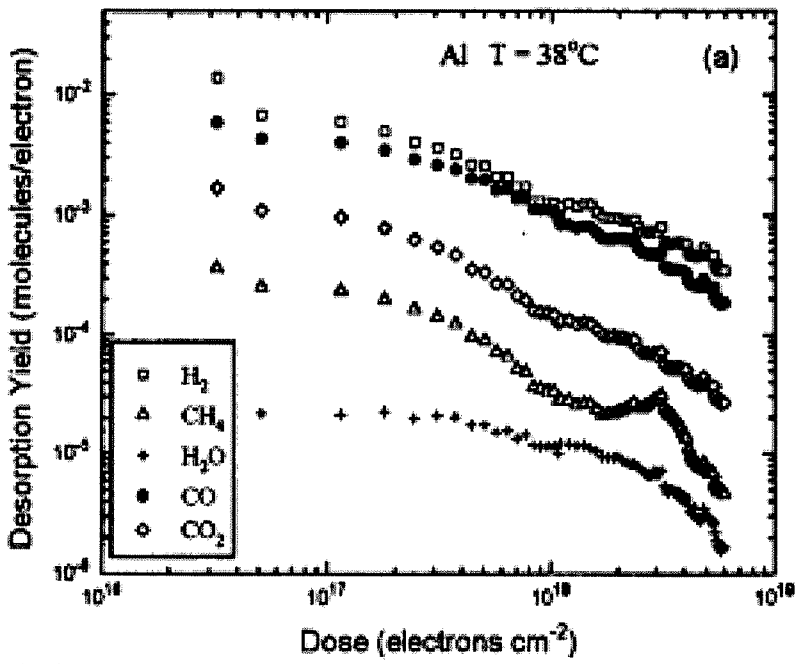

E_e = 300 eV

The positive effect of the accumulate dose on η is mostly lost when the bombarded surface is vented to air. A residual effect can be measured (memory effect) for a short stay in air.

④ The total quantity of desorbed gas molecules exceeds one monolayer. Some authors explain these results assuming a stimulated diffusion of C, O, H atoms from the bulk of the oxide layer.

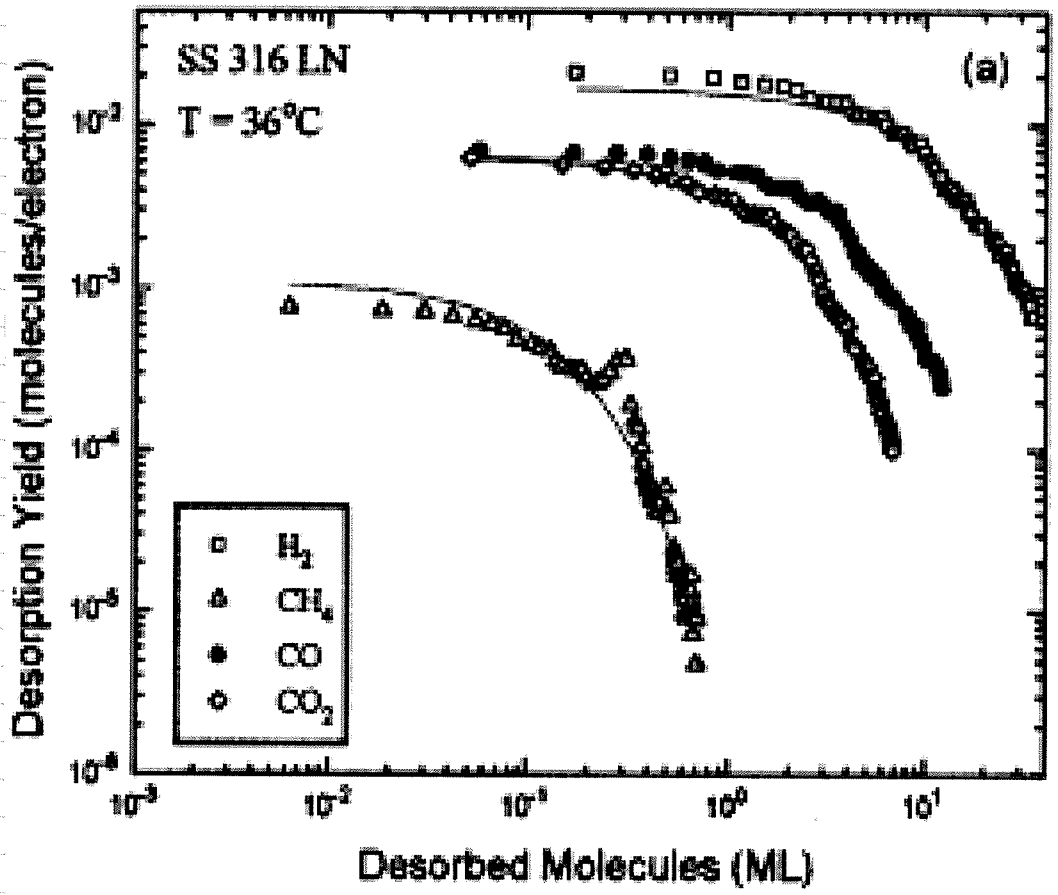

1ML=2x10^{15} molecules/ cm^2

The samples were baked at 150 C for 24 h and at 300 C for 2 h

7.1.2 The physical models of electron stimulated desorption

References
- T.E. Madey, D.E. Ramaker and R. Stockbauer, Ann. Rev. Phys. Chem. (1984), 35, p. 215-40
- R.D. Ramsier and J.T. Yates Jr., Surface Science Report (1991), 12, p. 243-378

The desorption mechanism can be described as a sequence of 3 steps:

1) a fast initial electronic excitation (10^{-16} s)
2) a decay of the exited state by displacement of atomic position in competition with other decay channels ($10^{-15} - 10^{-14}$ s)
3) a modification of the desorbing species as they get farther from the surface ($10^{-14} - 10^{-13}$ s).

$1\,\mathring{A} = 10^{-10}$ m $\quad E \cong 1$ eV $\rightarrow E = \frac{1}{2} m v^2 \rightarrow \sqrt{\frac{1.6\times10^{-19}\,J \times 2}{9.1\times10^{-31}}} \simeq 6\times10^{5}\ \frac{m}{s}$

electron mass

$\Delta t(1\mathring{A}) = \frac{\Delta s}{v} = \frac{10^{-10}}{6\times10^{5}} = \underline{\underline{1.6\times10^{-16}\ s}}$

electron movement involved

$\sqrt{\frac{1.6\times10^{-19}\,J \times 2}{2\times10^{-26}}} = 4000\ \frac{m}{s} \qquad \Delta t\,(1\mathring{A}) = \underline{\underline{2.5\times10^{-14}\ s}}$

carbon atom

atom movement involved

In the range of electron current recorded in particle accelerators, namely less than 10^{13} electrons $cm^{-2}\,s^{-1}$, the probability for an interaction among one molecule and more than one electron is negligible. Therefore the ESD is an isolate electron-adsorbate interaction.

When considering collisions between an incident low-energy particle ($E \sim 500$ eV) of mass m_e and a free particle of mass M, one can estimate the

order of magnitude of the maximun energy transferred (ΔE) during the process with classical kinematics.

For hard-sphere scattering the result is:

$$\frac{\Delta E}{E_e} = \frac{2 m_e M (1 - \cos\theta)}{(m_e + M)^2}$$

θ is the scattering angle in the centre of mass reference frame.

For $m_e \ll M$, which is always the case in ESD,

$$\frac{\Delta E}{E_e} \approx \frac{2 m_e}{M}$$

So the fraction of energy transfer is of the order of $2/1840 \approx 10^{-3}$ for electron - H collision. For typical energy of $E_e \approx 500$ eV $\Rightarrow \Delta E \approx 0.5$ eV which is much less than the observed 2-10 eV for heavier molecules.

$\Rightarrow$ The direct momentum transfer is not dominant in ESD $\Rightarrow$ electronic energy tranfer must be considered.

One of the earliest model to explain ESD was introduced in 1964 by Menzel, Gomer and Readhead (MGR model).

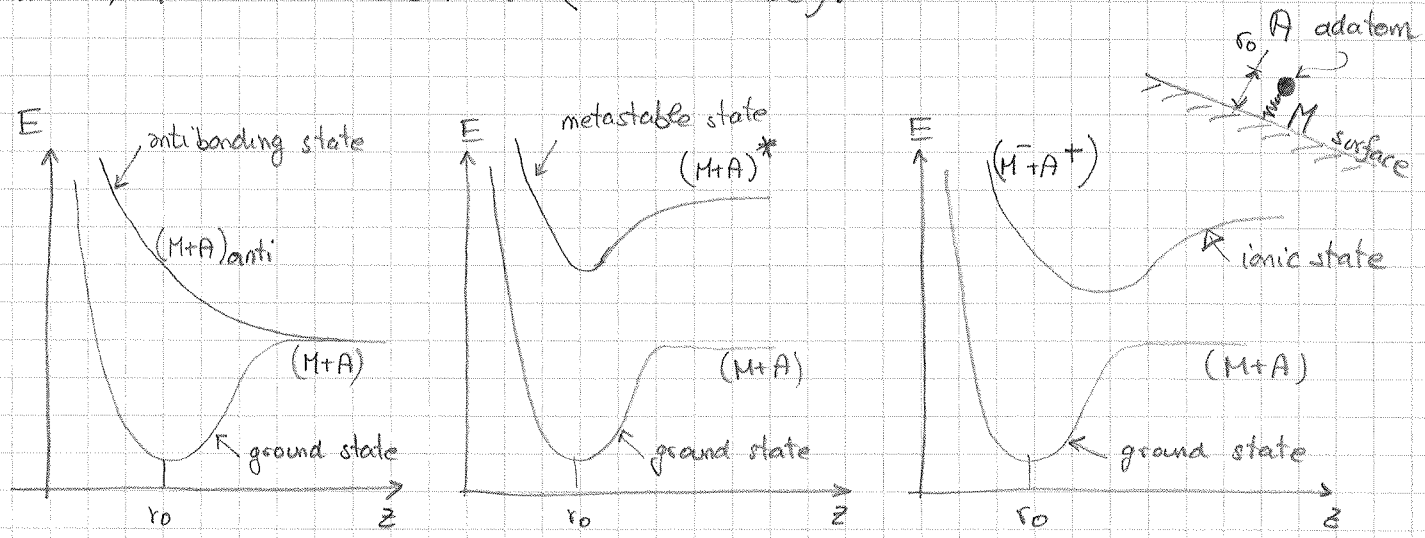

The MGR model assume that the M+A system is initially in its ground state (M+A). The interaction with the incident electron provokes an adiabatic transition (Franck-Condon principle) to exaited states,

antibonding, metastable or ionic. The Franck-Condon principle implies that the transition is vertical with respect to z, namely the electronic rearrangement is much faster than the nuclear movement.

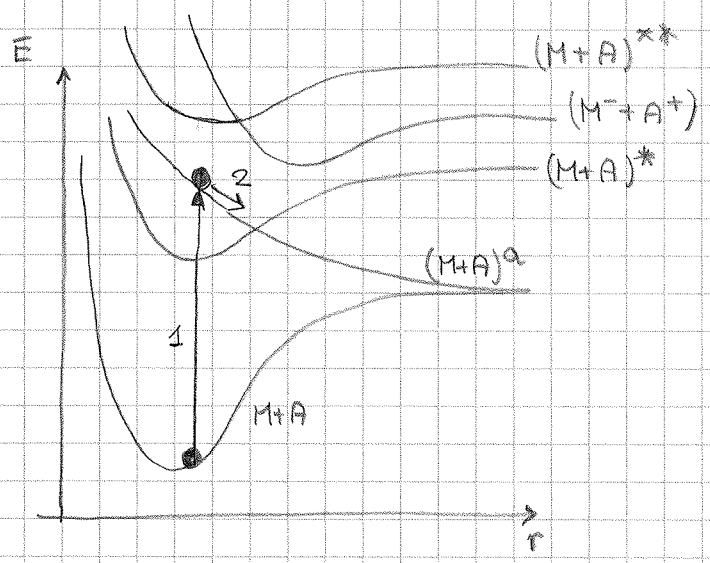

Adiabatic transition following electron collision.

After excitation, nuclear motion may occur over a time scale of $\approx 10^{-13} \div 10^{-14}$ s converting potential energy into traslational kinetic energy.
Potential curve crossing is possible resulting in different de-exitation pathways.

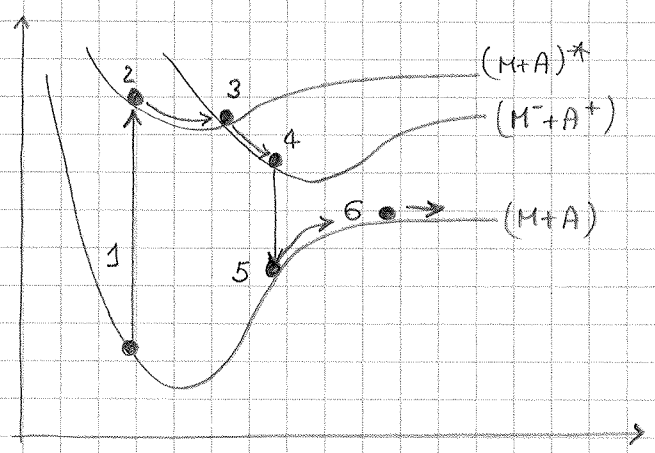

The ESD cross section can be written as

$$\sigma = \sigma_0 \cdot P_e$$

σ_0 ← primary electron exitation

P_e ← escape probability

The escape probability is higher when the adatom move faster beyond a critical distance r_c.

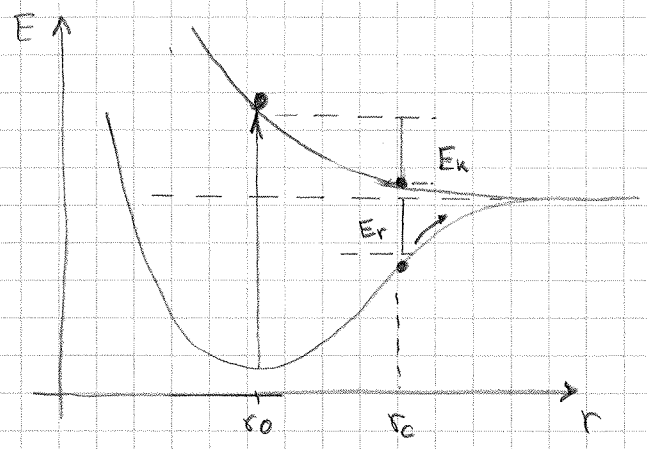

At the critical distance r_c, in case of de-exitation, the adatom has enough translational kinetic energy to escape.

The time needed to reach r_c is roughly:

$$t_c \approx \frac{r_c}{v} \approx \sqrt{M_a}$$

Because

$$P_e \propto e^{-t/\tau} \rightarrow P_e \propto e^{-\sqrt{M_a}}$$

$\Rightarrow$ The MGR model predict an isotope effect $\rightarrow$ experimentally verified.

7.2 PHOTON STIMULATED DESORPTION

Particle beams produce photons whenever they are accelerated, i.e. whenever their velocity vectors are changed, for example by bending magnets.
The emitted photons are adsorbed by the walls of the vacuum system and, as a result, gas molecules are desorbed.
There are experimental evidence that the desorption mechanism evolves in two steps:

1) the hitting photons extract photoelectrons with probability $\eta_e(\varepsilon)$ (ε = photon energy)
2) the emission and subsequent readsorption of the photoelectron provoke the desorption of gas molecules by ESD with probability η_d.

The total desorption flux is calculate by considering the number of photons emitted per second in a small interval of energy ε

$$\frac{dN(\varepsilon)}{dt}\, d\varepsilon$$

multiplying by the photoelectron yield at photon energy ε

$$\eta_e(\varepsilon) \cdot \frac{dN(\varepsilon)}{dt}\, d\varepsilon$$

and integrating photon energies:

$$\frac{dN_{e^-}}{dt} = \int_{\varepsilon_{min}}^{\infty} \eta_e(\varepsilon) \frac{dN(\varepsilon)}{dt}\, d\varepsilon$$

ε_{min} is the threshold for photoelectron extraction.

Finally multiplying by the electron desorption yield η_d:

$$\Rightarrow \quad Q = 2\eta_d \cdot \frac{dN_{e^-}}{dt} \Rightarrow \text{gas flux}$$

SOME ISSUES !

The number of photoelectrons extracted per photon is not well known for technological materials and it depends strongly on the surface cleanness. In addition the ESD yield of photoelectrons is not well defined because it depends on the photoelectron energy which is a priori not known.

For this reason the double step process is neglected and a global photodesorption yield η_{ph} is introduced.
In general η_{ph} is shown as a function of a typical synchrotron light parameter: the photon critical energy.

7.2.1 Photon power and energy spectrum

A particle moving on circular orbit radiate electromagnetic radiation with the following power:

$$P_{rad} = \frac{e^2 c}{6\pi \varepsilon_0 (m_0 c^2)^4} \cdot \frac{E^4}{\rho^2}$$

ρ = bending radius
E = beam energy
m_0 = rest mass
ε_0 = vacuum permittivity

Important consequence ⇒ the power emitted by electrons or positrons is much higher than that by protons:

$$\frac{P_{rad,e}}{P_{rad,p}} = \left(\frac{m_p c^2}{m_e c^2}\right)^4 = 1{,}13 \times 10^{13}$$

for the same bending radius and beam energy.

In practical units for electrons:

bending magnet field

$$P[W] = 1{,}59 \times 10^{-14} \cdot B^2[T] \cdot (\beta\gamma)^2 = 88{,}6 \, \frac{E^4[GeV] \cdot I[mA]}{\rho[m]}$$

- The synchrotron radiation power is a very important parameter for vacuum engineers in the phase of the vacuum system design. The power has to be collected, absorbed or transmitted. This defines shapes and materials of the vacuum chambers.

The <u>energy loss</u> per turn is:

$$U_0 = \oint P_{rad}\, dt = P_{rad} \cdot t_b = P_{rad} \cdot \frac{2\pi\rho}{c} = \frac{e^2}{3\varepsilon_0 (m_0 c^2)^4} \cdot \frac{E^4}{\rho}$$

t_b = travelling time in the bending magnets.

In practical units for electrons:

$$U_0\,[\mathrm{keV}] = 88{,}5\, \frac{E^4\,[\mathrm{GeV}]}{\rho\,[\mathrm{m}]}$$

IMPORTANT: The power emitted depends strongly on the beam energy.

- The synchrotron light at relativistic beam energy is emitted from the bending magnets in a very narrow cone:

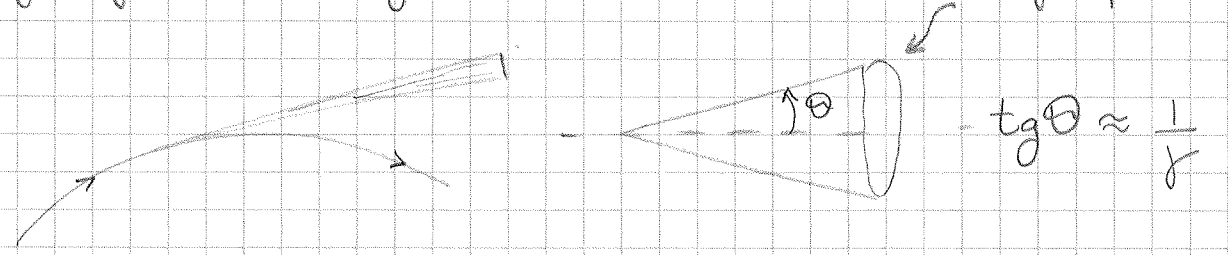

$$\mathrm{tg}\,\theta \approx \frac{1}{\gamma}$$

This means that an observer receives the radiation for a very short time Δt.

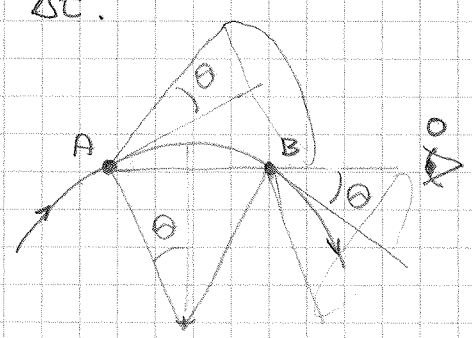

The observer receives the first light from A after:

$$t_1 = \frac{\overline{AB}}{c} + \frac{\overline{BO}}{c}$$

and the last:

$$t_2 = \frac{\widehat{AB}}{v} + \frac{\overline{BO}}{c}$$

Therefore the pulse lasts $\Delta t = \frac{\widehat{AB}}{v} - \frac{\overline{AB}}{c}$

$$\Delta t = \frac{2\rho\theta}{c\beta} - \frac{2\rho\sin\theta}{c} = \frac{2\rho}{c}\left(\frac{\theta}{\beta} - \theta + \frac{\theta^3}{3!} - \frac{\theta^5}{5!} + \dots\right)$$

$\theta \approx \frac{1}{\gamma}$ $\Rightarrow$ it can be shown that

$$\Delta t = \frac{4\rho}{3c\gamma^3} \rightarrow \text{very small number}$$

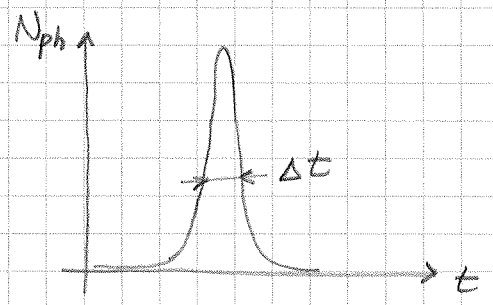

The Fourier transform of this short signal gives a very wide broad spectrum. The typical frequency is

$$\omega_{typ} = \frac{2\pi}{\Delta t} = \frac{3\pi c \cdot \gamma^3}{2\rho}$$

The critical frequency is defined as: $\omega_{CR} = \frac{\omega_{typ}}{\pi} = \frac{3c\gamma^3}{2\rho}$

As a consequence the critical energy is:

$$\boxed{\mathcal{E}_c = \hbar\omega_c = \frac{3}{2}\frac{\hbar c}{\rho}\gamma^3}$$

In practical unit:

$$\mathcal{E}_c\,[\text{keV}] = 2{,}218\,\frac{E^3[\text{GeV}]}{\rho} = 0{,}665\,E^2[\text{GeV}]\cdot B\,[T]$$

The critical energy divides the photon spectrum in two parts of equal power.

– The spectral photon density is given by:

$$\frac{d\dot{N}_{Ph}}{d\left(\frac{\varepsilon}{\varepsilon_c}\right)} = \frac{P_{TOT}}{\hbar\omega_c} \cdot S\left(\frac{\omega}{\omega_c}\right) \qquad \int_0^\infty S(\xi)\,d\xi = 1$$

$$\int_0^1 S(\xi)\,d\xi = \frac{1}{2}$$

The spectrum for a storage ring is fully determined by the three parameters:

$$I_b,\ E,\ \rho$$

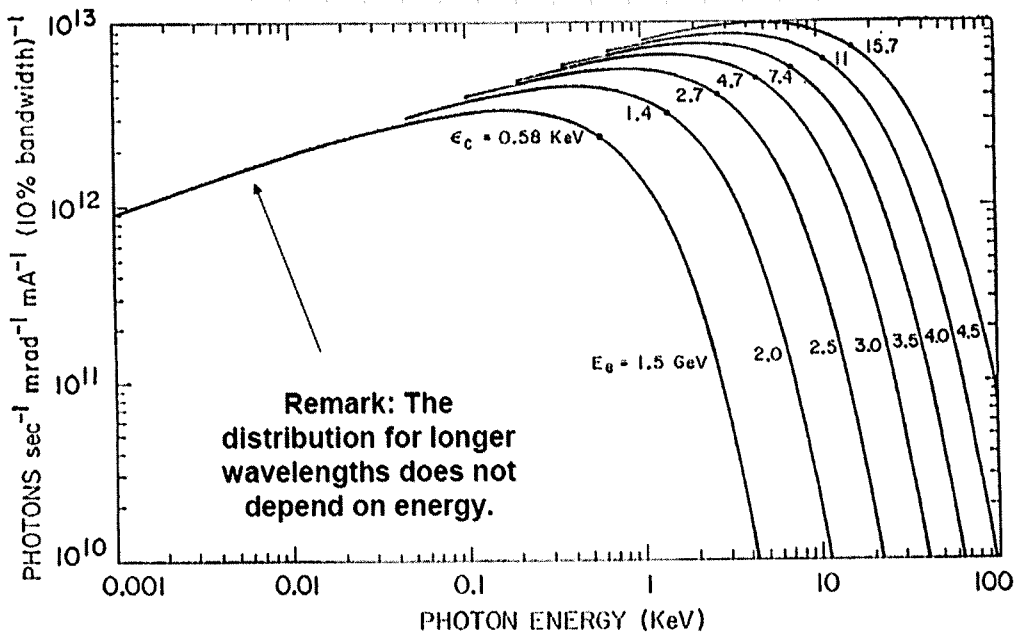

It can be shown that the number of emitted photon per second is

$$\dot{N} = \frac{15\sqrt{3}}{8} \cdot \frac{P}{\varepsilon_c}$$

and the mean photon energy is:

$$\langle \varepsilon \rangle = \frac{P}{\dot{N}} = \frac{8}{15\sqrt{3}}\,\varepsilon_c$$

In practical unit

$$\dot{N} = 8{,}08 \times 10^{17}\, I[mA] \cdot E[GeV]$$

and the linear flux (photons $m^{-1} s^{-1}$)

$$\frac{d\dot{N}}{ds} = 1{,}28 \times 10^{17}\, \frac{I[mA] \cdot E[GeV]}{\rho[m]}$$

The degassing rate is written as

$$Q = \eta_{ph} \cdot \dot{N}$$

where η_{ph} is the synchrotron ligth desorption yield. It is a measured value that averages the contribution of a large spectrum of photon energy.

<u>WARNING</u>: Do not confuse "power" and "number of photons"

50% power $\leftarrow \varepsilon_c \rightarrow$ 50% power

$\approx$ 90% of photons $\leftarrow \varepsilon_c \rightarrow \approx$ 10% of photons

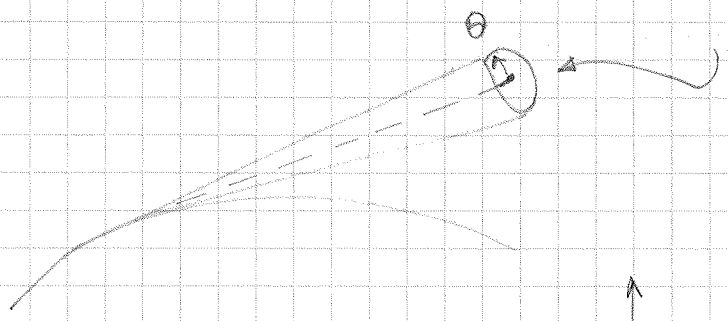

ligth cone:

power: $tg\,\theta \approx \frac{1}{\gamma}$

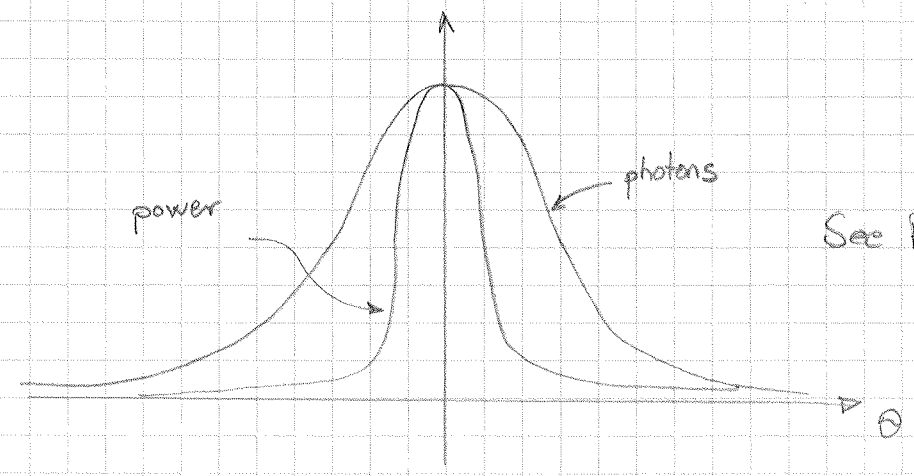

See Roberto's tutorial

7.2.2 The photon desorption yield of technological materials

The photon induced desorption yields have been measured by means of synchrotron radiation sources and dedicated setups. The results are in general plotted as a function of the dose of bombarding photons (p.ex. photons/metre).

- The desorption yields do not depend significantly on the photon dose up to about 5×10^{20} photons per metre of vacuum chamber. For higher doses, η_{ph} varies as a power law function of D:

$$\eta_{ph} \propto D^{-\alpha}$$

α has values similar to those of electron stimulated desorption.

- η_{PH} varies roughly linearly with the critical energy for $E_c < 280$ eV.

$$\eta_{ph} \approx A \cdot E_c^{\beta} \qquad 0{,}74 < \beta < 1{,}12$$

The orders of magnitude of η_{ph} for E_c of about $0.5 \div 1$ keV are:

for well cleaned and in situ baked Cu, and st. steel

$$\begin{cases} \eta_{H_2} \approx 10^{-3} \text{ molecules/photon} \\ \eta_{CO} \simeq \eta_{CO_2} \approx 10^{-3} \div 10^{-4} \text{ molecules/photon} \\ \eta_{CH_4} \approx 10^{-5} \text{ molecules/photons} \end{cases}$$

EASY TO REMEMBER: η_{PH} are about 2 orders of magnitude lower than η_e.

$\Longrightarrow$ photoelectron yields $\approx 10^{-2}$ electrons/photon for the material of interest.

Photons with energy lower than a threshold value should not contribute to the desorption process. The threshold should be equivalent to the photoelectron extraction threshold (work function):

$$E_{min} \approx 5 \text{ eV} \quad \Big\} \text{ for typical metals}$$

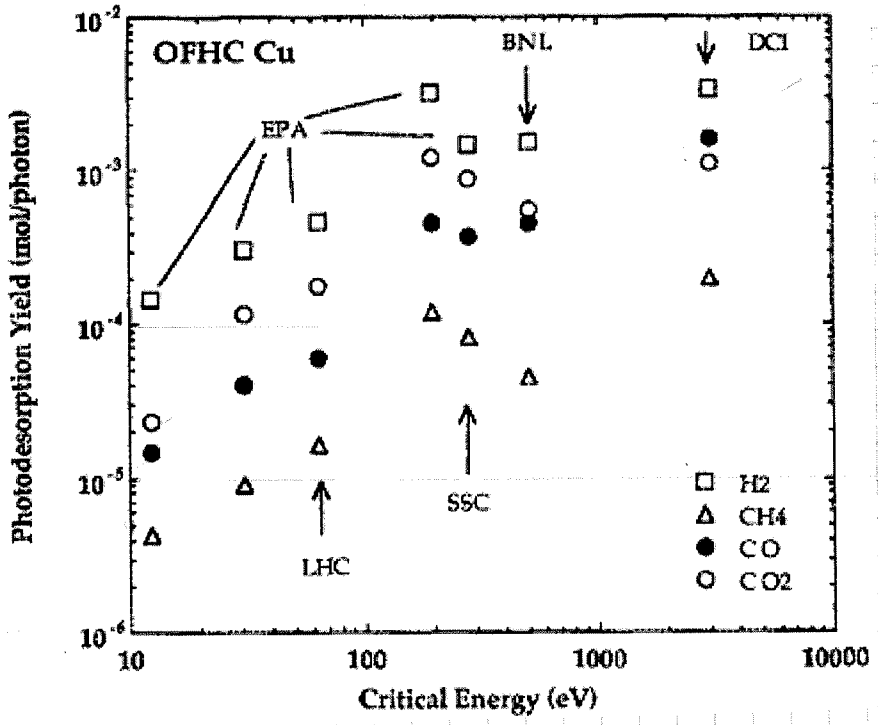

J. Gomez-Goñi et al. J. Vac. Sci. Tech A12, 1714 (1994)

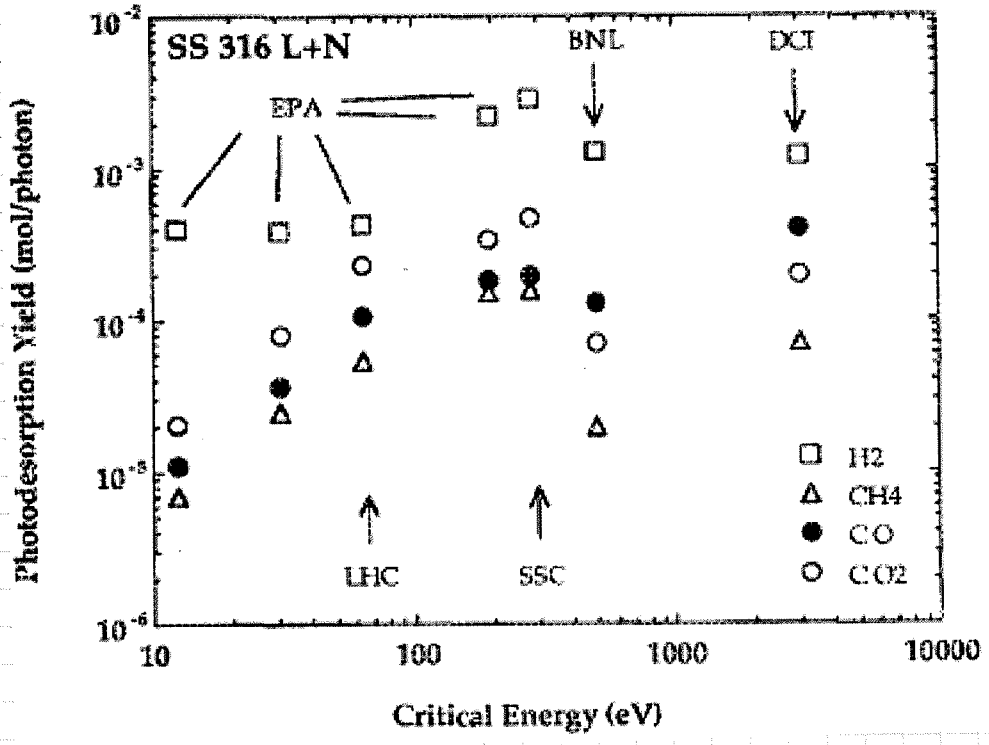

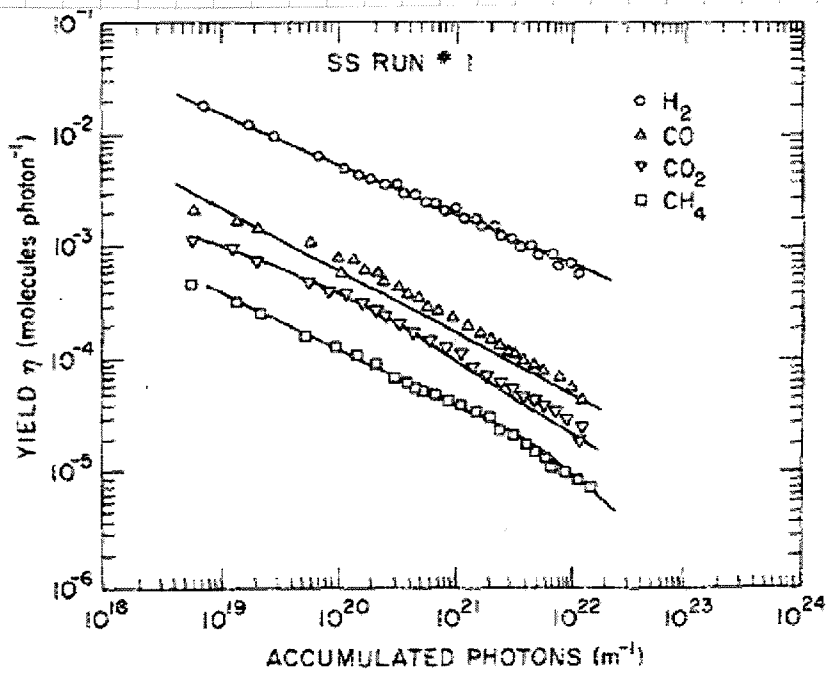

FIG. 2. Molecular desorption yields for prebaked stainless steel.

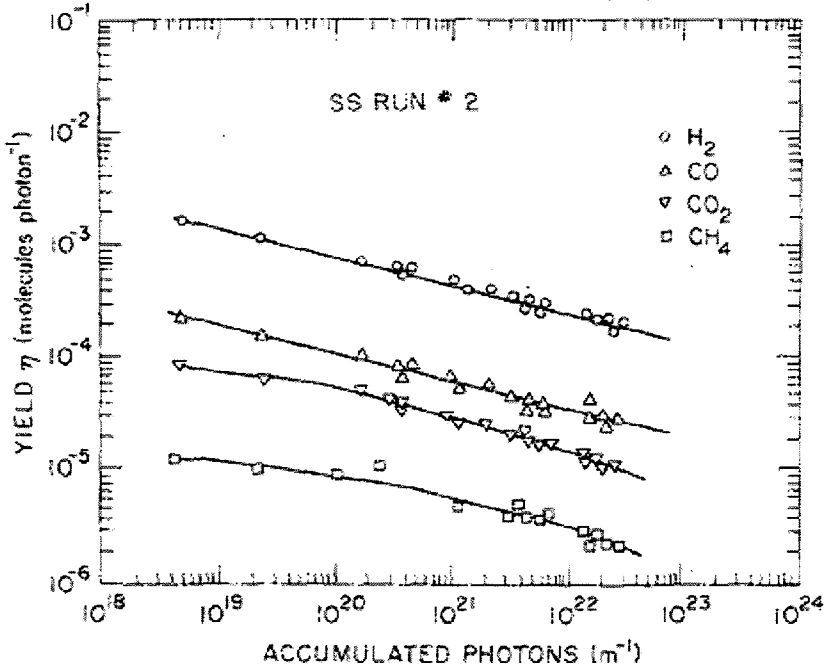

FIG. 3. Molecular desorption yields for *in situ* baked stainless steel.

Foerster, Halama, Lamm, J. Vac. Sci. and Tech A, vol 8, p. 2858, 1990

7.3 METHODS FOR THE REDUCTION OF ELECTRON AND PHOTON INDUCED DESORPTION.

The gas desorbed by electrons or photons is located on the surface of the vacuum chamber materials or very close to it. It goes without saying that a state of art surface cleaning is essential to avoid excessive induced desorption.

An additional mitigation is provided by in situ bakeout at temperature in the range 120°C ÷ 350°C. Heating the vacuum material results in a reduced quantity of gas onto the surface and in the oxide layer. However, the effect on the η values is limited and in general less than an order of magnitude.

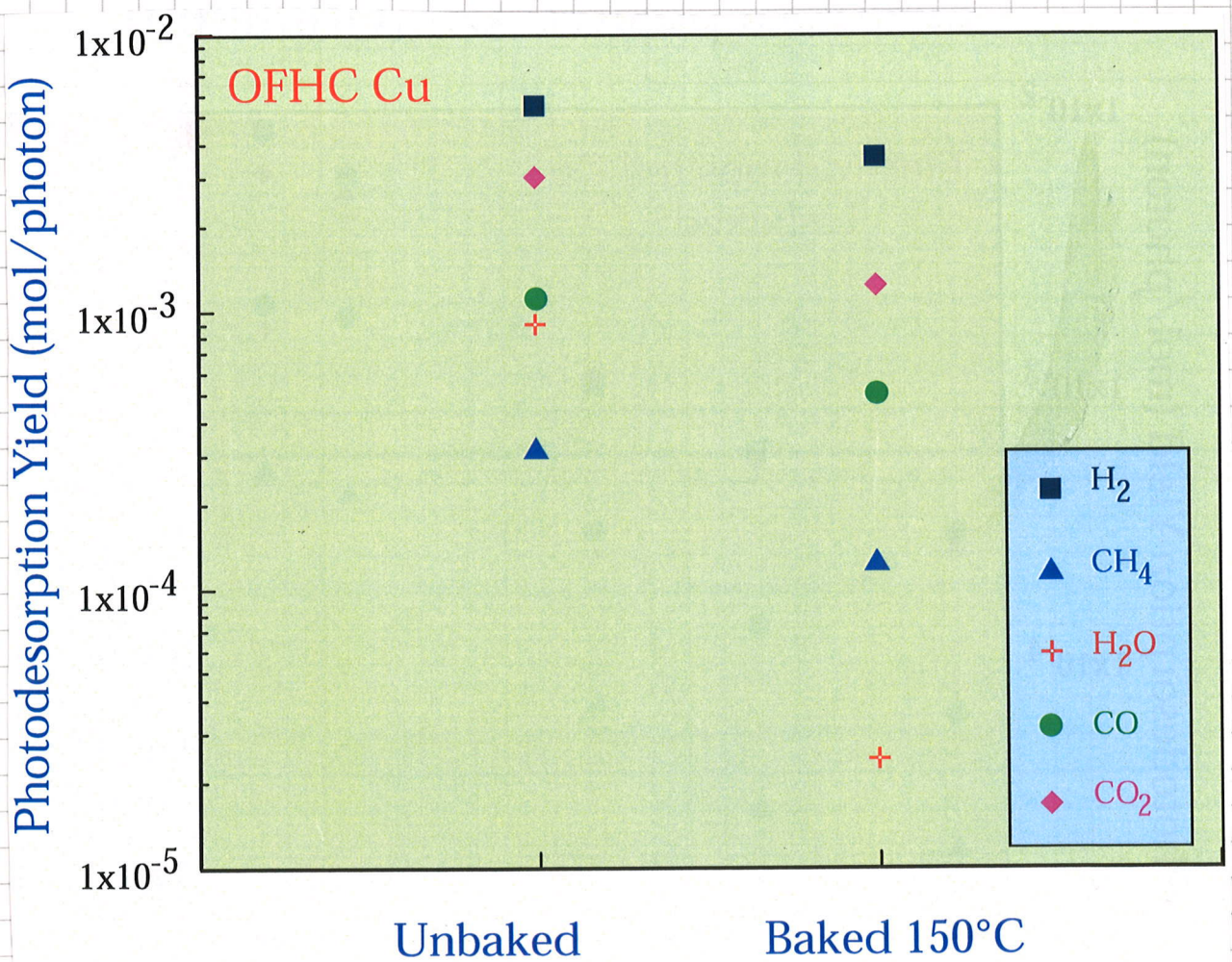

H_2 : 1,5 CH_4 : 2,5 H_2O : 36,7 CO : 2,2 CO_2 : 2,5

Electropolishing and vacuum firing have a very limited effect on η.

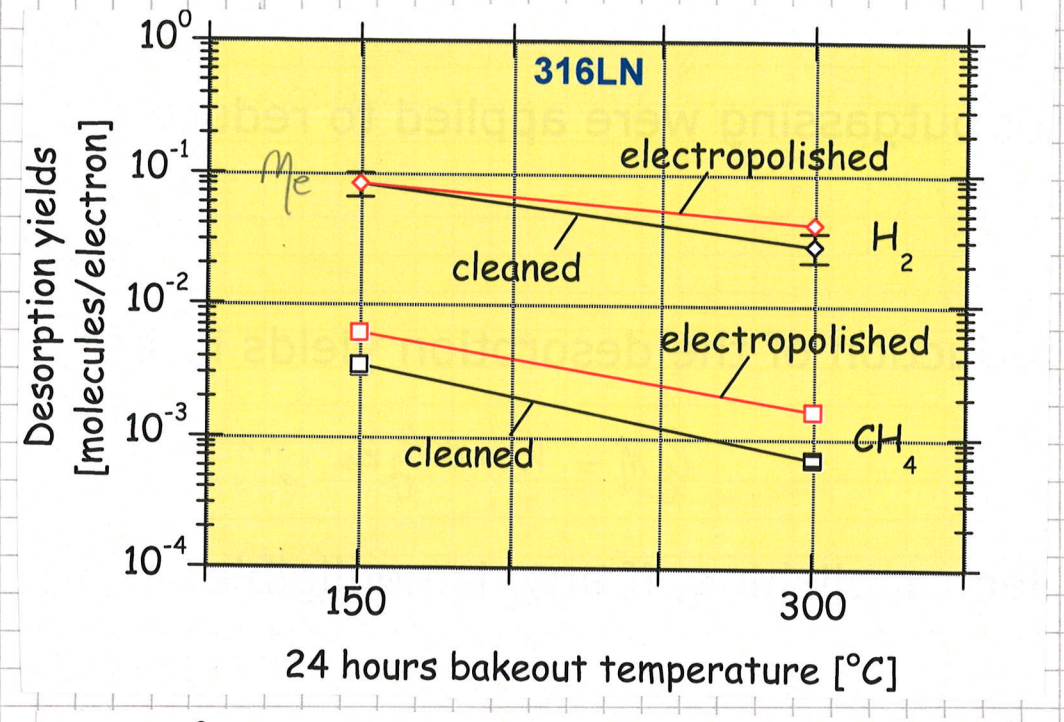

Austenitic st. steel

$E_e = 500$ eV

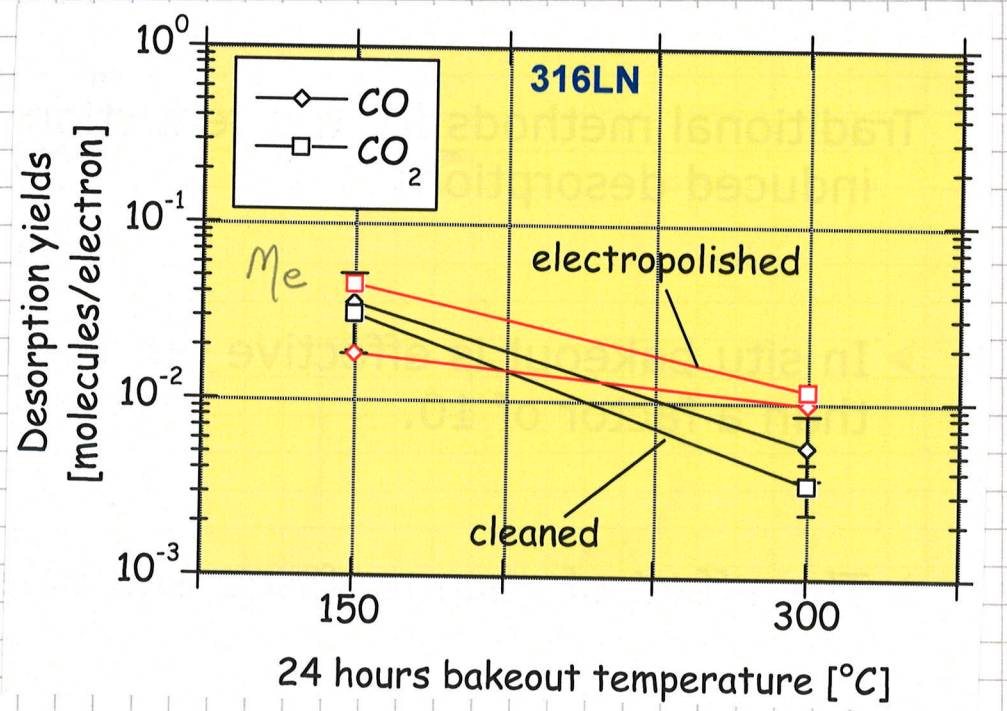

After these treatment, vacuum materials are re-exposed to air. A new oxide layer is formed, which is considered as the source of gas.

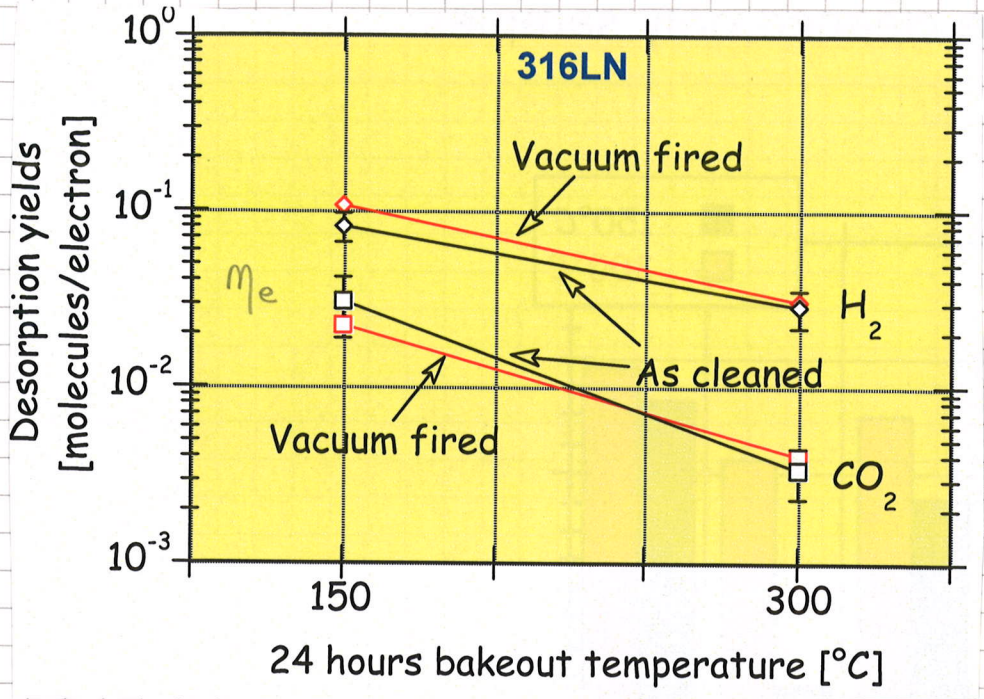

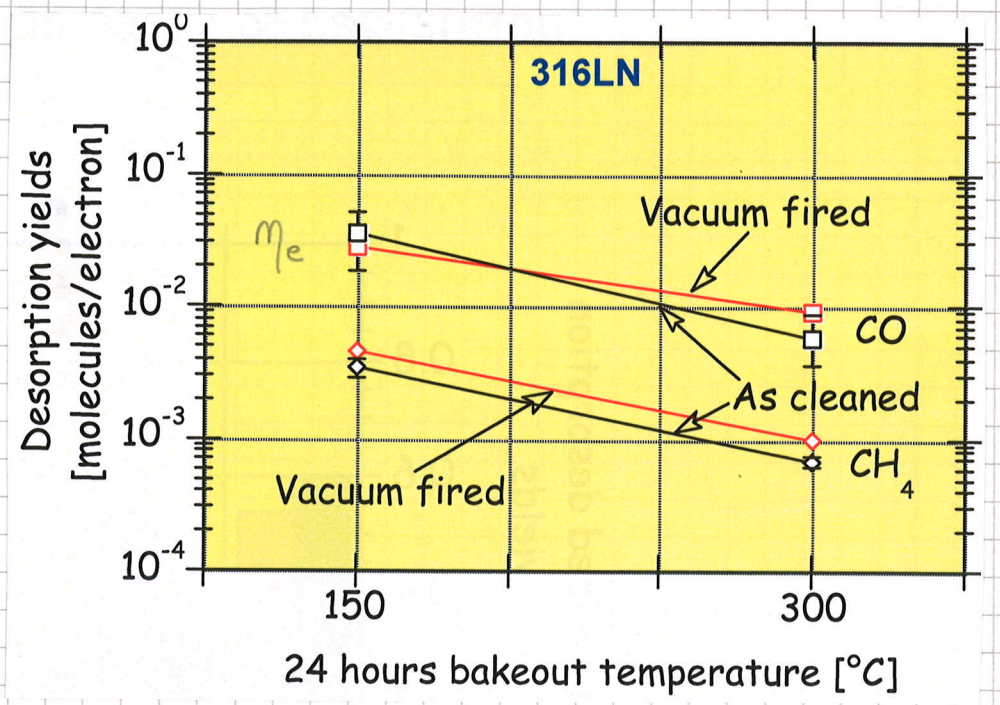

Stainless steel components that are preliminarily air baked shows η sligtly lower than those reported for as cleaned surfaces, despite a thicker oxide layer.

- The accumulation of electron or photon doses is very effective in the reduction of η as shown above for Cu. The particle bombardment produce an additional surface cleaning and a change in the surface chemistry.

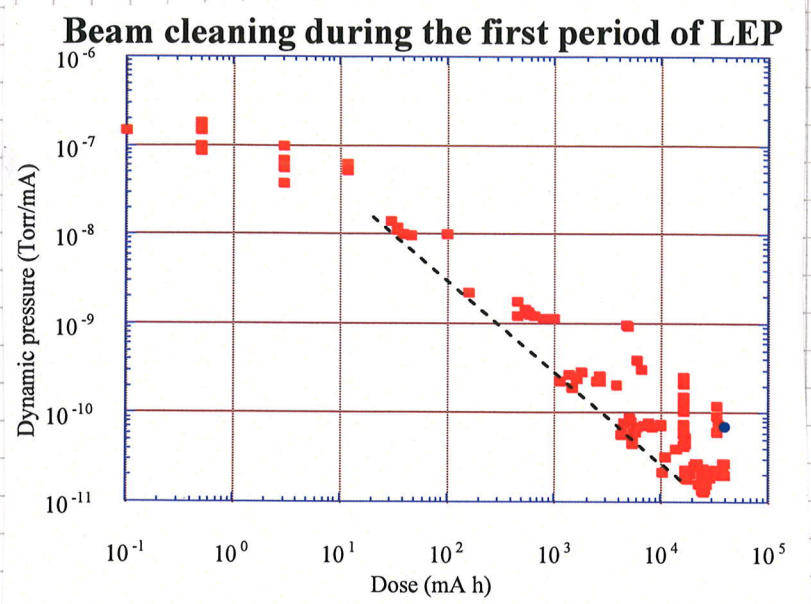

O. Gröbner. Vacuum 43 (1992) 27-30

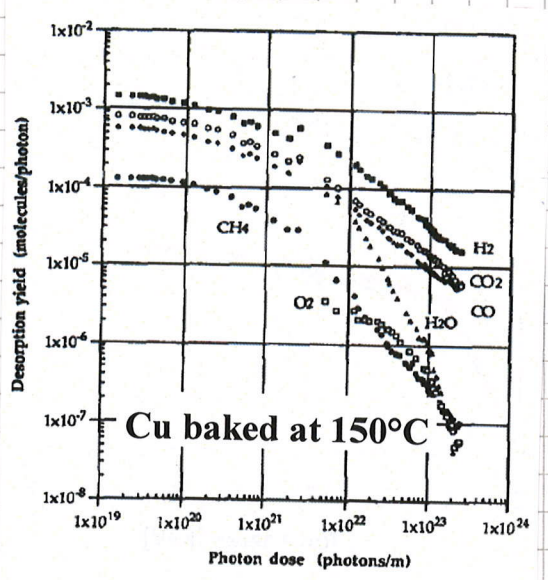

O. Gröbner *et al.* J.Vac.Sci. 12(3), May/Jun 1994, 846-853

Particle accelerators for which induced desorption is a serious limitation can be run for some day, at a limited current, to reduce η. This operation is refered to as "BEAM CONDITIONING" or "BEAM SCRUBBING".

In section 3 we will consider another method to change the surface composition with a consequent radical reduction of η: non-evaporable getter thin film coating.

7.3 ION INDUCED DESORPTION

Ion induced desorption is in general studied in two diffent conditions.

→ single ionized gas molecules found in vacuum system

→ highly ionized heavy atoms

- The first considers the fact that beam particles can collide with the residual gas molecules and ionize them. The gas molecule ions acquire kinetic energy interacting with the ⊕ beam electric potential. The energy of impact on the beam pipes' wall is in the range eV to KeV. The desorption yieds η_{ION} are measured in laboratory set-up.

- In the second case, the heavy ions are produced on purpose in ion-sources and then accelerated for collisions. Typical ions are Pb^{53+}, U^{73+}, Ar^{10+} ... The desorption studies are performed in the range 1 MeV/u to 100 GeV/u by set-up integrated in particle accelerators.

7.3.1 Gas molecule ions at low energy.

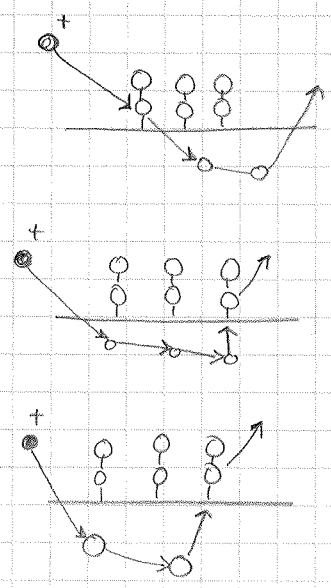

The desorption by ions (H_2^+, CH_4^+, CO^+, CO_2^+, Ar^+) can be depicted as the effect of a series of collisions among the impinging ion, the atoms of the metal and adsorbate.
(see J. Schou, CERN Accelerator School, Vacuum in Accelerators)

Typical values for the desorption yield for low ion doses are :

Ion energy $\approx$ 1 KeV
Baked copper or stainless steel

$$\left\{\begin{array}{l} \eta_{H_2} \overset{<}{\approx} \eta_{CO} \approx 1 \\ \eta_{CO_2} \approx \eta_{CO}/5 \\ \eta_{CH_4} \approx \eta_{H_2}/10 \end{array}\right\}$$

ion desorption yields are higher than electron and photon desorption yields

The desorption yield depends on;

- ion mass
- ion energy
- nature of the desorbed gas
- material of the vacuum chamber

see G. Hulla
CERN-THESIS-2009-026
05/03/2009

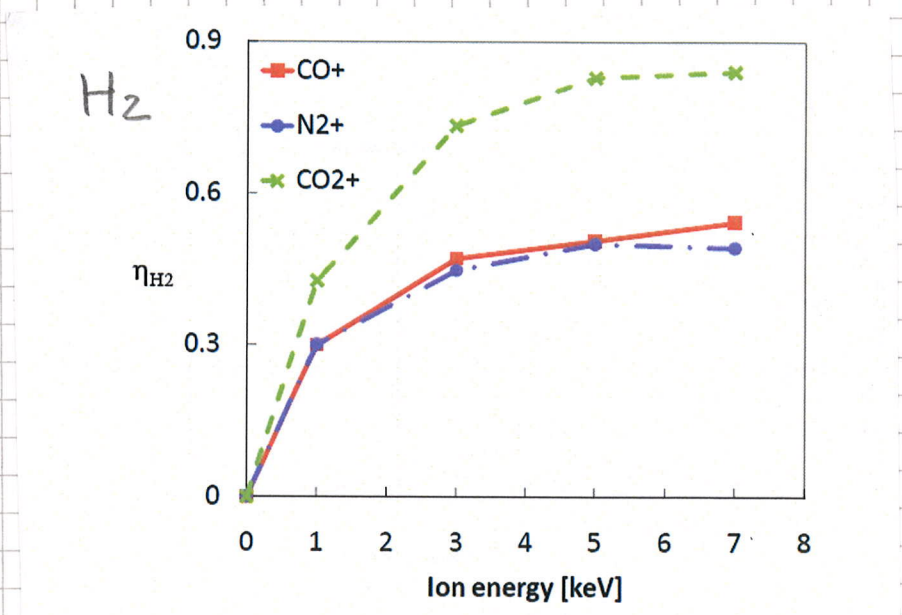

Figure 6.14: H_2 desorption yields of N_2^+-ions and oxygen containing ions incident on copper as function of the ion energy.

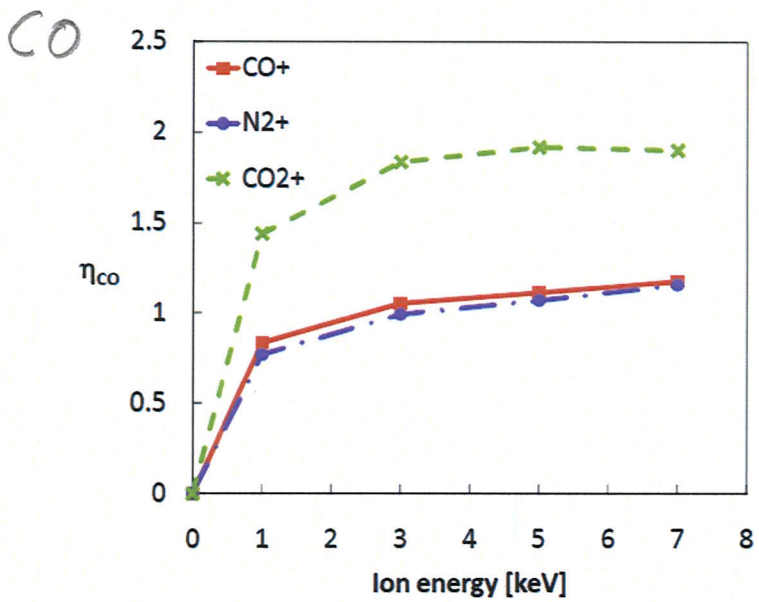

Figure 6.16: CO desorption yields of N_2^+-ions and oxygen containing ions incident on copper as function of the ion energy.

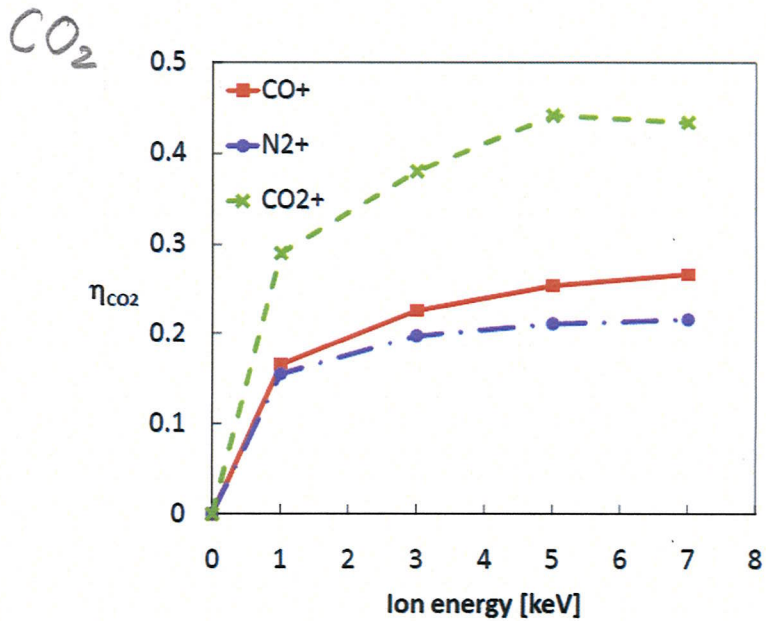

Figure 6.18: CO_2 desorption yields of N_2^+-ions and oxygen containing ions incident on copper as function of the ion energy.

The dose effect is visible for more than 10^{15} ions/cm^2. Saturation of the η values was measured for doses higher than 10^{16} ions/cm^2 ($\approx$ 10 times lower than the η at zero dose).

- The role of ion mass and energy and of the material of the substrate can be calculated in terms of <u>energy loss</u>. The key quantity is the <u>stopping power</u>

$$\frac{dE}{dx} = N \cdot S(E)$$

N = number density of atoms in the solid

$S(E)$ = stopping cross section which depends on the energy E of the impinging ion.

$S(E)$ can be divided in two contributions:

$$S(E) = S_n(E) + S_e(E) \begin{cases} S_n(E) = \text{nuclear stopping cross section} \\ S_e(E) = \text{electronic stopping cross section} \end{cases}$$

The "nuclear" part takes into account the energy transfered to nuclei as in sputtering processing. The primary ions undergoes several scattering and a complete change of trajectory. This energy transfer mechanism is dominant up to about 50 keV ion energy.

The electronic part considers the energy transfered to electrons belonging to the solid, first to break the bonding with the nuclei and then to accelerate them. This process prevails on the nuclear one at high energy ($E > 1$ MeV).

The energy loss model, considering the nuclear part only, can fit the experimental data of ion induced adsorption at low energy.

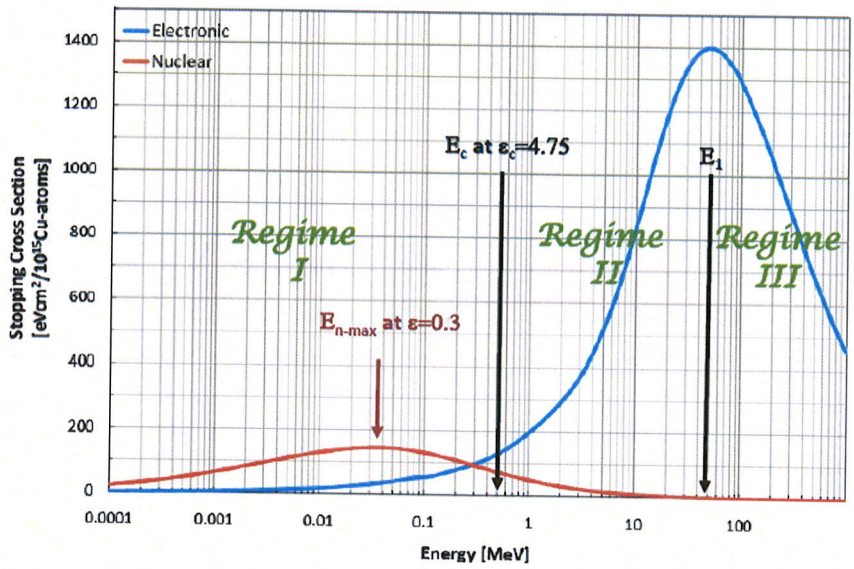

Figure 4.3: Electronic and nuclear stopping cross sections for Ar^+-ions incident on copper.

7.3.2 Heavy ion induced desorption

- In the last 15 years, several experiments have shown that high energy ($E > 1$ MeV/u) ions can induce the desorption of a huge quantity of gas. Desorption yields up to 10^5 molecules/ion were measured for In^{49+} at 158 GeV/u at the CERN SPS.
  A review of data can be found in E. Mahner, Phys. Rev. ST Accel. Beams 11, 104801 (2008).

- Here again M_{ION} is reduced by increasing the dose of impinging ions.

- It has been shown that the M_{ION} can be obtained by the electronic energy loss:

$$M_{ION} = k \left(\frac{dE}{dx}\right)_e^n$$

$$2 < n < 3$$

The transfer of energy to electron provokes a thermal spike that results in the desorption.

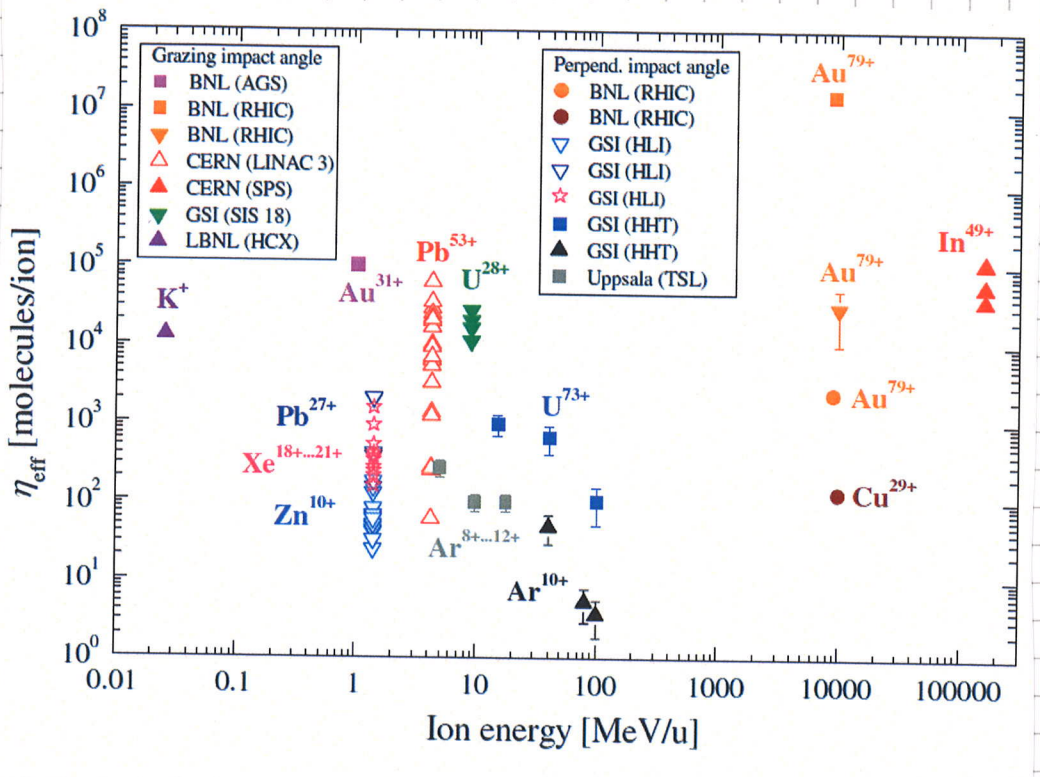

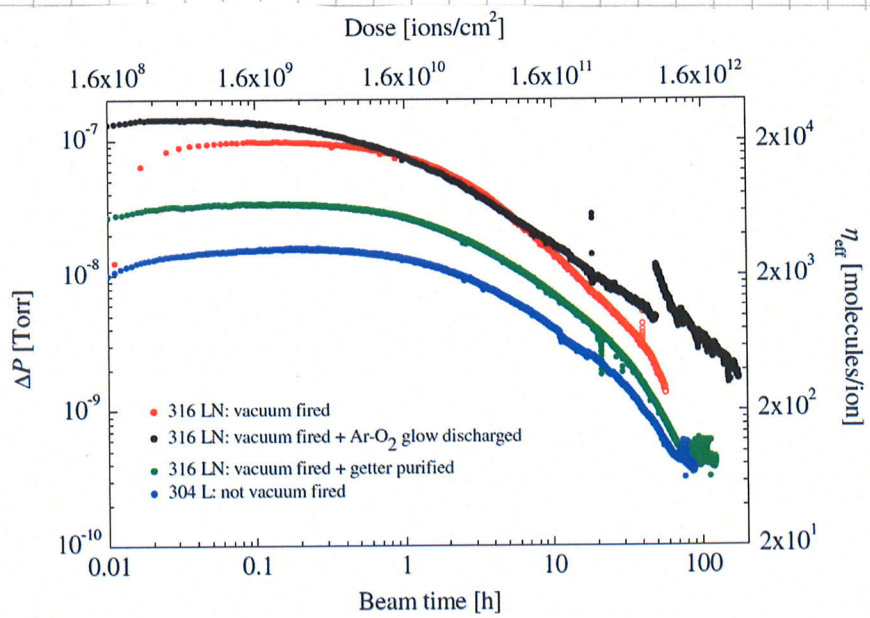

FIG. 7. (Color) Beam cleaning measurements for four different stainless steel (316LN, 304L) vacuum chambers continuously bombarded with 1.5×10^9 Pb^{53} ions (per shot) under $\theta = 89.2°$ grazing incidence. The shown desorption measurements were done with 4.2 MeV/u lead ions at LINAC 3; all four vacuum chambers were cut afterwards and samples of each chamber were studied with ERDA [70]. The obtained ERDA results are displayed in Fig. 3.

7.3.3 Pressure runaway provoked by ion induced desorption.

Ion induced desorption can trigger a rapid pressure rise in particle accelerators that results in a limitation of the beam current. This phenomenon was shown at the ISR in the '70 when increasing the proton beam current to about 1 A.

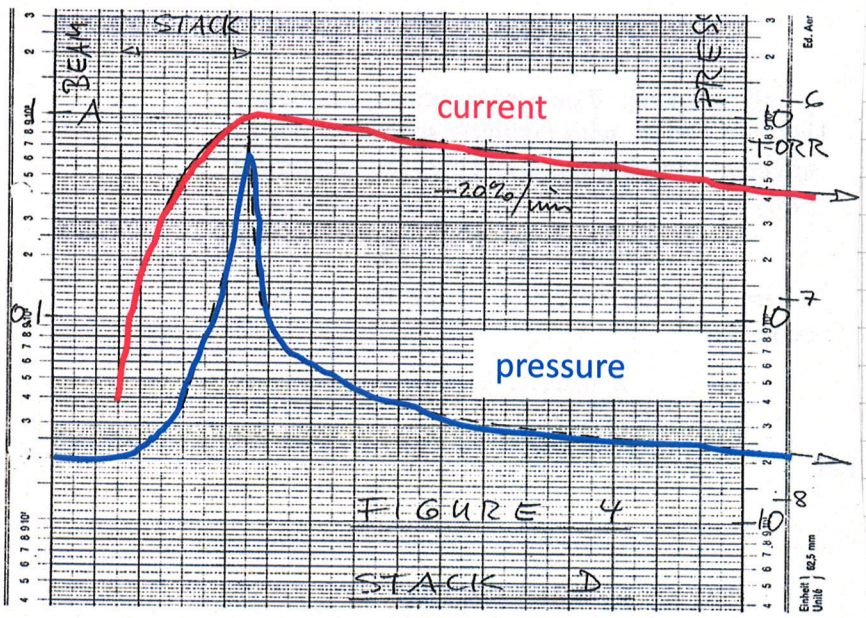

First documented pressure bump in the ISR

E. Fischer/O. Gröbner/E. Jones 18/11/1970

The instability can be easily understood:

- the residual gas is ionized by the positive particle beam
- the ions are accelerated by the beam potential toward the beam pipe walls
- the impinging ions induce gas desorption

The process can have a positive feedback.

The total flux of desorbed molecules per unit length of vacuum chamber is

$$Q = \eta_{ion} \cdot \sigma_i \cdot \frac{P \cdot I}{e} + Q_{th} \quad \left[\frac{Torr \cdot \ell}{s}\right]$$

where: σ_i is the cross section of ionization of the gas molecules

I is the beam current

Ionization probability for a proton $\frac{\sigma \cdot n \cdot A \cdot 1}{A} = \sigma \cdot n$ ← gas density; A ← cross section area of beampipe

Q_{th} is the thermal outgassing

The pressure in the beam pipe is

$$P = \frac{Q}{S_{eff}} = \frac{\eta_{ion}\, \sigma_i\, P\, I}{e \cdot S_{eff}} + \frac{Q_{th}}{S_{eff}}$$

S_{eff} = effective pump. speed per unit length $[\ell/(s \cdot m)]$

$$\Rightarrow \quad P = \frac{Q_{th}}{S_{eff} - \eta_{ion}\, \sigma_i\, \frac{I}{e}}$$

The pressure diverges for $S_{eff} - \eta_{ion}\, \sigma_i\, \frac{I}{e} = 0$, which defines a critical value for the current:

$$S_{eff} - \eta_{ion}\, \sigma_i\, \frac{I_c}{e} = 0 \Rightarrow \boxed{I_c = \frac{S_{eff} \cdot e}{\sigma_i \cdot \eta_{ion}}}$$

	σ_i $[10^{-18}\ cm^2]$	
H_2	0,22	0,37
He	0,23	0,38
CH_4	1,2	2,1
CO	1,0	1,8
Ar	1,1	2,0
CO_2	1,6	2,8
	⇑ 26 GeV	⇑ 7 TeV

Example:

$S_{eff} \simeq 10\ \ell/(s \cdot dm)$ $\quad 1\,\ell = 1\,dm^3$

$\sigma_{CO} = 1 \times 10^{-18}\ cm^2 = 10^{-16}\ dm^2$ $\quad \eta_{ion} = 1$

$$I_c = \frac{10 \times 1{,}6 \times 10^{-19}}{10^{-16} \times 1} = 1{,}6 \times 10^{-2}\ A$$

UNIT 3 !

PUMPS FOR PARTICLE ACCELERATORS

3.1 INTRODUCTION

In this unit, we consider only pumps (gas sinks) working in the molecular regime, namely when a molecule collides much more frequently with the walls of the vacuum system than with any other molecule.

For typical beam pipes the transition to molecular regime is at about 10^{-3} Torr. Pumps working at higher pressures are mechanical pumps that trap the gas, compress it and expel it from the vacuum system.

- Gas in molecular regime cannot be considered as a fluid and, as a consequence, it cannot be removed by suction because the molecules cannot tranfer energy and momentum amongst them.
- In molecular regime, pumps act on each molecule singularly.

- They can be classified in two big families:

1) Momentum transfer pumps
2) Capture pumps

In the first family, the molecules receive a momentum component pointing toward the pump outlet where the gas is compressed and finally evacuated by pumps working in viscous regime.
In the second one, the molecules are not evacuated; they are "captured" on the walls of the pump where they are bound or borried by other atoms.
These pumps are much more selective than the first ones.

3.2 MOMENTUM TRANSFER PUMPS: MOLECULAR PUMPS

The momentum transfer can be obtained either by impact on surfaces attaining speed close to the mean velocity of molecules or by collision with the molecules of a fluid projected toward the outlet of the pump at supersonic speed ($M \approx 3$ to 8)

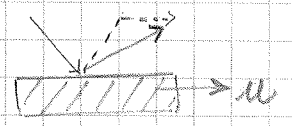

MOLECULAR PUMPS

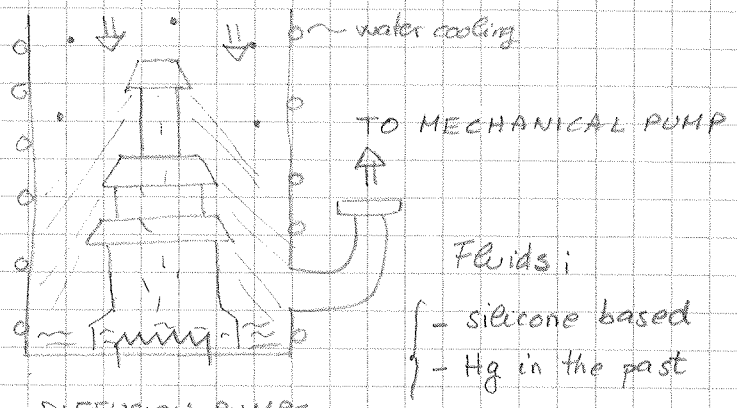

DIFFUSION PUMPS

Diffusion pumps are not anymore used in modern particle accelerators.

Molecular pumps are based on the fact that gas molecules that collide on a surface is adsorbed for a finite time.
On desorption, their velocity distribution is isotropic and corresponds to the wall temperature. If the surface moves with velocity u, then the velocity distribution will be superimposed by the drift velocity $\Rightarrow$ a moving wall produce a gas flow.

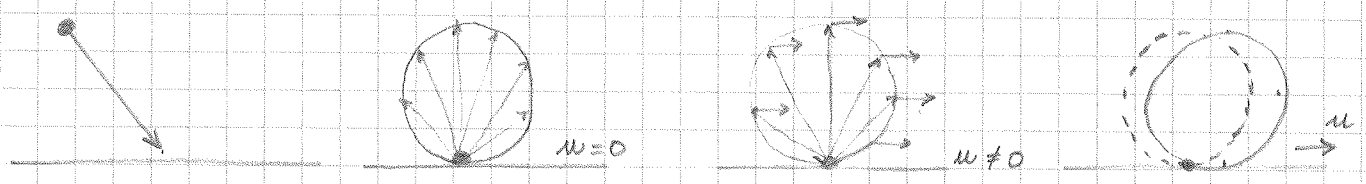

The first molecular pump was invented by W. Gaede. In the original design, the molecules entering from the inlet hit a rotor revolving at high frequency.

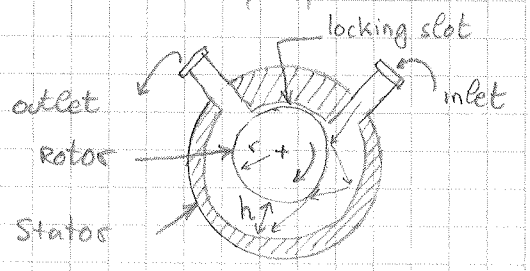

To prevent backstreaming, inlet and outlet must be separated by a very thin slot (locking slot). This aperture is of the order of 1/100 mm.

The two most important characterists of a molecular pump are

- pumping speed $\Rightarrow S = \frac{Q}{P_{IN}}$
- compression ratio = maximum $\frac{P_{OUT}}{P_{IN}} = K_0$

The parameters of pump and gas that determine S and k_0 can be identified with the help of a simple geometrical model.

Consider a plane section of the Gaede pump:

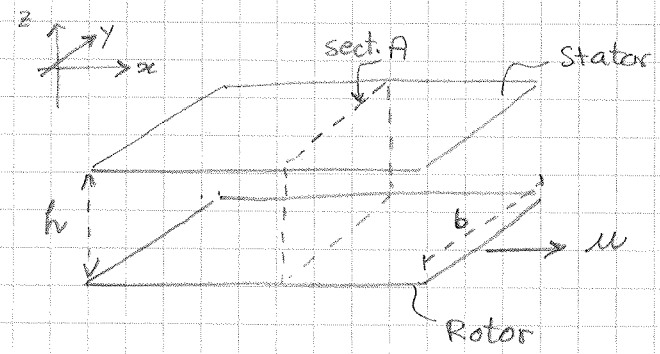

at any point in time half of the molecules has just collided with the rotor and drift in the x direction with velocity u. The other half comes from the stator where the drif component is lost. The flow of molecules toward an imaginary section (A) is:

$$q_N = \frac{1}{2} \cdot \underbrace{n}_{\text{density of molecules}} \cdot \underbrace{u \cdot bh}_{\text{volume of the gas passing through A in one second.}}$$

$$\Rightarrow \underbrace{q_N = \frac{1}{2} \frac{P}{k_B T} \cdot ubh}_{\text{molecule units}} \Rightarrow \underbrace{Q_P = \frac{1}{2} P(ubh)}_{\text{P.V units}}$$

$$\Rightarrow S = \frac{Q_P}{P} = \frac{1}{2} u \cdot (bh)$$

FIRST CONCLUSION: the pumping speed of a molecular pump is proportional to the speed of the rotor and, in the frame of this simple model, does not depend on the nature of the gas.

The gas flow from the entrance toward the exit generates a pressure gradient (higher pressure at exit). This gradient causes a backflow that can be written as:

$$Q_{bf} = -\bar{C} \cdot \frac{dP}{dx}$$

$\bar{C}$ is the conductance of a unit length duct which section is $b \times h$

The net flux is therefore:

$$Q = Q_p - Q_{bf} = \frac{1}{2} P w (bh) - \bar{C} \frac{dP}{dx}$$

When the net flux is zero:

$$\frac{dP}{P} = \frac{1}{2} \frac{w b h}{\bar{C}} dx$$

Integrating between inlet and outlet:

$$\frac{P_{OUT}}{P_{IN}} = \exp\left(\frac{w b h L}{2 \bar{C}}\right)$$

L = length of the duct.

The unit-length conductance of a rectangular duct is

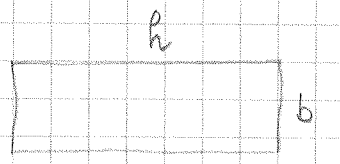

$$\bar{C} = \frac{2}{3} \cdot \frac{v_{th} (b \cdot h)^2}{b + h}$$

for $h << b$

v_{th} = thermal velocity

$$\Rightarrow \frac{P_{OUT}}{P_{IN}} \simeq \exp\left(\frac{6}{8} \cdot \frac{u}{v_{th}} \cdot \frac{L}{h}\right)$$

For zero net flux, the pressure ratio is the maximum; it is called the maximum compression ratio K_0:

$$K_0 \simeq \exp\left(\frac{6}{8} \frac{u}{v_{th}} \cdot \frac{L}{h}\right)$$

To attain high K_0, the revolution speed of the rotor has to be the highest possible, in any case close to the molecular thermal velocity.

In addition, the pumping channel has to be long and narrow.

Because the thermal velocity is:

$$v_{th} \propto \frac{1}{\sqrt{M_t}}$$

$$\Rightarrow \quad K_0 \simeq \exp\left(\alpha \cdot u \cdot \sqrt{M_i} \cdot \frac{L}{h}\right) \qquad \alpha = \text{constant at constant } T$$

SECOND CONCLUSION: The maximum compression ratio depends on the mass of the gas molecule

. The ultimate pressure at the output depends on the characteristic of the mechanical pump (primary pump) $\Rightarrow$ we expect the worst ultimate pressures for H_2 in the vacuum system. (smallest M_i)

3.2.1 Turbomolecular pumps

The development of molecular pumps was hindered by the very small gap between stator and rotor; these pumps had poor reliability and low pumping speed.

In 1957, Becker invented the first turbomolecular pump. It is based on rapidly rotating blades.

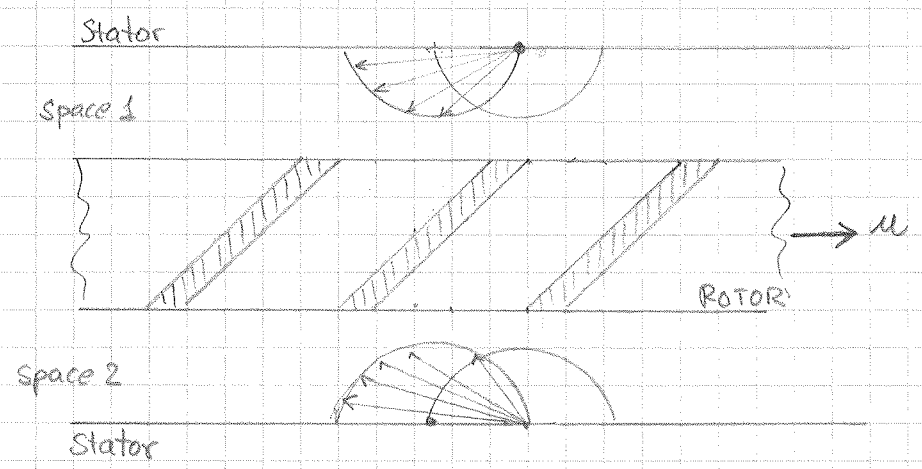

The molecules seen from the blade have a velocity much more oriented toward the blades' channel when they come from space 1. From space 2, most of the molecules hit the blades and are backscattered. Of course this works only if the deformation of the velocity angular distribution is significant, namely if

$$u \approx v_{th}$$

In a real pump, the gas enters through the pump's flange and is compressed by several turbomolecular stages. Any blade series must be followed by a series of static blades (stator).

To increase the compression ratio, the gas compressed by the turbomolecular pump is transported to a classical molecular pump. Finally it is removed by a backing pump

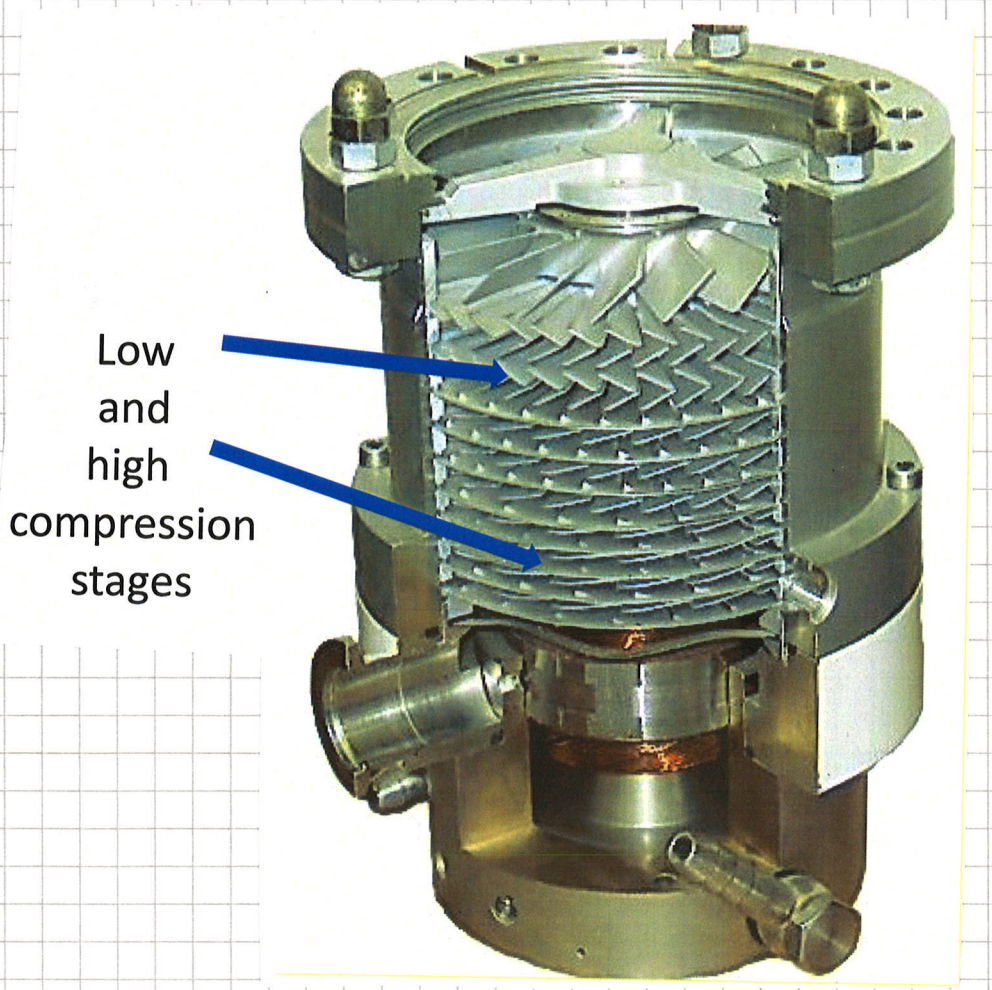

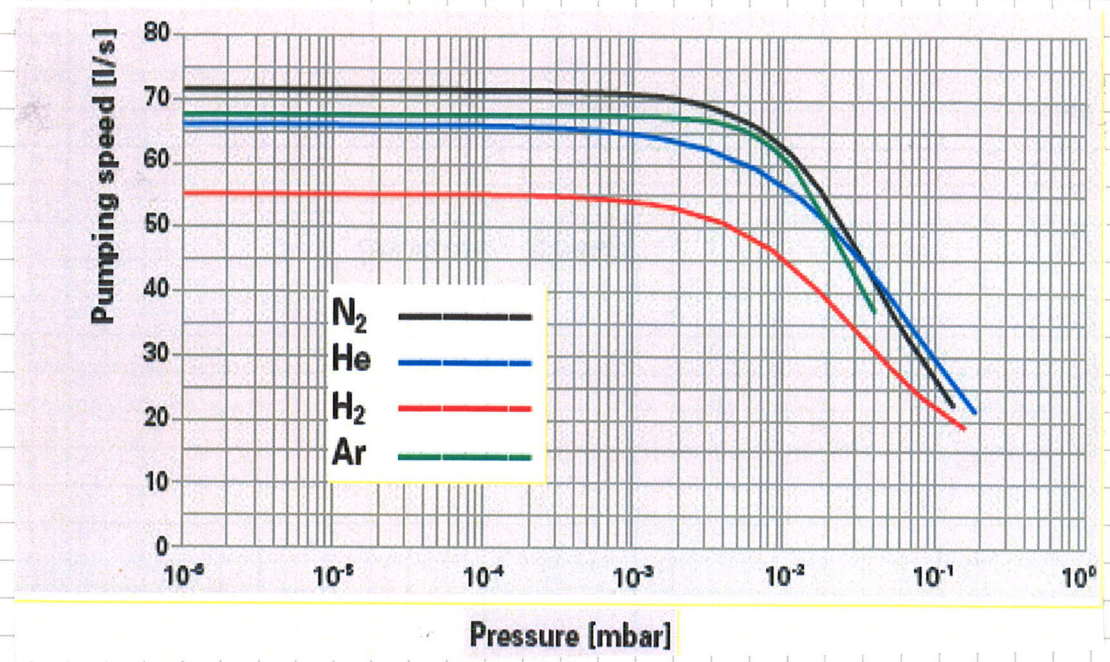

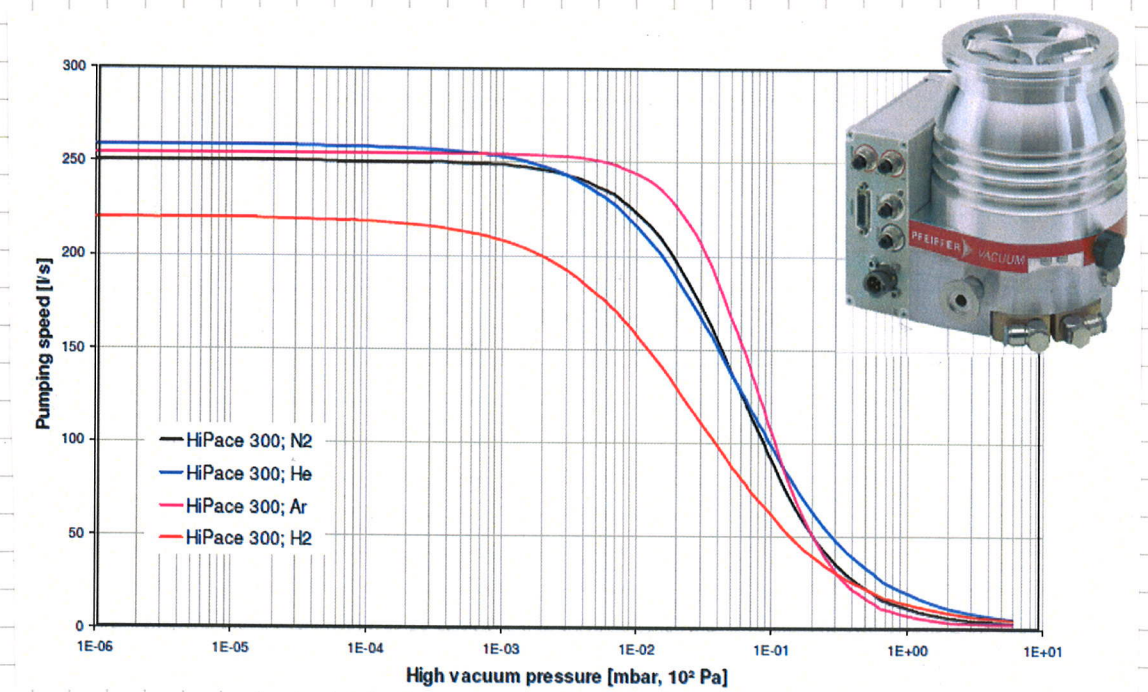

As expected, the mass of the molecule has a small influence on S.

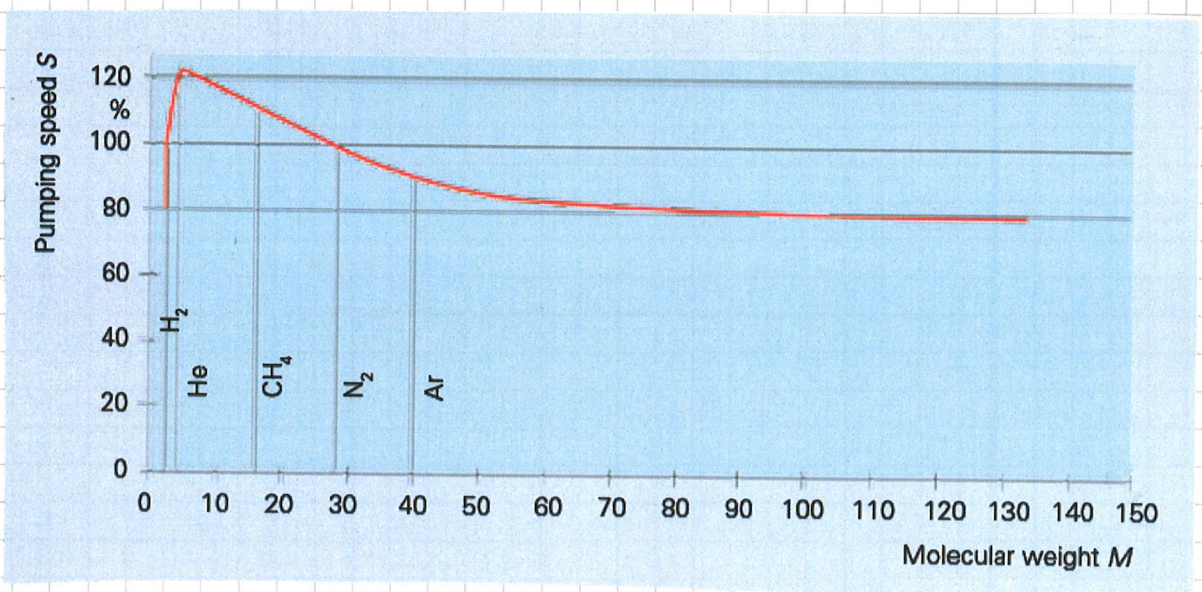

The rotor blades are made of high-strength aluminium alloys. They reach circumferential speeds up to 500 m/s; for 100 mm diameter pump this implies a rotation frequency of roughly 1 kHz.

The pumping speed range of turbomolecular pumps varies from 10 to 3000 l/s.
The pumping speed is constant in the molecular regime ($P < 10^{-3}$ Torr).

As expected the lowest compression ratio is the one for H_2; in classical design it was limited to 10^3. Nowadays values up to 10^6 can be obtained.

In general, turbomolecular pumps and backing pumps are assembled in pump units which include power supplies and instrumentation.

In particle accelerators, they are largely used to evacuate beam pipes to pressures at which capture pumps can safely work. In some specific cases, when high flux of gas must be removed, the turbo pumps the vacuum system continuously. This is the case of H^+, H^- or ion sources.

The lowest pressure that can be attained by turbomolecular pumps is in the order of 10^{-11} Torr (baked and all-metal systems).

MAIN ADVANTAGES:
- constant pumping speed in large range of pressure.
- no memory effect nor selectivity.
- start working at relatively high pressure.

MAIN DISADVANTAGES:
- mechanical fragility.
- intrinsic limitation in ultimate pressure
- risk of venting the system in case of damage

- relatively high cost per given l/s
(including backing pump and maintenance)

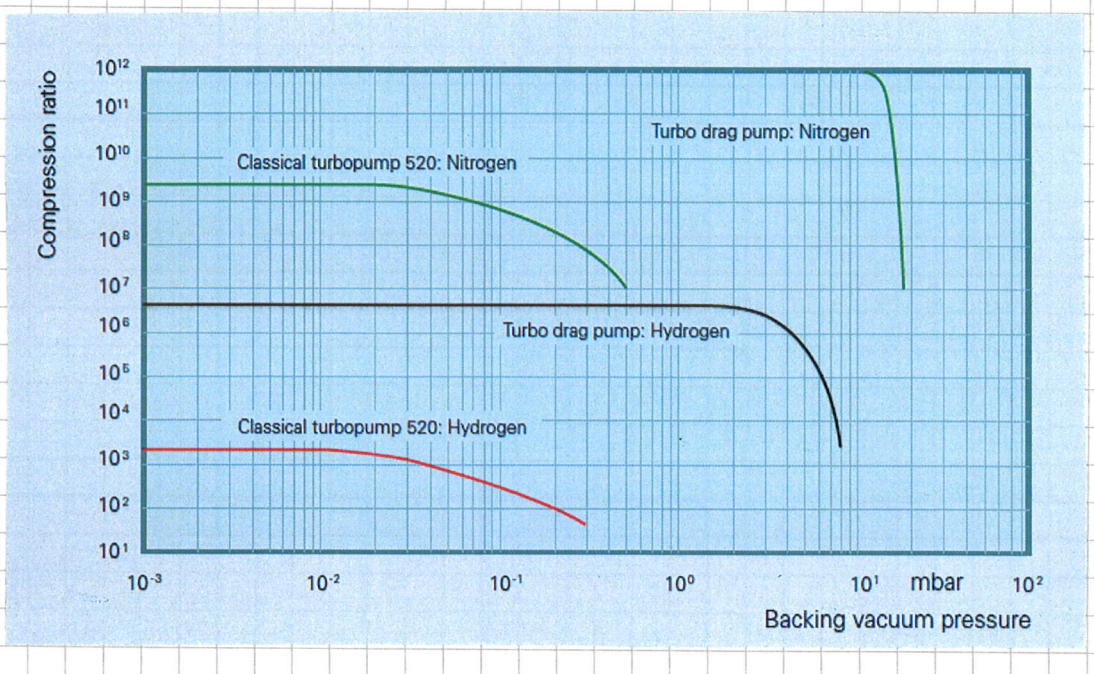

3.3 CAPTURE PUMPS

As already written, capture pumps remove gas molecules by fixing them to a surface.

The sorption mechanism is based either on chemical bonding on reacting surfaces or physisorption on cooled walls. Both mechanisms results in a long mean sojourn time τ_s :

physisorption $E_a \leq 0.4$ eV/molec.
chemisorption $E_a > 0.4$ eV/molec.

$$\tau_s = \tau_0 \cdot e^{E_a / k_B \cdot T} \qquad \tau_0 \approx 10^{-13} \text{ s}$$

Energy [eV/molecule]		τ_s 300 K [s]	τ_s 4.3 K [s]
He physisorption	4×10^{-3}	$\sim 10^{-13}$	$5 \cdot 10^{-9}$
H_2 physisorption	6.5×10^{-2}	$\sim 10^{-12}$	10^{63}
Ar, CO, N_2, CO_2 phisis.	0,15	$\sim 10^{-11}$	∞
H_2 chemisorption	0,87	100	
CO chemisorption on Ni	1,3	$\sim 10^{9}$ (100y)	
O chemisorption on W	6,5	> age of universe	

definition
- pumping by low T → cryopumps
- pumping by high E_a → chemical pumps → getter pumps

Another family of capture pumps associates chemical pumping with physical burying by reactive metal atoms. These pumps are named sputter ion pumps. They are the most important pumps in particle accelerators.

3.3.1 Sputter-ion pumps (SIP)

In sputter ion pumps the residual gas is ionized in a Penning cell.
The ions are accelerated toward a cathode made of a reactive metal.
The collision generates sputtering of the reactive metal atoms that are deposited on the nearby surfaces.
The deposited atoms adsorb gas molecules that are then covered by other metal atoms.
In general the reactive metal is Ti.

Schematically a SIP consist of two electrodes (anode and cathode) and a permanent magnet.

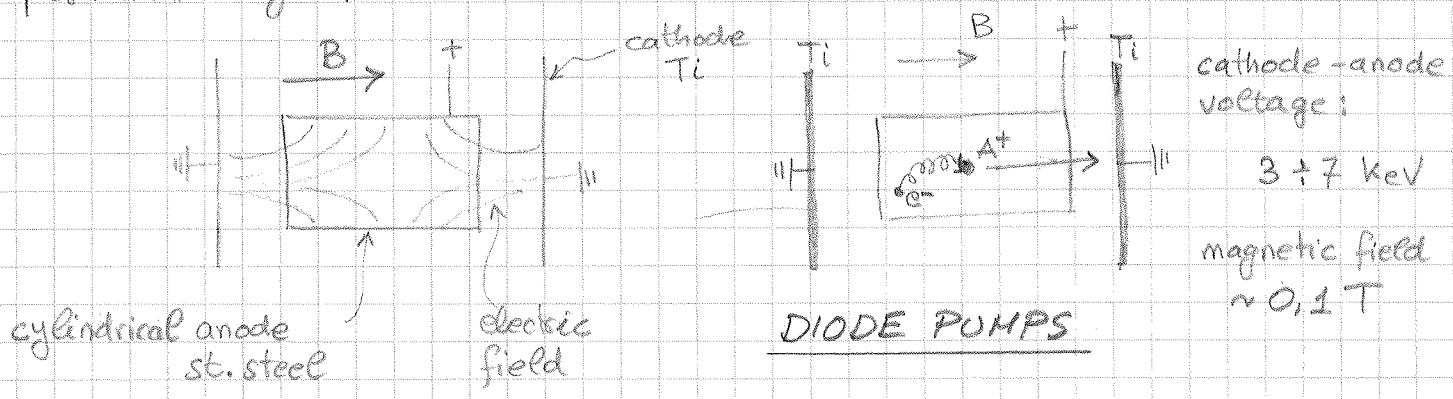

DIODE PUMPS

The anode is an open cylinder and the magnetic field is parallel to the cylinder axis.
In this configuration, the crossed electrical and magnetic field trap electrons in long helical trajectories resulting in an increased probability of gas ionization.
The created ions are accelerated to the cathode.
The ions collide on the Ti cathode and they:

- sputter Ti atoms on the nearby surface (mainly anode)
- can be implanted in the cathode
- can rebound as a neutral and be implanted in the

Ti film.

- The Ti film reacts with most of the gas species and definitely remove them from the gas phase.

- Noble gases can be pumped only by implantation in the cathode or in the Ti film.
  In the cathode the pumping is reversible because, soon or later, the progressive erosion frees the implanted atom.
  In the Ti film, the pumping is permanent because the implanted atoms are covered by additional Ti atoms.

  In addition H_2 can also be pumped by dissolution into the cathode once the native oxide layer covering the Ti sheets is removed by sputtering.

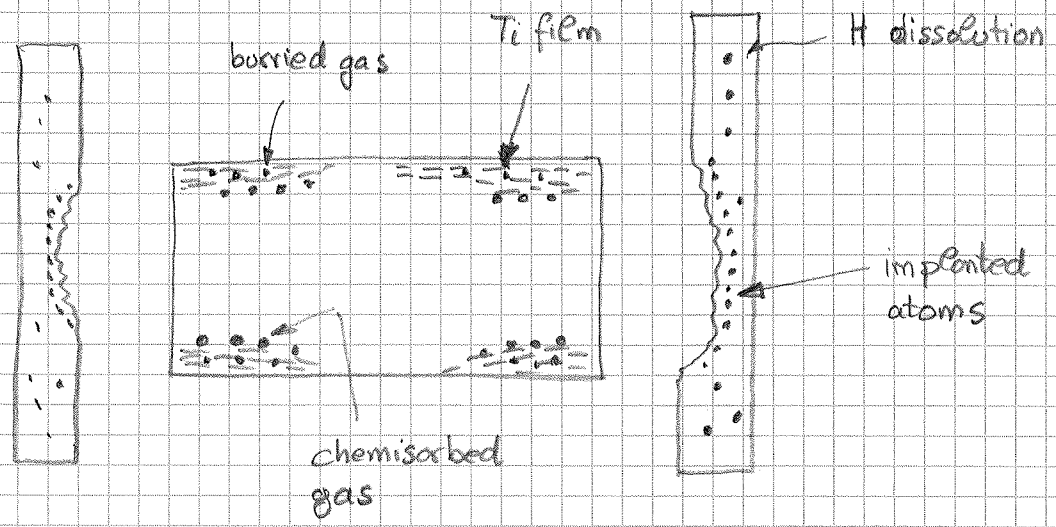

An excessive quantity of noble gas implanted in the cathode can produce pressure instabilities. In fact, the continuous erosion can extract noble gas implanted; as a result the pressure increases and the erosion is accelerated. The feedback is positive; a pressure spike is producede. The pressure rise terminate when most of the noble gas is implanted again but in a deeper zone. A new pressure spike appears when the erosion reaches the new noble atoms' front.

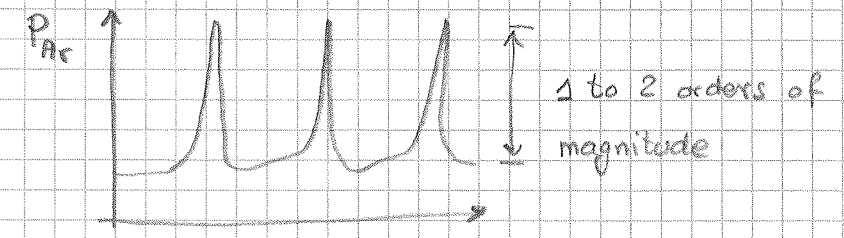

To increase the pumping efficiency for noble gases, the number of ions implanted in the cathode has to be reduced while increasing the rebouncing neutralized atoms and their probability to be buried by Ti on the anode.

Two different approches:

1) change material.

2) change geometry of the penning cell.

In the first case Ta is used instead of Ti for the cathode. Ta atoms are much heavier (Ta = 181 amu, Ti = 48 amu). Gas ions, once reneutralized, rebounce at higher energy when colliding with Ta and, as a consequence, have a much higher probability to be implanted into the anode. The quantity of gas implanted in the cathode is reduced because most of the gas ions rebound. This kind of pump is called "noble diode" or "differential ion pumps".

In the second case, a new arrangement is chosen based on 3 "electrodes". This pump is called "triode pump"

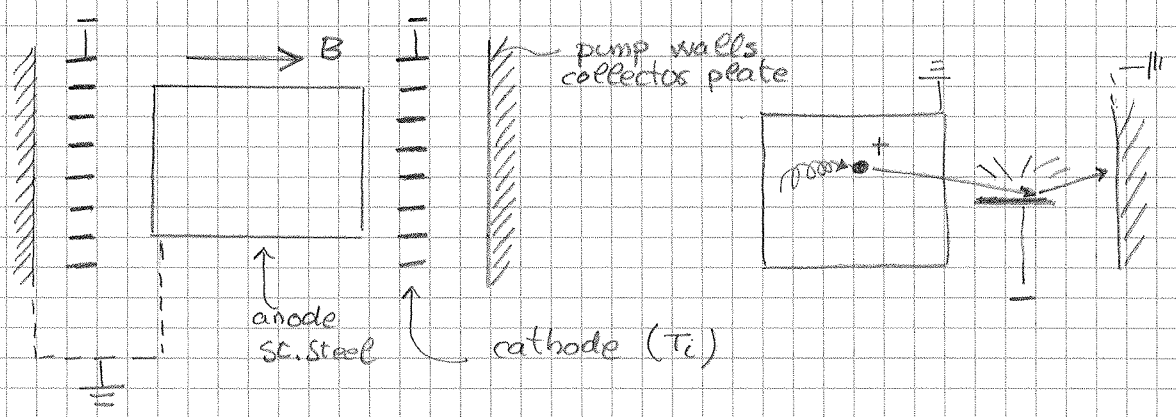

In this pumps, the cathode consists of a series of small Ti plates aligned along the cell axis. In this configuration the collisions ion-cathode are at glancing angle.

The glancing angle collisions increase the sputtering rate → more Ti on the collector plate and anode. In addition, the ions have higher probability of neutralization and rebounce at higher energy → more efficient implantation in the collector plate.

An improved triode pump is the StarCell (produced by Agilent Vacuum).

In commercial pumps, many penning cell are assembled to form honeycomb structures.

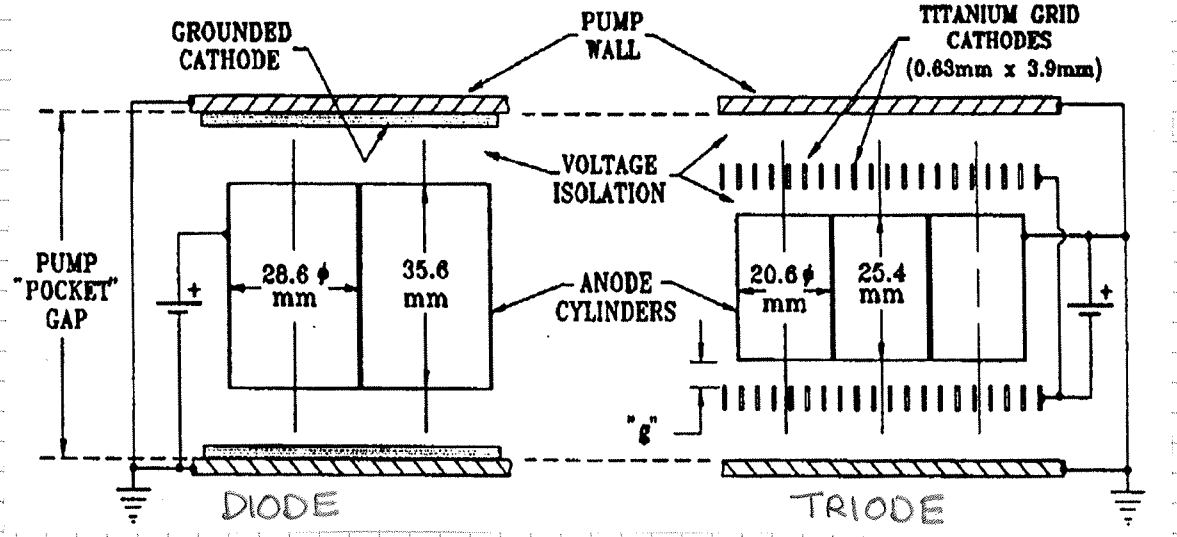

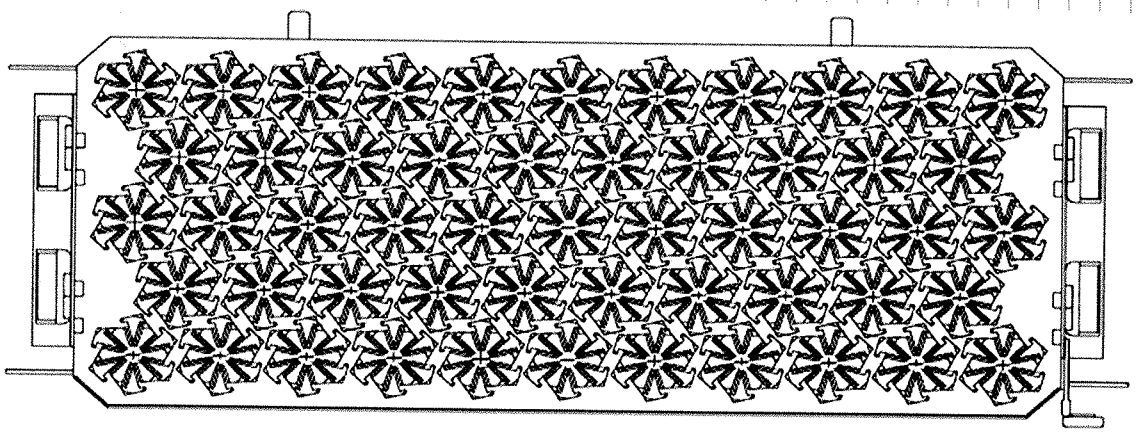

STAR CELL ION PUMP DESIGN

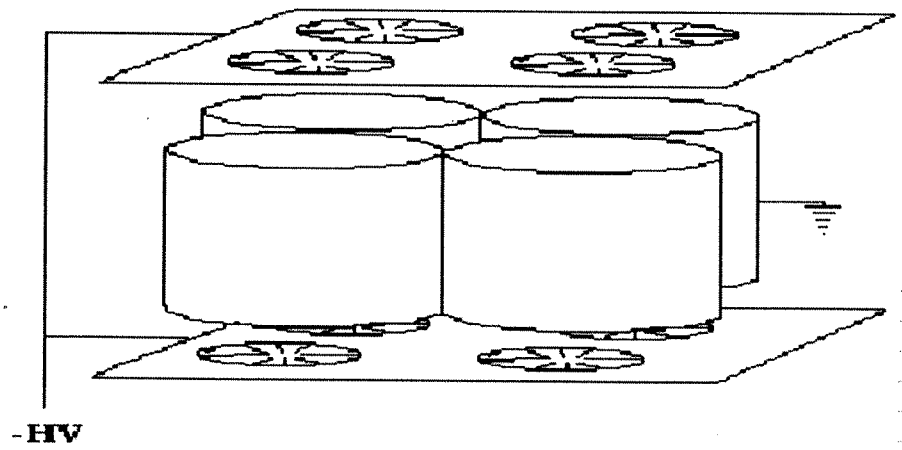

PRESSURE VERSUS PENNING DISCHARGE CURRENT

The discharge current of the penning cells is proportionate to gas pressure for $P < 10^{-4}$ Torr. In the lower pressure range, pressure lower than 10^{-9} Torr cannot be measured by standard power supplies because of leak current (field emission).

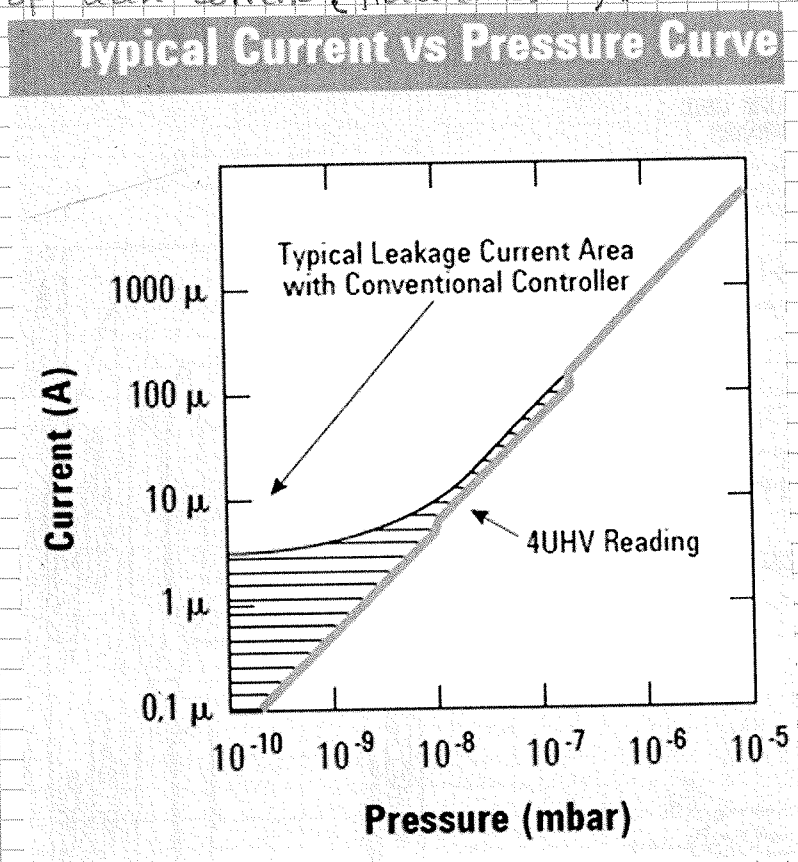

Ion pumps are extensively used in particle accelerators for the measurement of pressures.

PUMPING SPEEDS

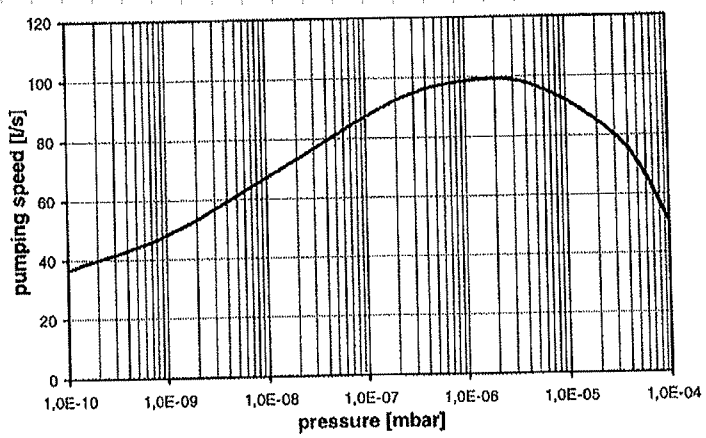

Fig. 5 Pumping speed vs pressure for a standard diode with S_N = 100 l/s (for air after saturation).

Pumping speed for ion pumps depends on

- the pressure at the inlet;
- the nature of the gas

DN	S [l s^{-1}]
63	50
100	70/125
150	240/500

pumping speed for N_2 nominal (starcell) →

- The pumping speed in general reaches a smooth maximum at about 10^{-6} Torr. This is due to the fact that at lower pressure there are less ionizations, so a lower number of electron to maintain the discharge.

- The gas molecules that are chemisorbed by Ti have high pumping speed. The noble gases have lower pumping speed.

GAS	DIODE PUMPS	TRIODE PUMPS
AIR	1	1
N_2	1	1
O_2	1	1
H_2	1,5-2	1,5-2
CO	0,9	0,9
CO_2	0,9	0,9
H_2O	0,8	0,8
CH_4	0,6-1	0,6-1
Ar	0,03	0,25
He	0,1	0,3

normalized to S for air

Typical nominal pumping speed for air varies from a few l/s to ~ 1000 l/s.

DISTRIBUTED ION PUMPS

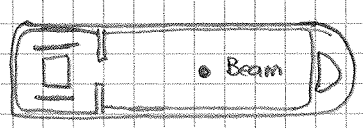

Ion pumps can also be distributed along the beampipe of accelerators. The magnetic field is provided by the dipole magnets that steer the beam.

The development of this pump was hindered by the B field limitation during beam injection and also by the introduction of getter ribbon and films.

3.3.2 Getter pumps

Some definitions:

a) sticking probability: $\alpha = \dfrac{\text{nr of molecules captured by a surface}}{\text{nr of molecules impinging on a surface}}$

= probability of pumping for a molecule.

$$0 \leq \alpha \leq 1$$

For $\alpha = 1$, all impinging molecules are pumped

$$\Rightarrow \quad q_p = \frac{1}{4} n v_{th} = \frac{1}{4} \cdot \frac{p}{k_B T} \cdot v_{th} \Rightarrow \frac{q_p}{p} = \frac{1}{4} \frac{v_{th}}{k_B T}$$

in pressure-volume units $S = \dfrac{Q_p}{p} = \dfrac{1}{4} v_{th}$ (conductance of unit area)

$\Rightarrow \alpha = 1 \quad S_{H_2} \cong 44 \ \ell/s \quad S_{N_2} \cong 11{,}7 \ \ell/s \quad S_{H_2O} = 14{,}7 \ \ell/s$

b) monolayer coverage:

the quantity of gas needed to cover the unit area (depends on roughness and porosity); for "technical" surface:

$$N_{ML} \cong 10^{15} \text{ molecules} = \frac{10^{15}}{3{,}3 \times 10^{19}} = 3 \times 10^{-5} \text{ Torr} \cdot \ell$$

c) monolayer formation time:

for $\alpha = 1$ and a smooth surface, for N_2:

$$t_{sat} = 10^6 \cdot p \ [s]$$

For 10^{-6} Torr $\rightarrow$ 1 s is needed to cover a surface.

Getter surface adsorb most of the gas molecules present in vacuum system. They react with the gas and form stable chemical elements.

This is possible only if their surface is clean, free of contamination and native oxide layer. The metal atoms have to be free to exchange electrons with the gas molecules.

Depending on how the clean, metallic, surface is produced two family of getters can be defined:

1. evaporable getters: the active surface is generated by sublimation of a metal in-situ.

2. non-evaporable getters (NEG): the active surface is produce by dissolving the surface contamination into the getter bulk by heating in vacuum. The dissolution process is called "ACTIVATION".

3.3.2.1 EVAPORABLE GETTERS (SUBLIMATION PUMPS)

For particle accelerators, Ti is the metal of choice.
Ti alloy rods are heated up to 1500°C, therefore attaining a Ti vapour pressure of about 10^{-3} Torr.

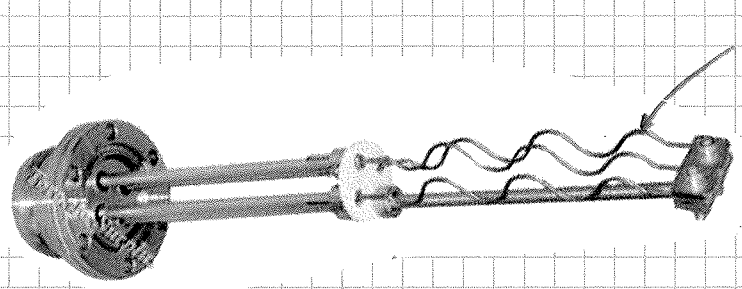

The material of the rods is not pure Ti because otherwise cross-section of lower dimensions would result in higher temperature, higher sublimation, faster diameter reduction and finaly melting.
In case of Ti-Mo, the Ti sublimation increases the concentration of Mo which reduces the sublimation rate of Ti and melting point.

In commercial rods: Ti-Mo(15%).

Sticking probabilities α for Ti sublimated at 300°C are:

H_2 : $1-5 \times 10^{-2}$
CO : 0,4 - 0,8

α depends on the quantity of gas already pumped: $S = S(Q)$. The molecules already adsorbed block adsorption sites. The S reaches negligible values when Q approches a saturation values that depends on the gas nature.
For CO: $Q_{SAT} \simeq N_{ML}$; for O_2: $Q_{SAT} \simeq 5 \div 10\, N_{ML}$; for N_2: $Q_{SAT} \simeq N_{ML}/(3 \div 6)$

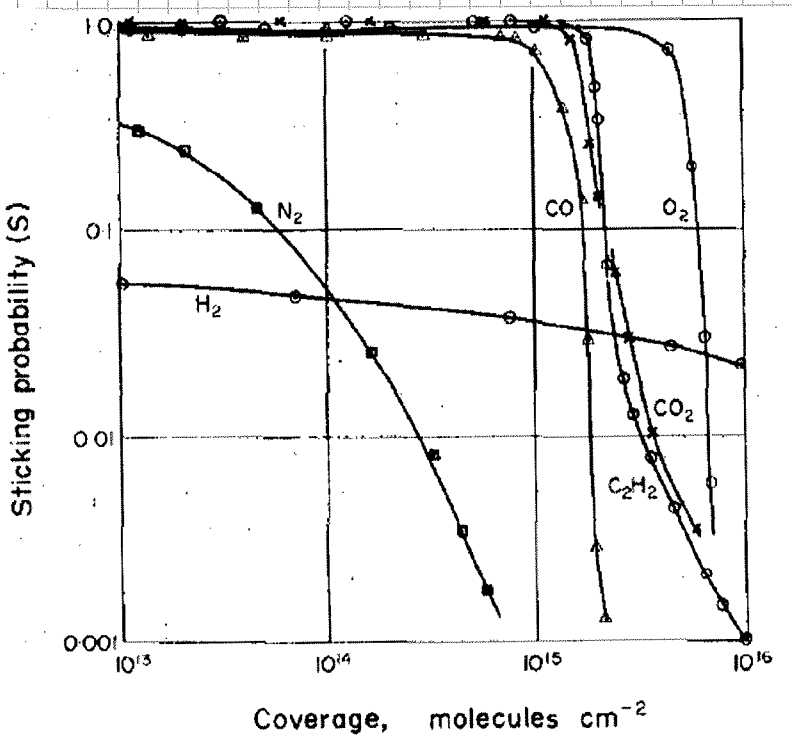

Figure 4. Room temperature sorption characteristics for pure gases on batch evaporated clean titanium films.

When Ti is sublimated on a surface at 77 K, the Q_{SAT} increases → the roughness of the film is higher.

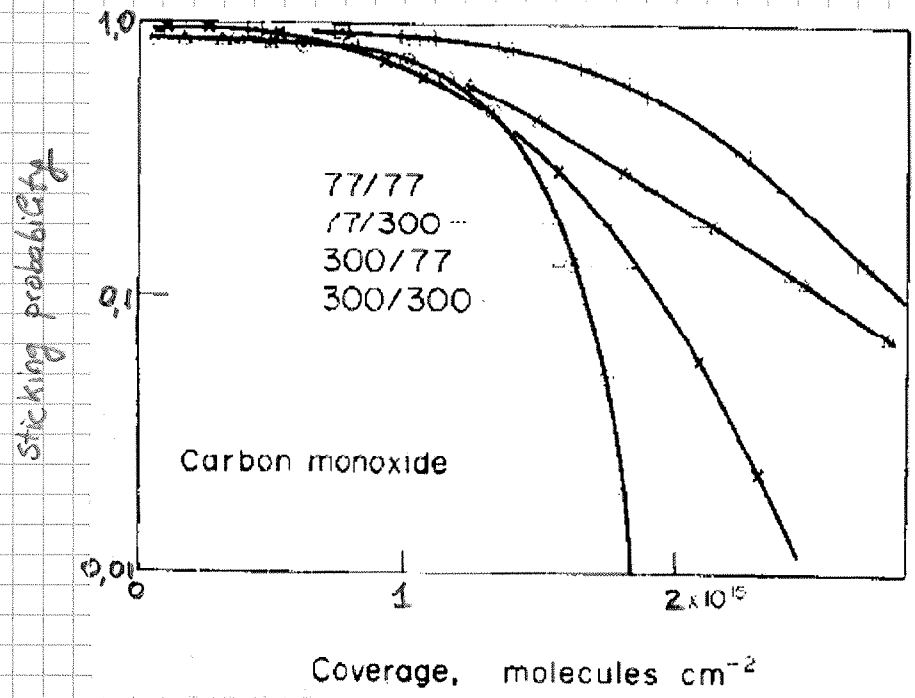

The experimental curves $S = S(Q)$ indicate that at room temperature all gases adsorbed on Ti remain on the surface. The only exception is H_2: this gas, after molecular dissociation, diffuses in the Ti film. As a result the quantity of gas already pumped has a limited effect on the pumping speed.

When the surface is saturated, the pumping capacity can be restored by additional sublimations.

This pump does not adsorb rare gases and CH_4 at room temperature. As a consequence, it is always coupled with other kind of pumps, in general with sputter ion pumps.

Ti sublimation pumps do not have intrinsic pressure limitations. One of the lowest ever measured pressures at room temperature was produced by Ti subl. pumps + sputter ion pumps ($\sim 2\times10^{-14}$ Torr).

With this pump, distributed pumping is unfeasible along beam pipes.

3.3.2.2 NEG pumps

NEG materials are produced in industry by powder technology. Small grains of very reactive metals are sintered to form pellets, discs or plates. In addition, the grain can be pressed onto a metallic substrate to form ribbons.

These pumps are based on the exception high oxygen solubility limit of the element of the 4th group:

Sc	Ti	V
Y	Zr	Nb
La	Hf	Ta
1-4%	20÷30%	1-2%

O solubility limit at RT in the 3rd, 4th, 5th groups

O solubility limit ⇒ in a oxygen-metal system, it is the concentration of oxygen in the solid solution in equilibrium with the oxide. It depends on temperature.

Zr is in general the metal of choice.

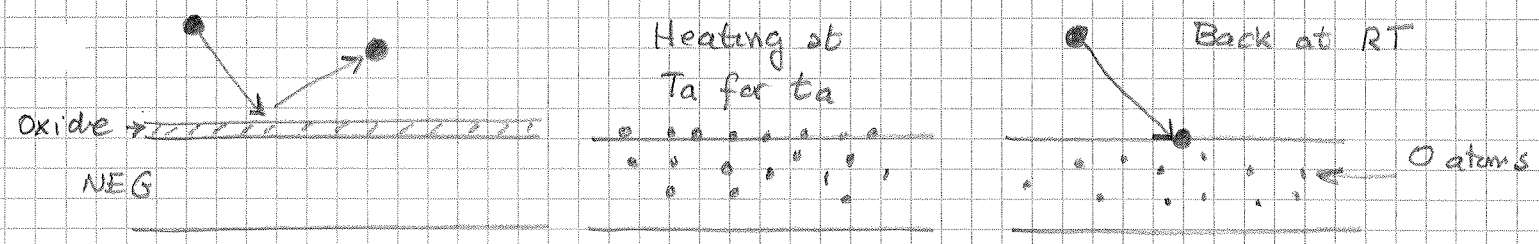

To reduce the activation temperature, other elements are added to increase the O diffusivity ⇒ faster O dissolution.

A typical alloy is St 707 (produced by SAES Getters, Milan, I)

St 707:
- Zr 70% wt. ← high solubility
- V 24,6% wt. ← increase diffusivity
- Fe 5,4% wt. ← reduce pyrophoricity

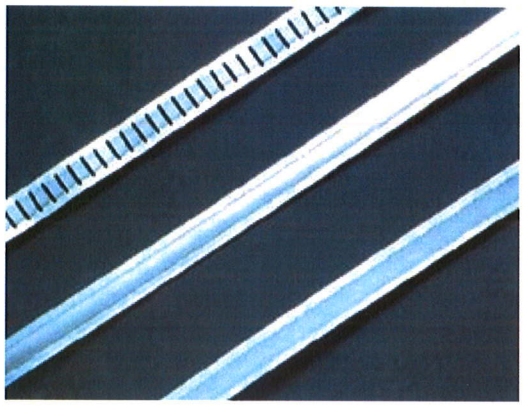

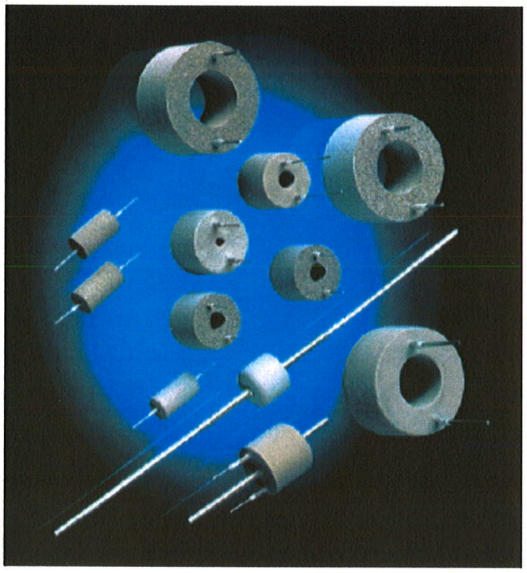

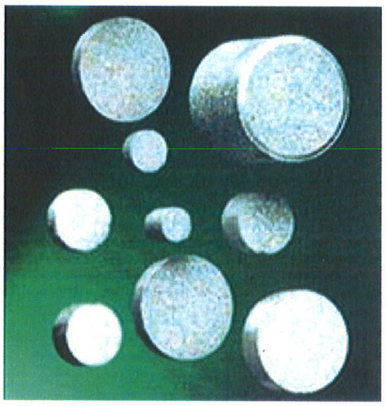

Typical activation temperatures: 400°C x 45' min / 300°C x 24 h

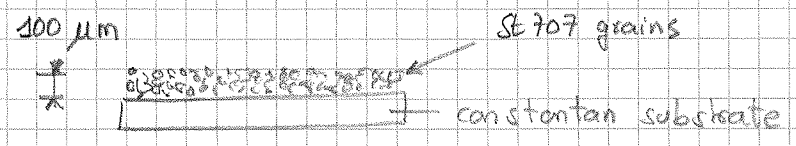

If compared to Ti sublimation pumps, NEG pumps present the risk of powder peel-off due to excessive heating or H_2 embrittlement (excessive hydride formation). However NEG may provide distributed pumping in beam pipes. In the LEP, NEG ribbons provided more than 90% of the pumping speed. The alloy was Zr-Al (St 101) activated at 750°(45')

LEP vacuum chamber cross section

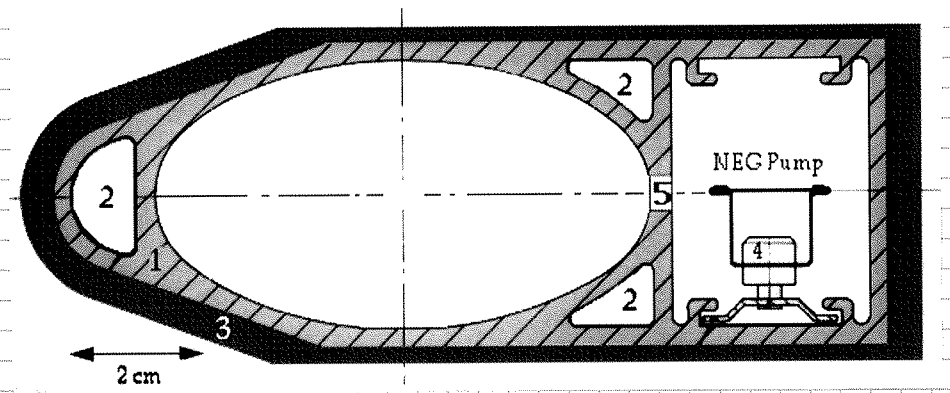

The pumping speeds for St 707 are shown in the next figures.

The general behaviour is the following:

- NEGs do not pump CH_4 + noble gases
- At room temperature, the adsorbed gas molecules progressively saturate the surface and reduce the pumping speed, except for H_2 that is dissolved in the NEG bulk
- CO inhibits the pumping of other gases
- N_2 has a small surface blocking for the other gases
- H_2 does not block the adsorption of the other gases

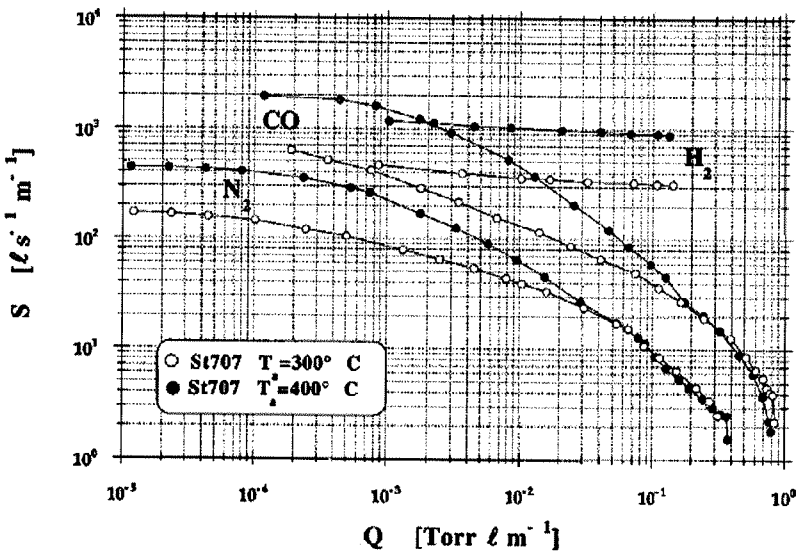

FIG. 1. Pumping speed of the St707 NEG after 45 min activation at 300 and 400 °C as a function of the pumped quantities of CO, N_2, and H_2.

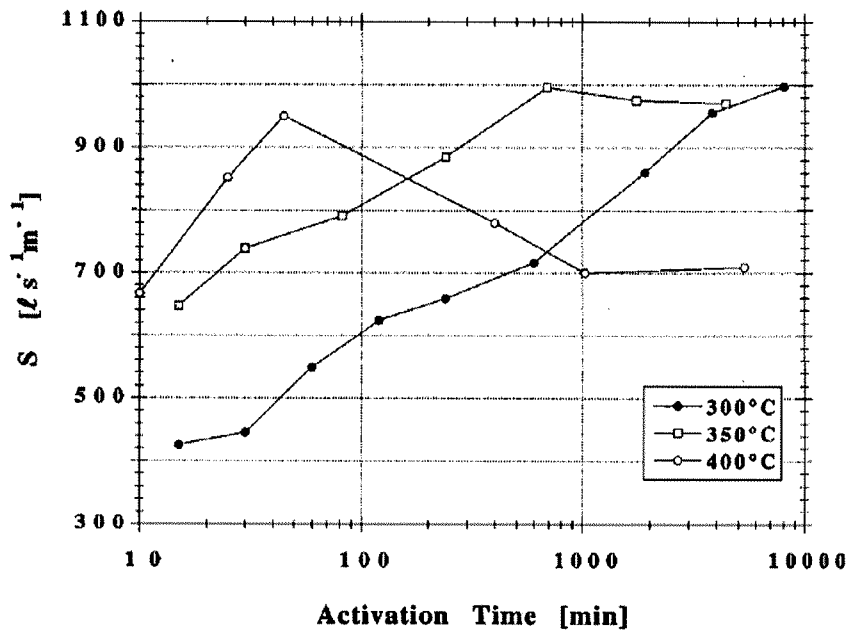

FIG. 7. Variation of the initial pumping speed for H_2 of a St707 NEG as a function of the heating time and for various heating temperatures.

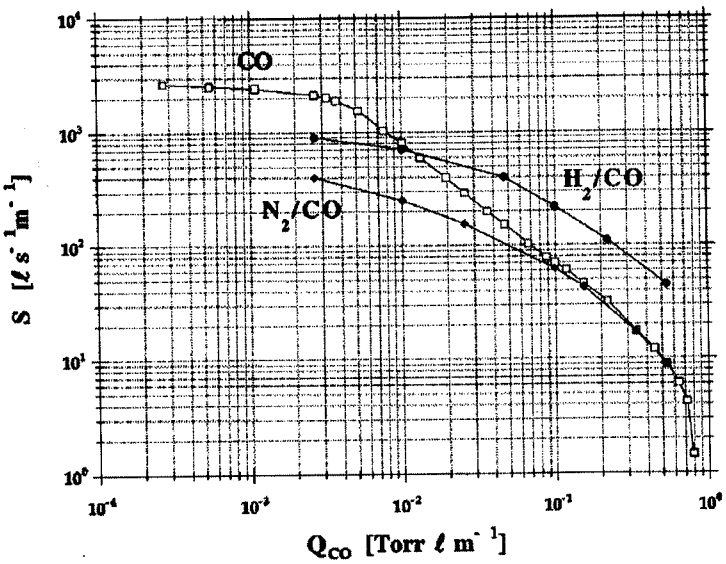

FIG. 8. Variation of the measured pumping speed for H_2, N_2, and CO as a function of the adsorbed quantity of CO.

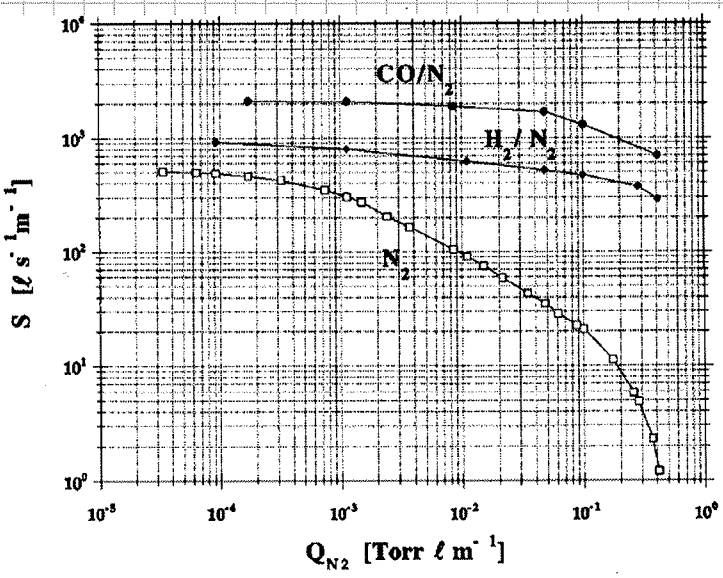

FIG. 9. Variation of the measured pumping speed for H_2, N_2, and CO as a function of the adsorbed quantity of N_2.

All gases are pumped irreversibly, except for H_2.
This gas can enter and exit from the NEG material at a rate that depends on temperature and hydrogen concentration. An equilibrium condition is attained. The H_2 equilibrium pressure is also called dissociation pressure.

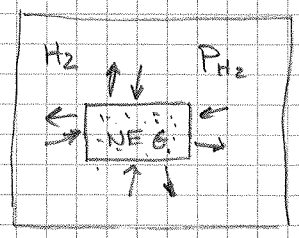

$$H_2 + Me \rightleftarrows 2H \text{ (in metal)} + Me$$

$$K_{eq} \propto \frac{P_{H_2}}{C_H^2} \longrightarrow P_{H_2} = \tilde{K} \cdot C_H^2$$

$$\tilde{K} = \tilde{K}_0 \, e^{-E_s/RT}$$

$$\longrightarrow \lg P_{H_2} = \lg \tilde{K}_0 - \frac{E_s}{RT} + 2 \lg C_H$$

For St 707:

$$\lg P_{H_2} = 5{,}14 - \frac{6250}{T} + 2 \lg C_H$$

P [mbar] C_H [mbar l/g]
T [K]

The H_2 equilibrium pressure increases when increasing T. If a NEG has been charged with H_2, it can always come back to the initial condition by stopping the external gas load, increasing the temperature to accelerate hydrogen desorption and then cooling down to room temperature.

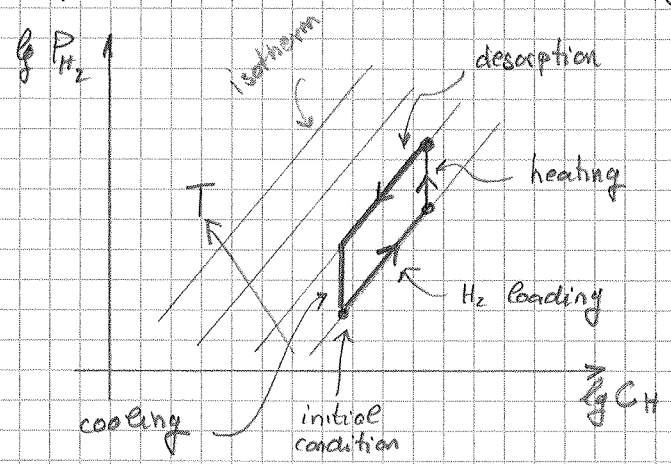

The inner walls of a vacuum pipe can be covered by NEG St 707 ribbon, activated during the bakeout at a temperature $T \geq 300°C$.
Very low pressures are achieved coupling the NEG with sputter ion pumps for the pumping of CH_4 and rare gases.

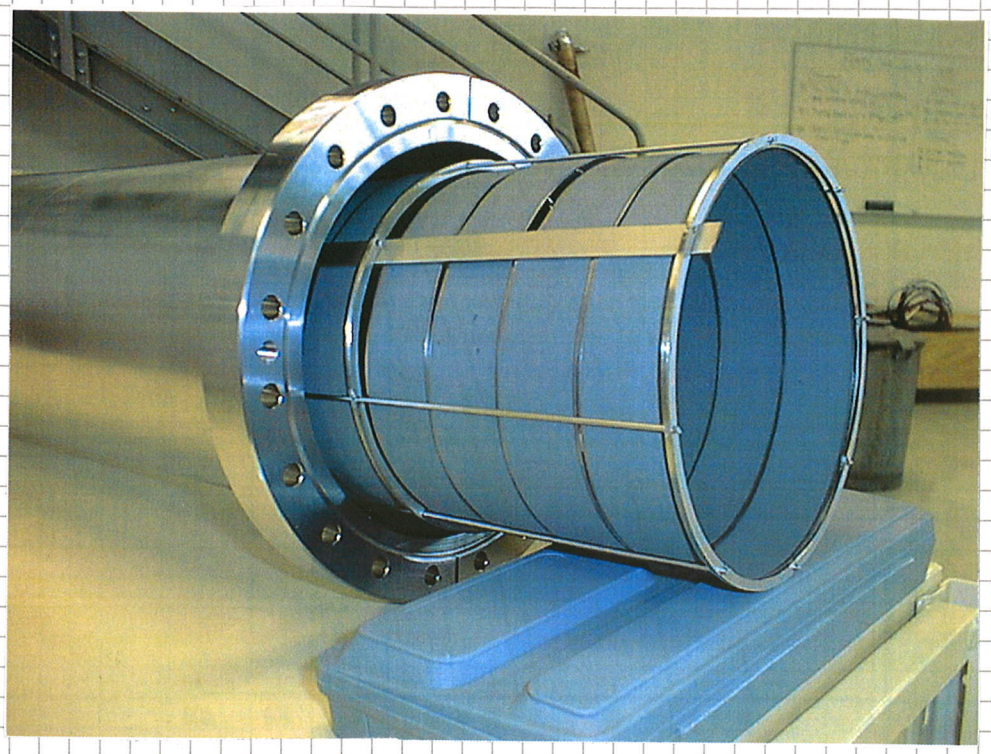

PUMP EVOLUTION

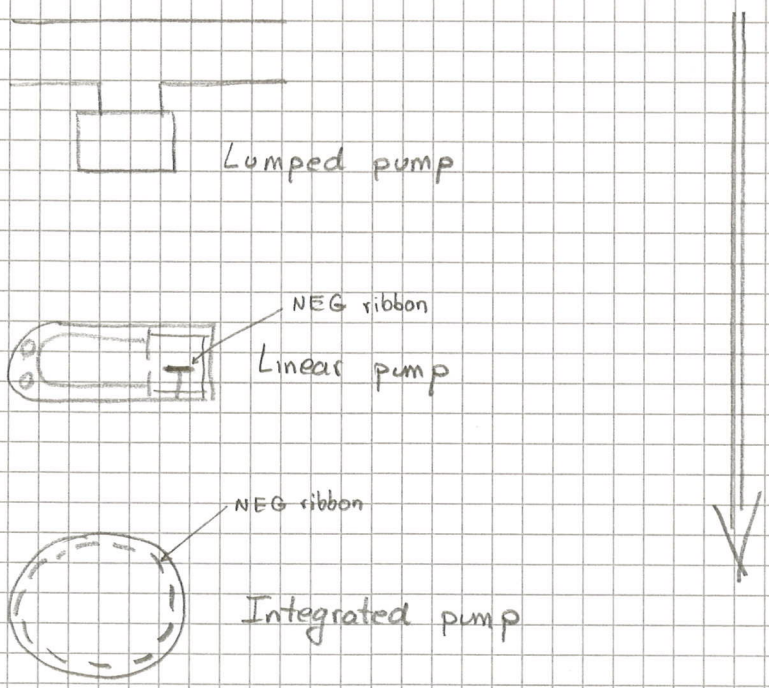

The pump has moved closer to the gas source.

NEXT STEP ⟹ COATING THE WALLS OF THE BEAM PIPE BY NEG THIN FILMS.

(see ppt presentation)

... where the NEG film was born in 1996!

NEG thin film coatings

Paolo Chiggiato

How a pumping vacuum chamber can be obtained:

...by sputter coating its inner wall with a non-evaporable getter film before the installation in the accelerator.

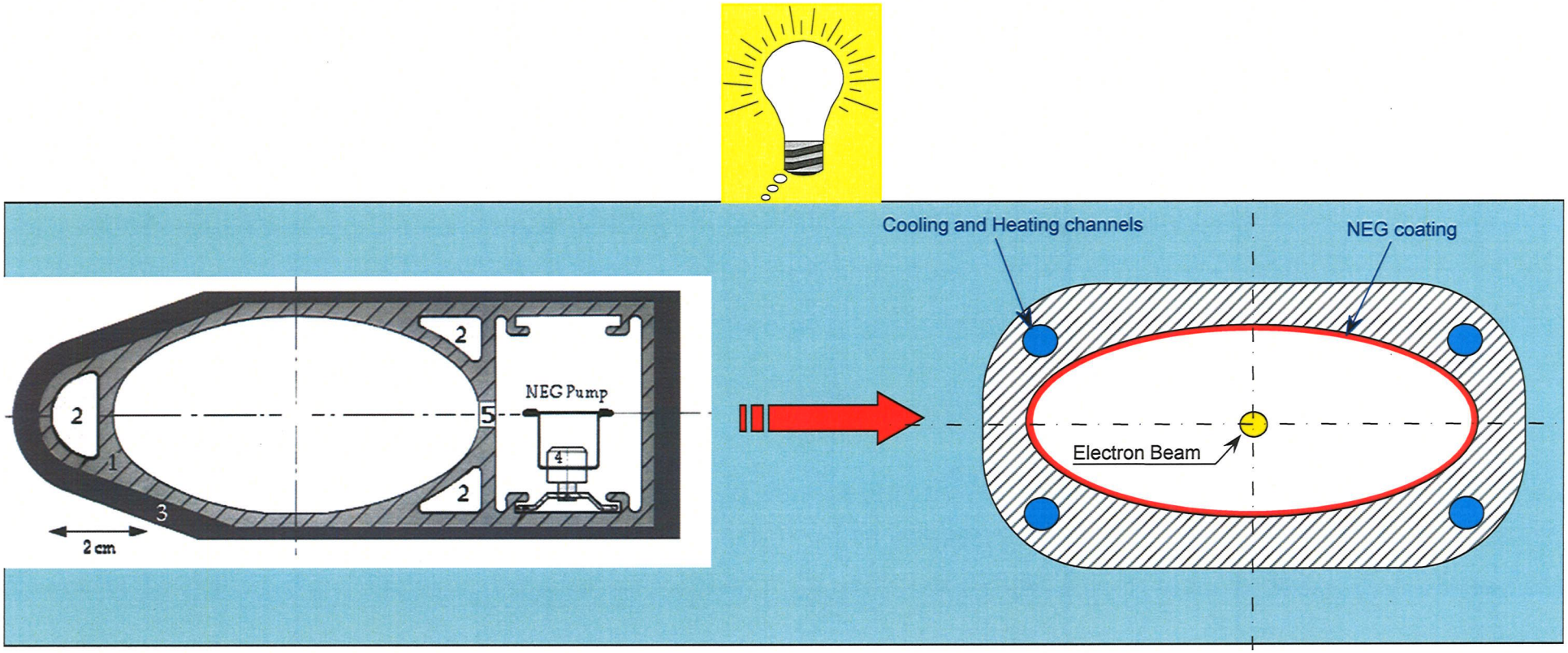

Getters are materials capable of chemically adsorbing gas molecules. To do so they need to be activated

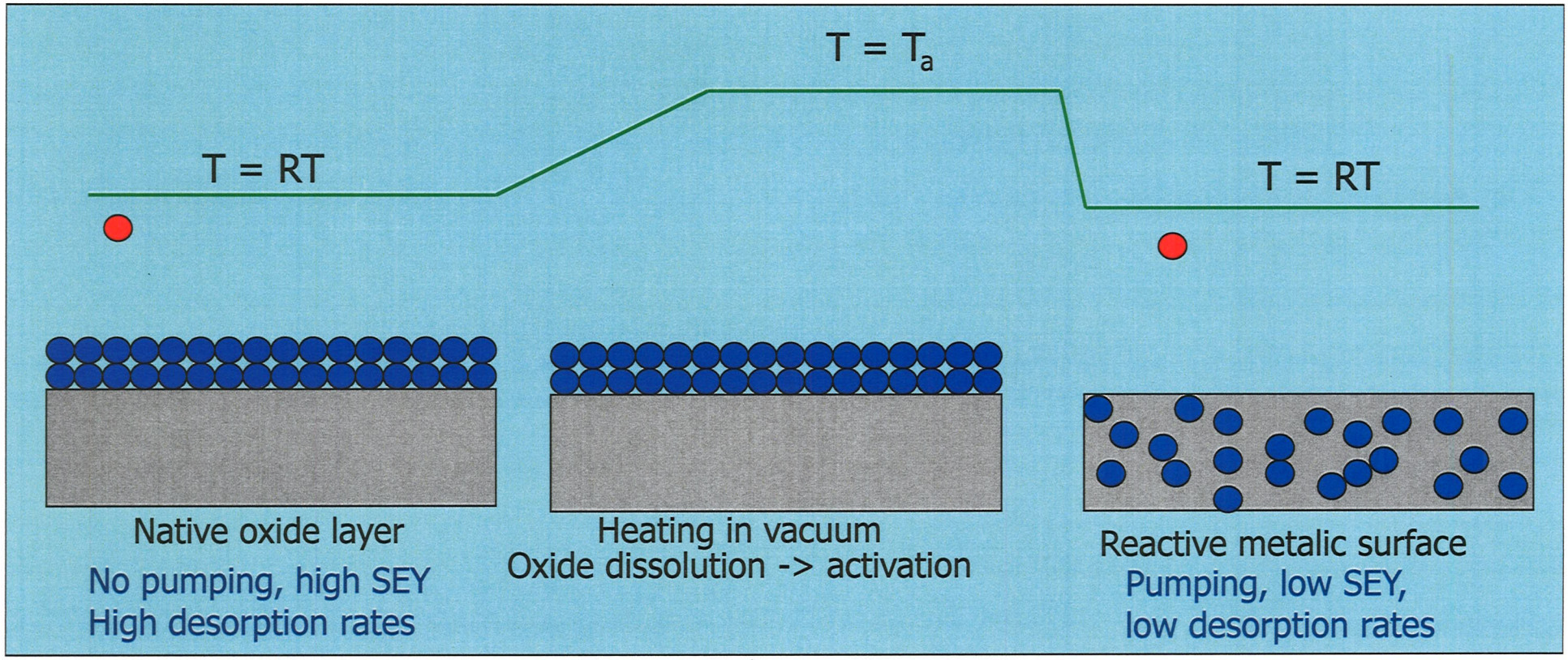

NEGs pump most of the gas except rare gases and methane at room temperature

The activation temperature has to be compatible with the substrate materials:

St. steel < 400 °C

Copper alloys < 250°C

Aluminum alloys < 200 °C

Lowest activation temperature obtained by sputtering Ti-Zr-V alloys:

180 °C

(24 hours heating in vacuum)

in a large range of composition in the Ti-Zr-V system

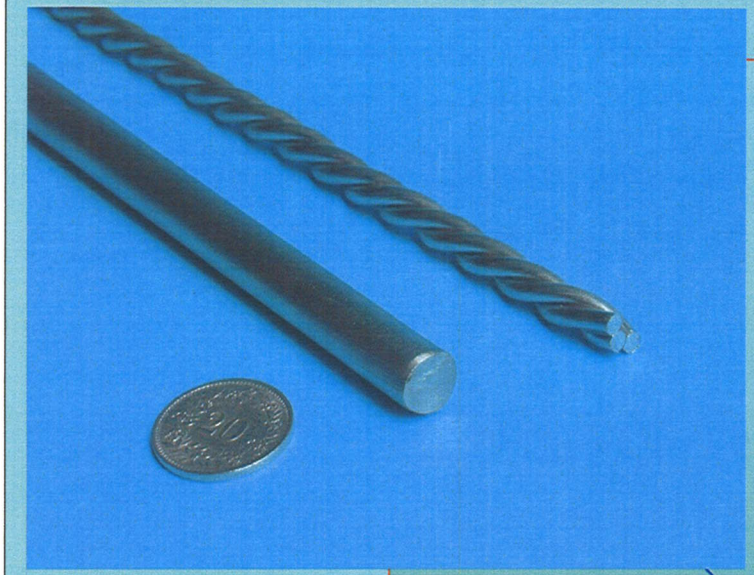

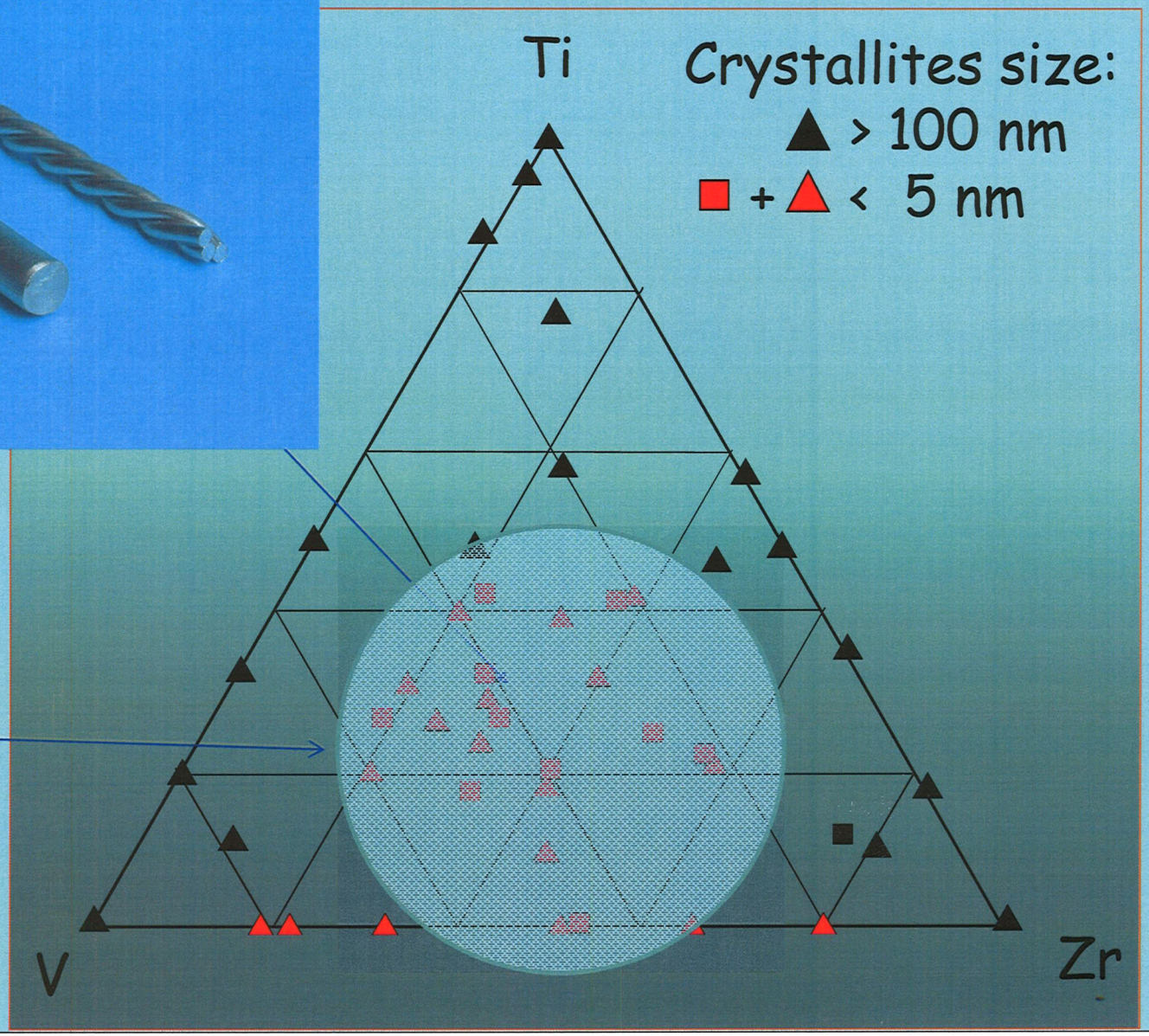

Low activation temperature

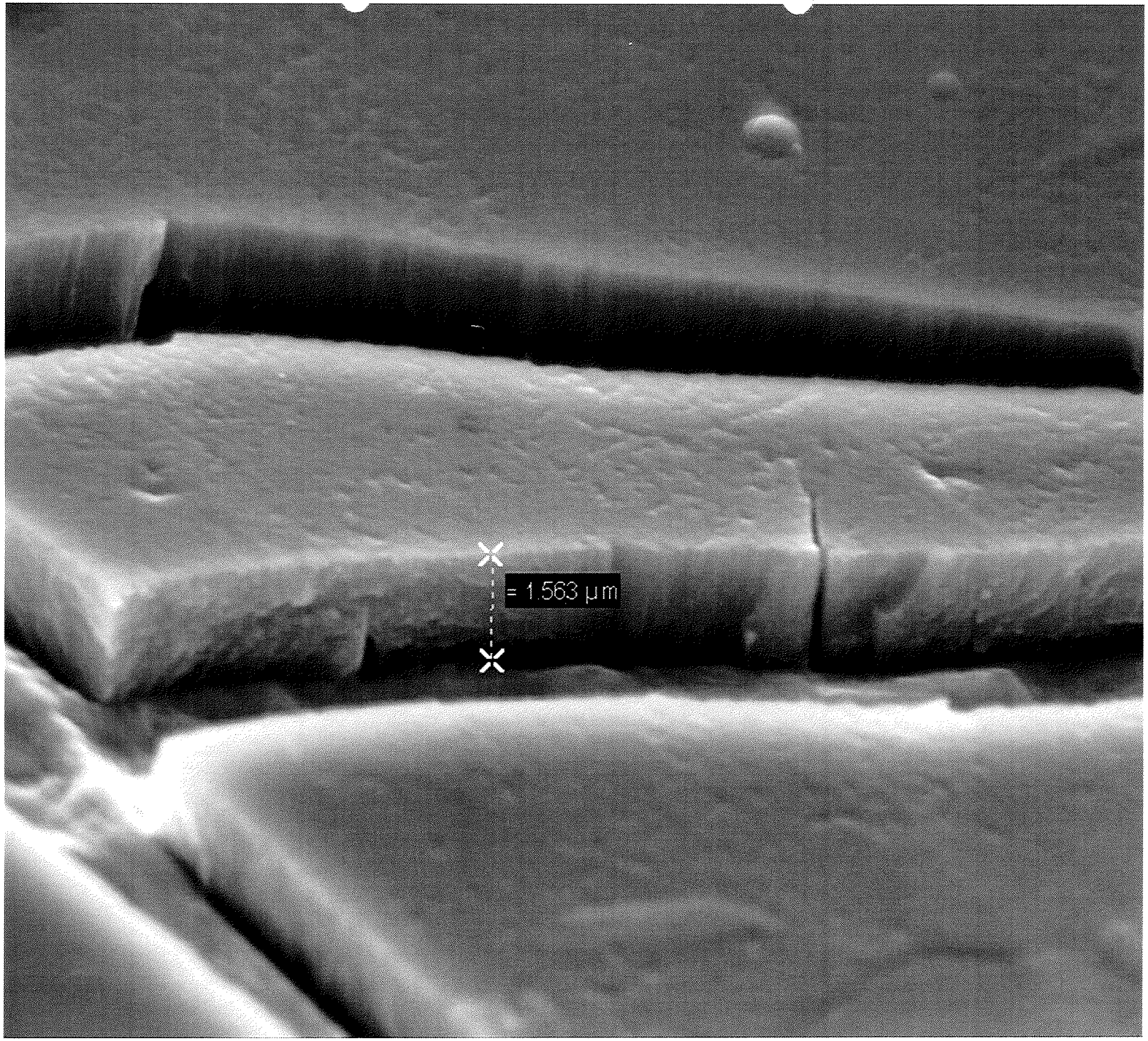
= 1.563 µm

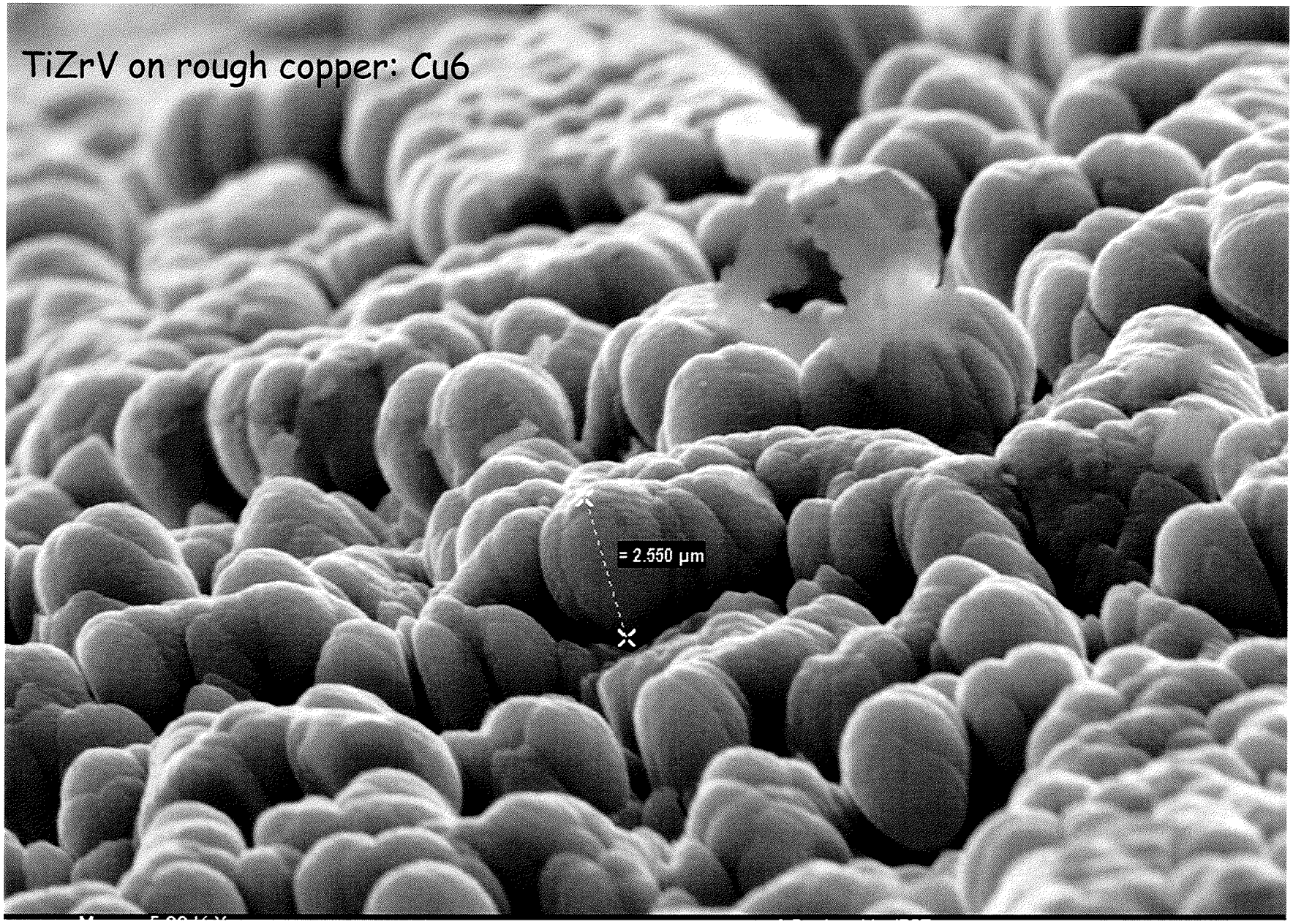
TiZrV on rough copper: Cu6
= 2.550 µm

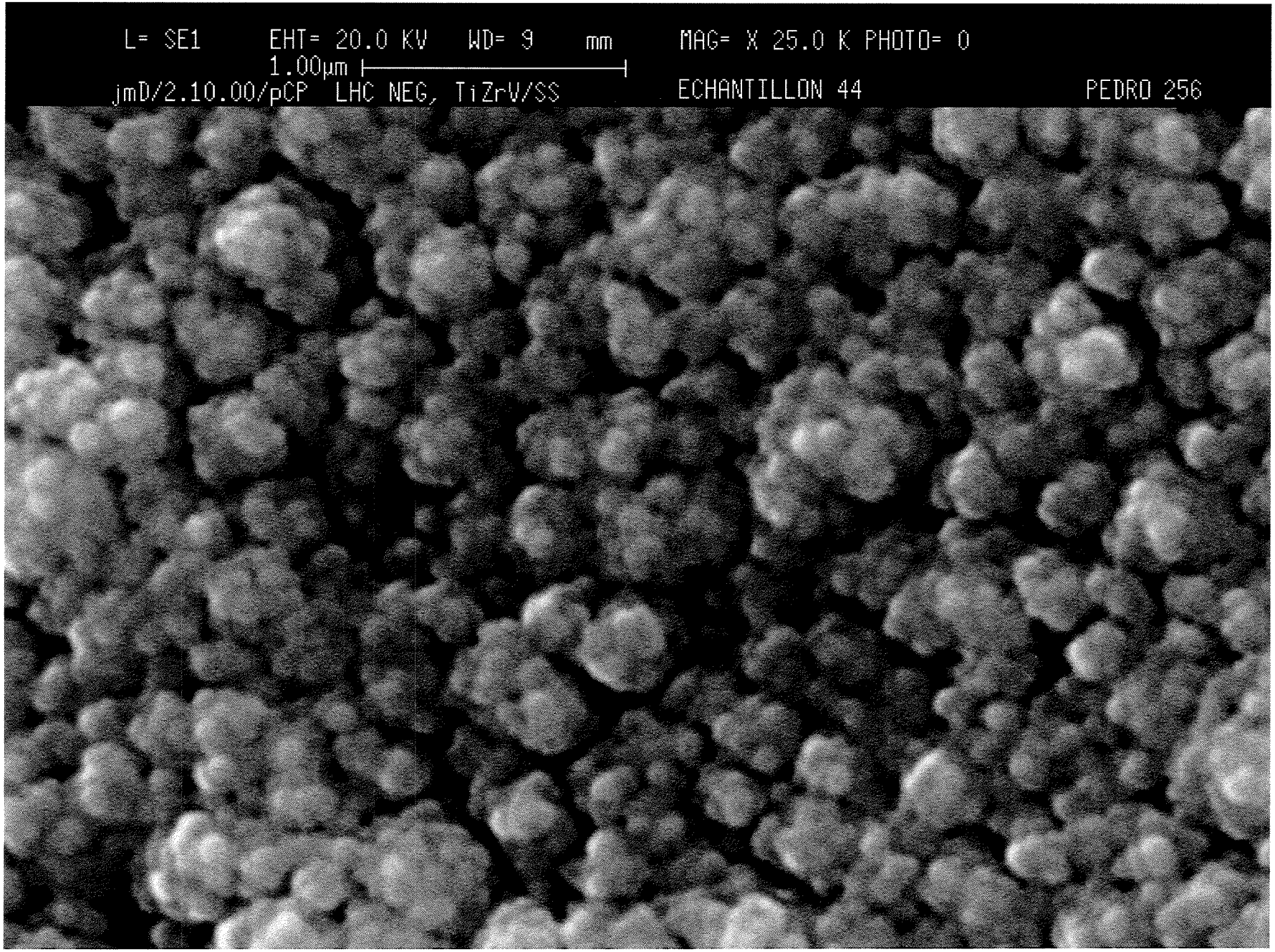
L= SE1 EHT= 20.0 KV WD= 9 mm MAG= X 25.0 K PHOTO= 0
1.00µm
jmD/2.10.00/pCP LHC NEG, TiZrV/SS ECHANTILLON 44 PEDRO 256

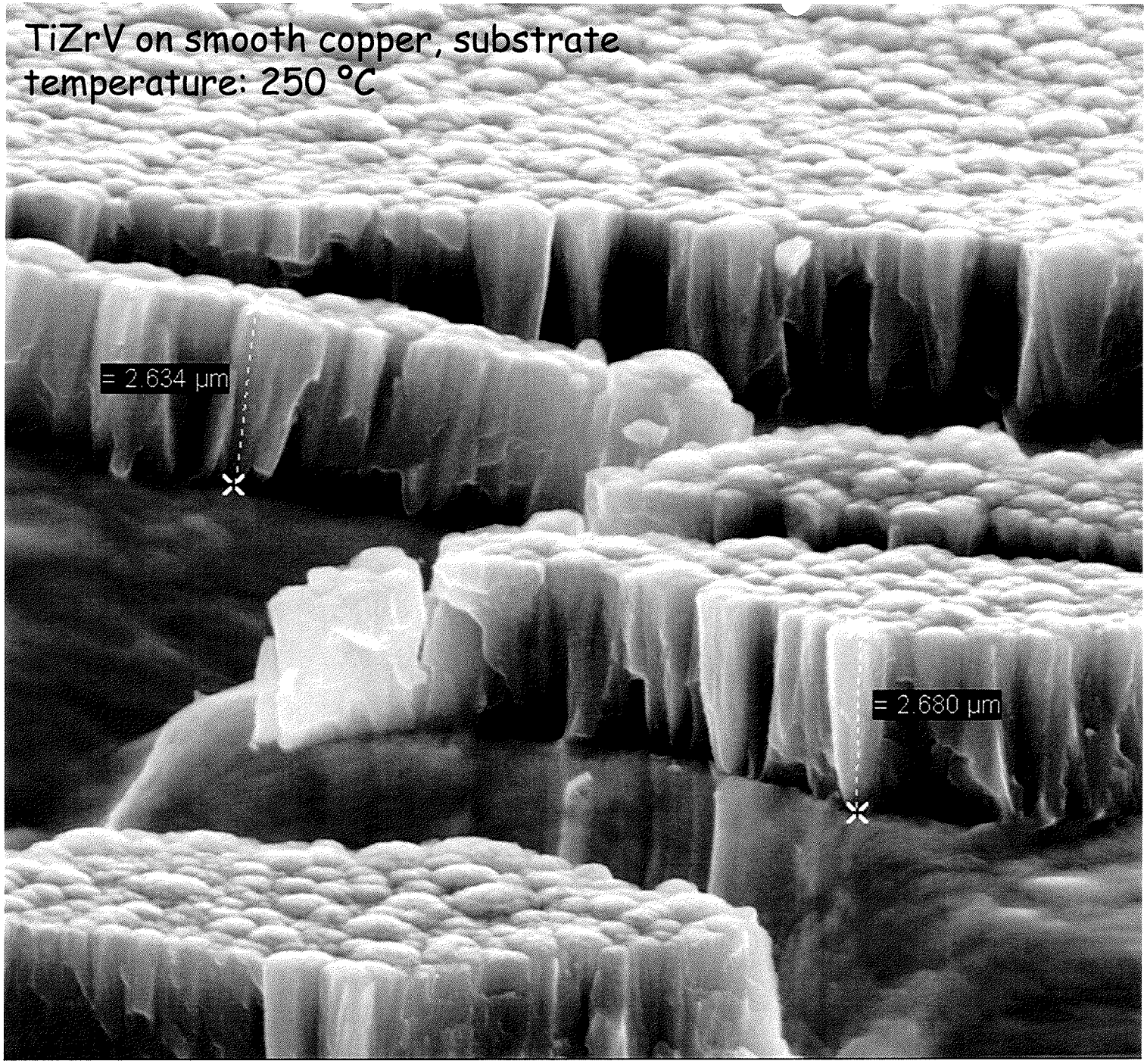
TiZrV on smooth copper, substrate temperature: 250 °C
= 2.634 µm
= 2.680 µm

✓ **Role of the substrate material on the activation process and on the film morphology.**

Does not affect the film crystallinity

Does not affect the activation process

Affects the film morphology

Substrates studied

Glass
Stainless steel
Copper
Aluminium
Glidcop
Beryllium
Al-Be

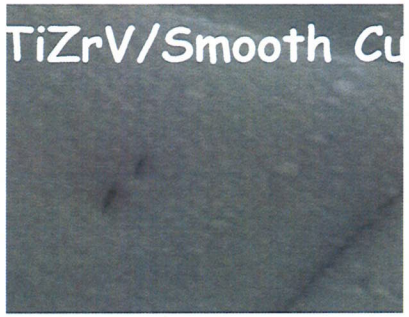

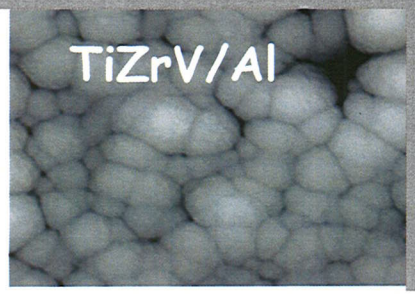

✓ Influence of the substrate temperature during coating.

Influence of the substrate temperature

On film crystallinity:
increased grain size for T≥ 300°C

250 °C is the highest substrate temperature at which a grain size below the threshold value of 5 nm is still preserved.
For T>300°C the activation process is delayed

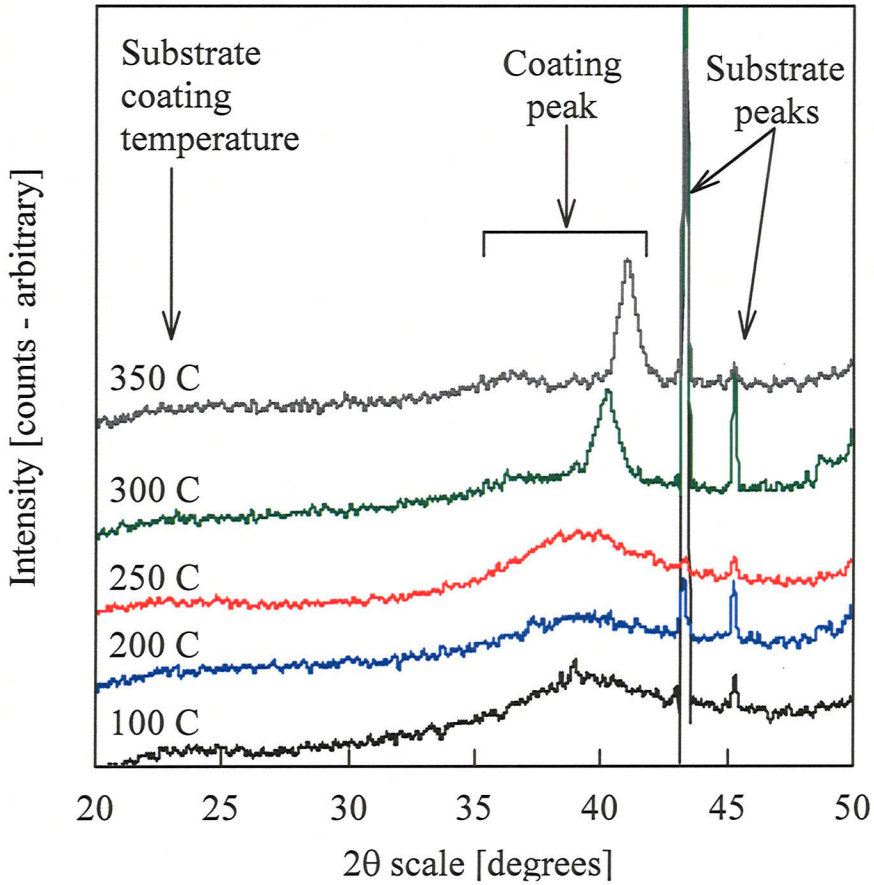

✓ Influence of the substrate temperature during coating.

Influence of the substrate temperature

On film morphology:
increased roughness for T> 200°C

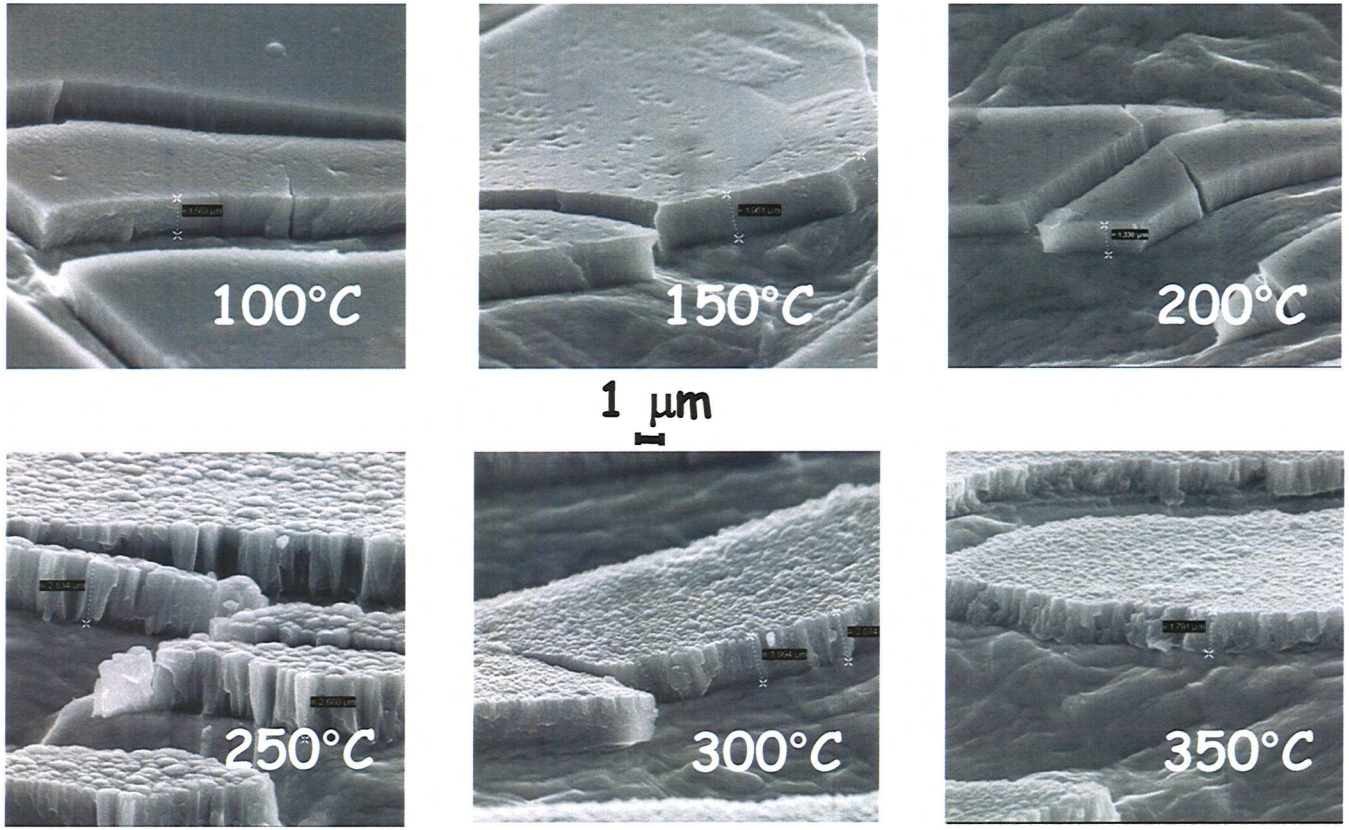

✓ Functional properties:

Large and uniformly distributed pumping speed for most of the residual gases: ≈ 0.5 l $s^{-1}cm^{-2}$ for H_2 and ≈ 5 l $s^{-1}cm^{-2}$ for CO .

Monolayer surface capacity for CO (about 10^{15} molecules cm^{-2}).

Photon and electron desorption yields lower than those for standard vacuum materials.

Extremely low CH_4 and Kr outgassing rate: $\leq 10^{-17}$ Torr l $s^{-1}cm^{-2}$ (Kr desorption energy = 21±1 Kcal mol^{-1})

Typical initial H content of the order of 10^{-3} at. fraction. Dissociation pressure negligible at room temperature; 10^{-10} Torr at 180°C, 10^{-8} Torr at 250°C.

Safe H charging limit at room temperature: 10 Torr l g^{-1} ($\approx 2x10^{17}$ H_2 molecules cm^{-2} μm^{-1}).

Low SEY ($\approx$1.1 at peak value)

TiZrV functional properties: pumping speed

Smooth coating

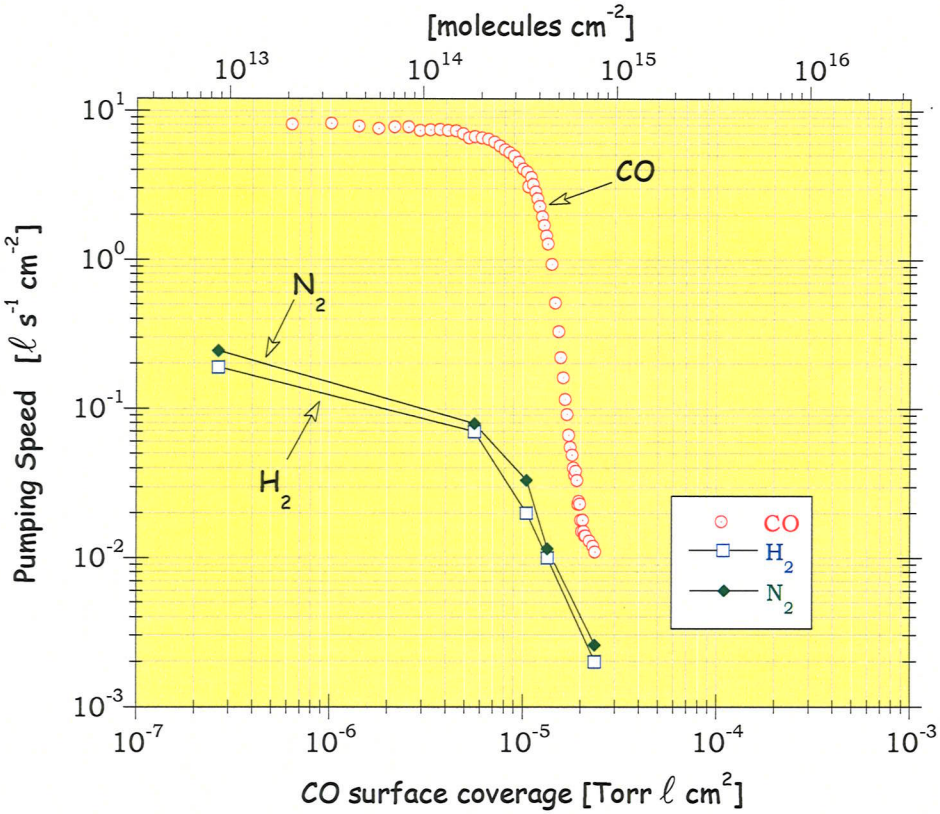

Rough coating

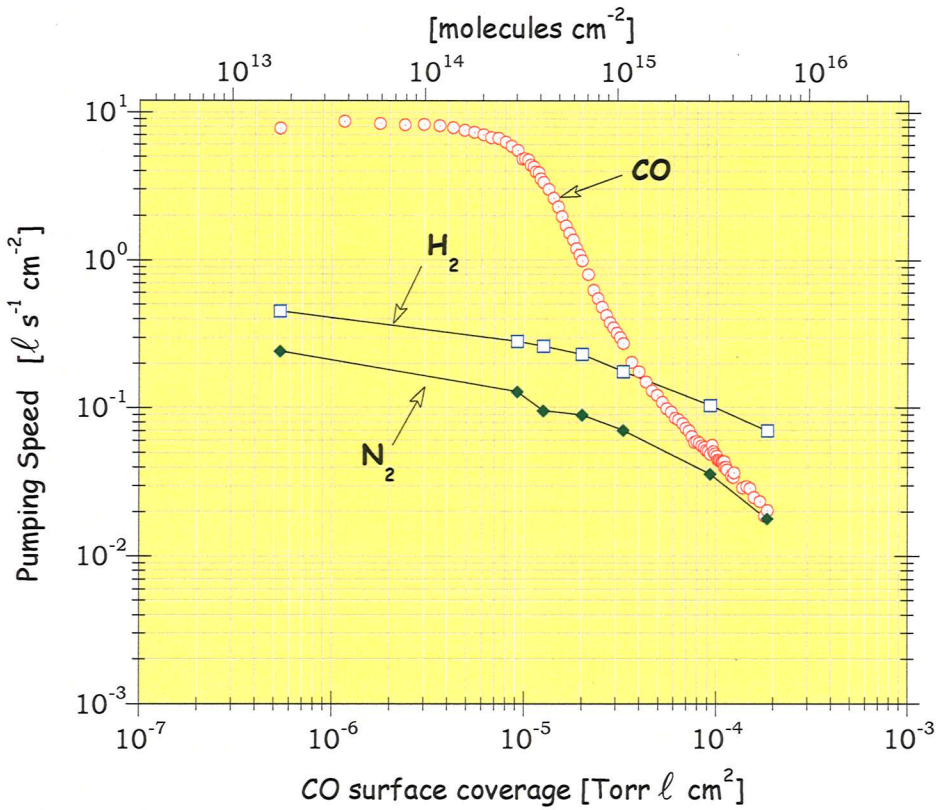

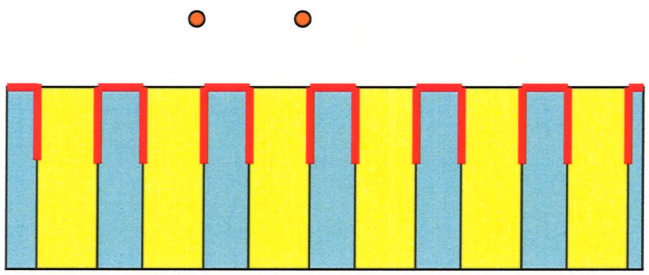

TiZrV functional properties: secondary electron yield

B. Henrist et al./Applied Surface Science 172 (2001) 95–102

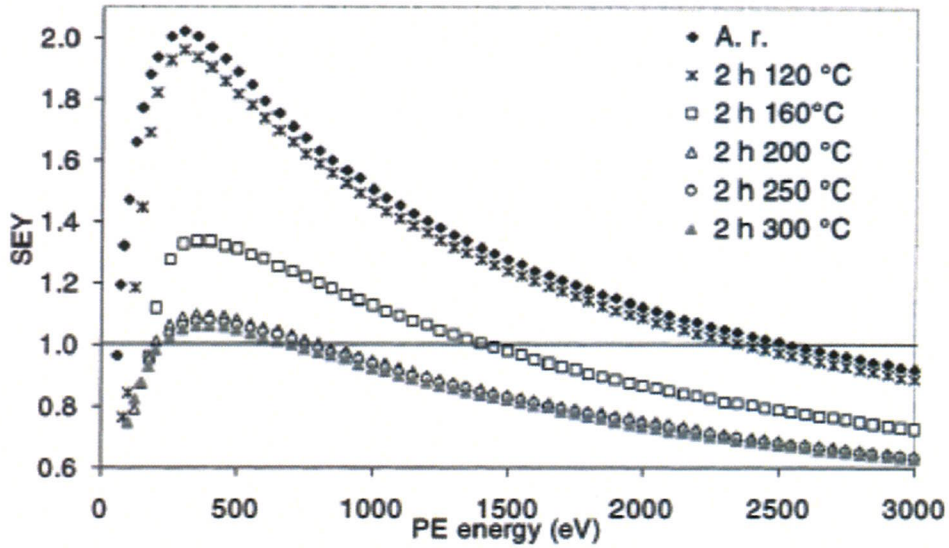

SEY versus PE energy of the TiZrV NEG coating:
as received and after 2h heating at 120, 160, 200, 250 and 300 °C.

Influence of CO exposure on the SEY of a TiZrV coating activated 2 h at 300 °C and cooled at 60°C before CO exposure

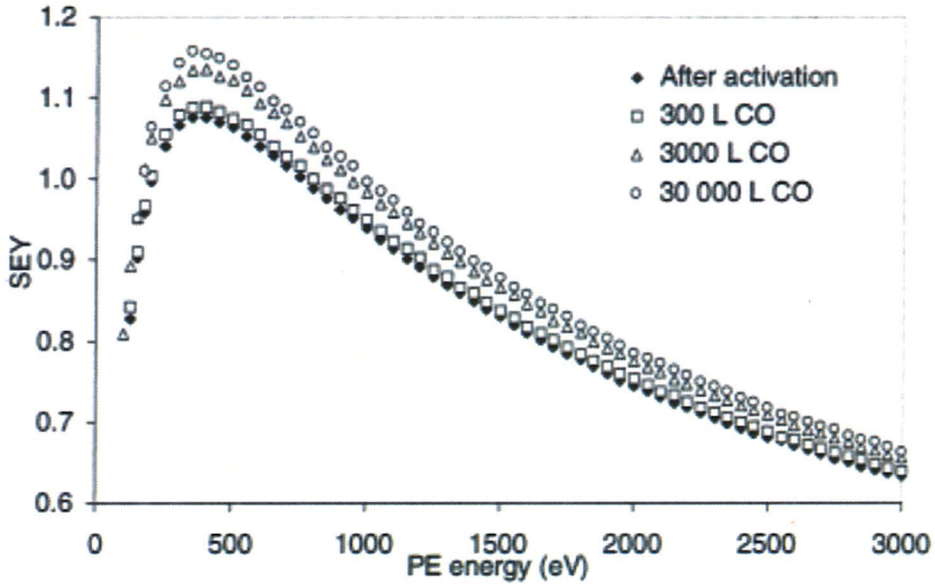

TiZrV: synchrotron radiation induced desorption

Angle of incidence = 25 mrad

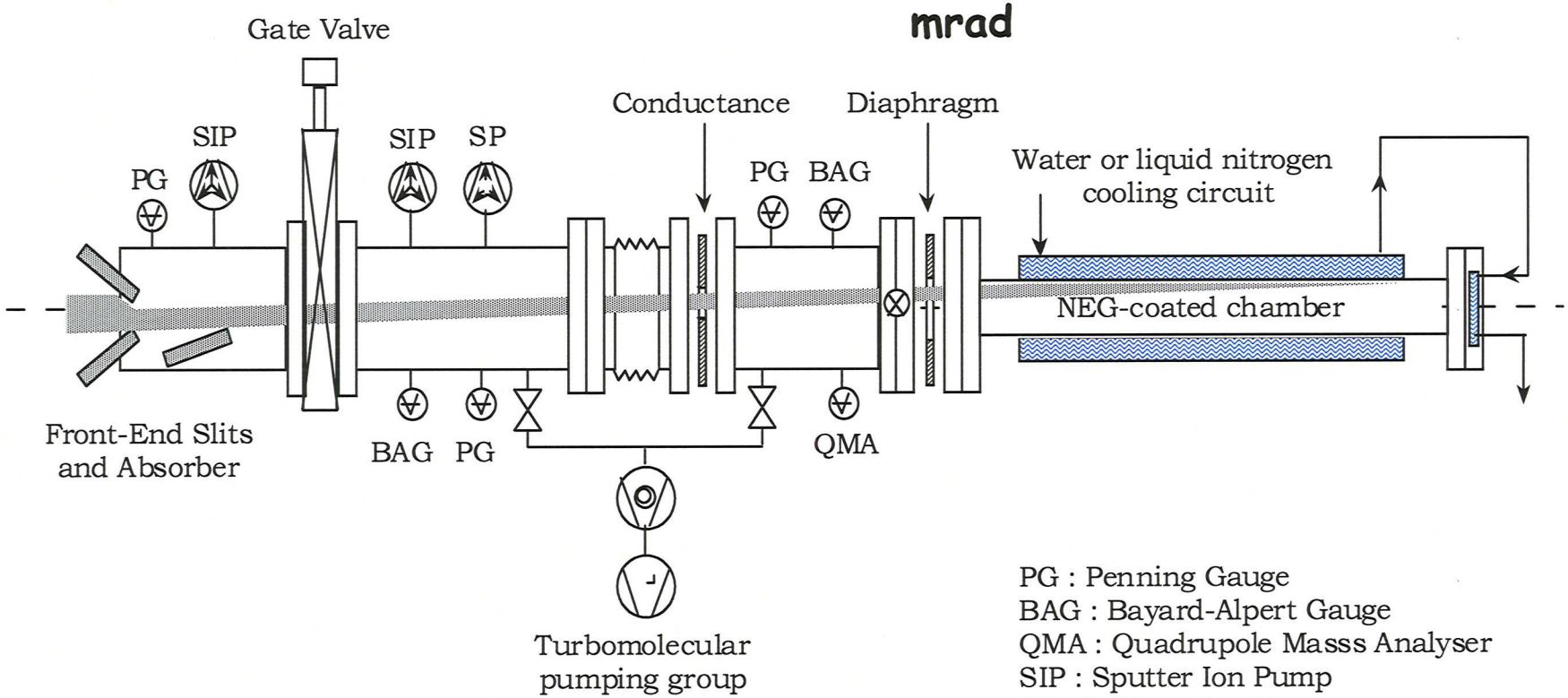

PG : Penning Gauge
BAG : Bayard-Alpert Gauge
QMA : Quadrupole Masss Analyser
SIP : Sputter Ion Pump
SP : Sublimation Pump

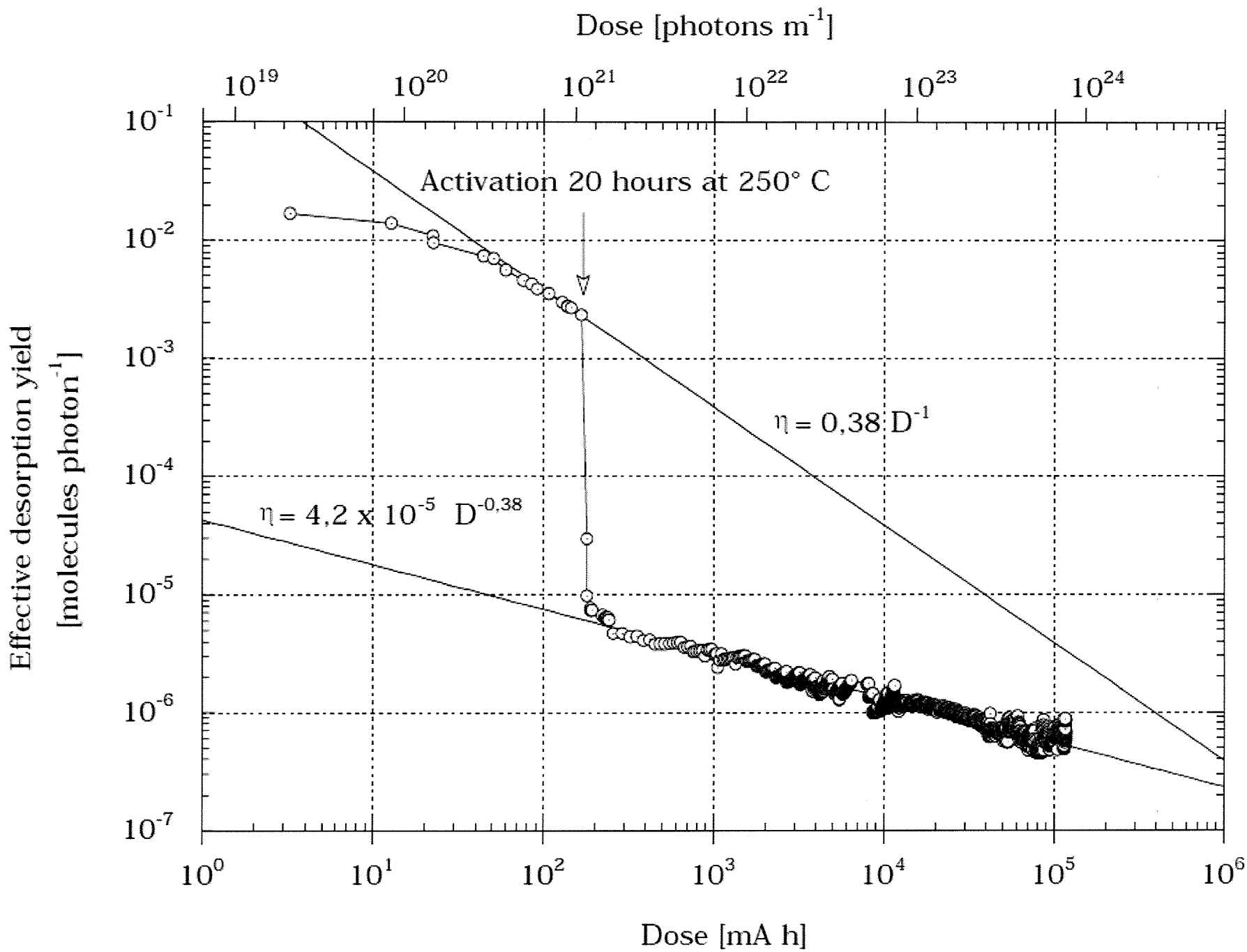
Dose [photons m-1]
10^19
10^20
10^21
10^22
10^23
10^24
Activation 20 hours at 250° C
η = 0,38 D-1
η = 4,2 x 10-5 D-0,38
Effective desorption yield
[molecules photon-1]
10-1
10-2
10-3
10-4
10-5
10-6
10-7
10^0
10^1
10^2
10^3
10^4
10^5
10^6
Dose [mA h]

✓ Performances deterioration:

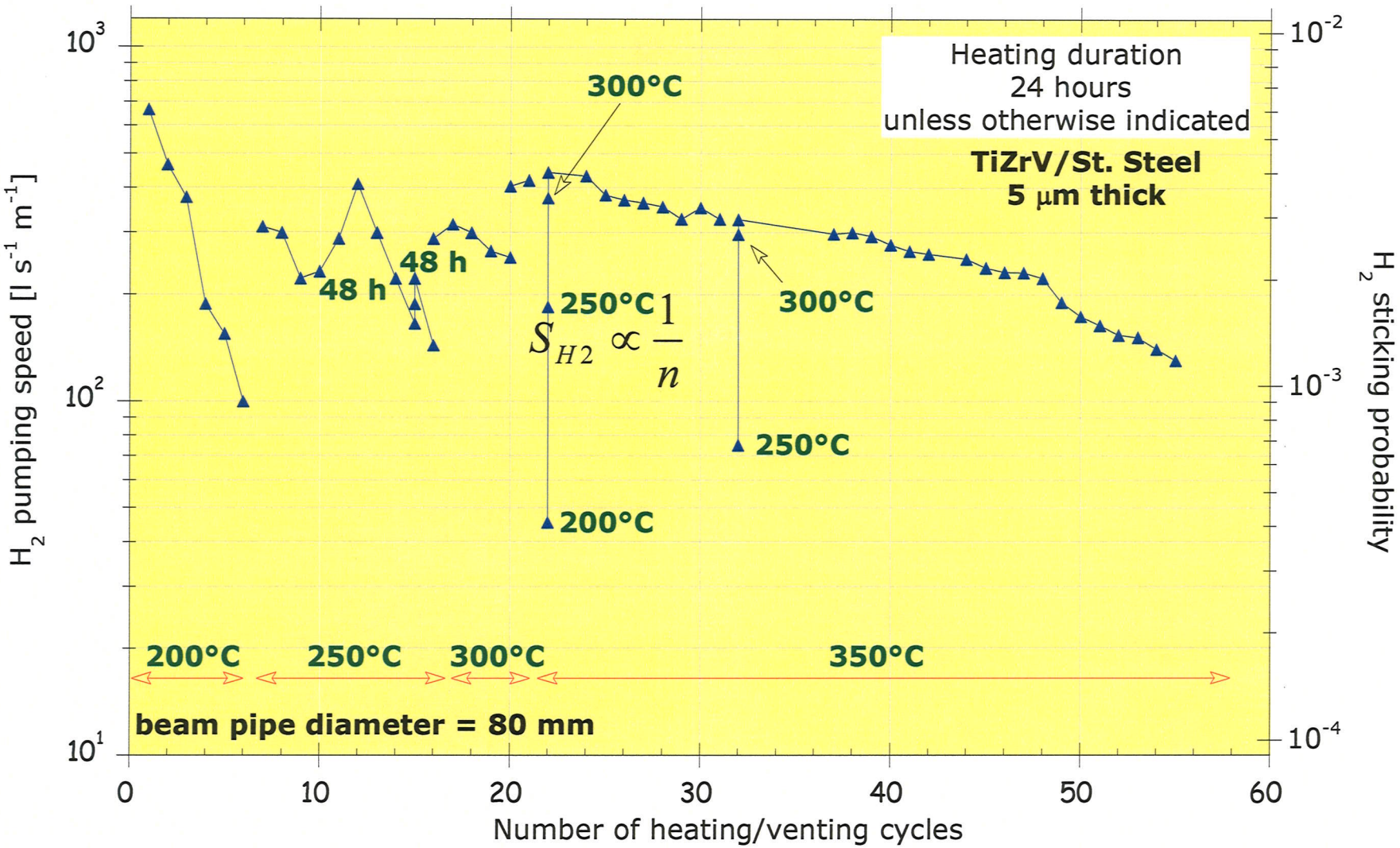

Performances deterioration: ageing

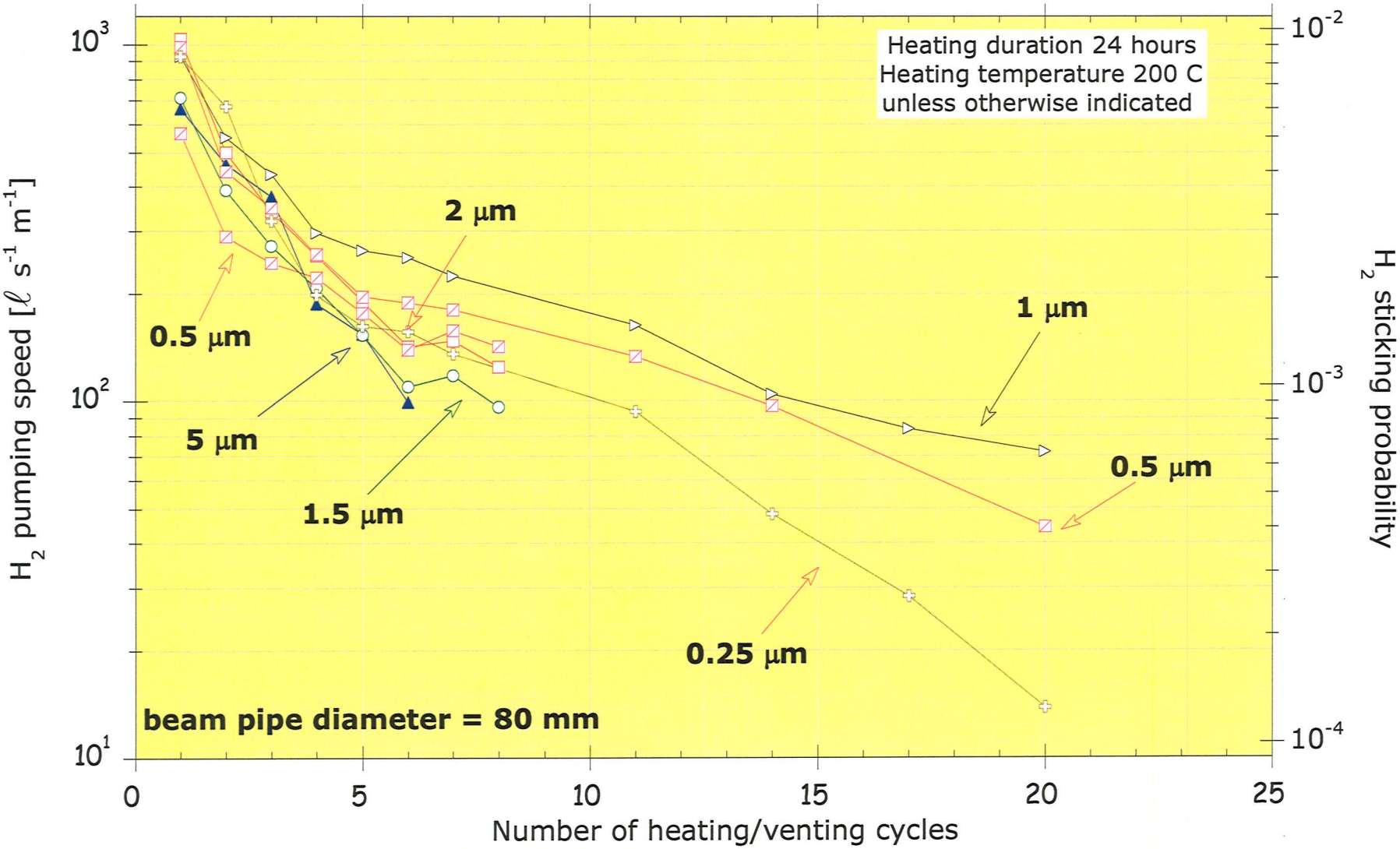

✓ Performances deterioration:

- The pumping speed shows a gradual decrease after each venting-activation cycle.

- The decrease of performance depends on the heating temperature; higher the temperature, lower the loss. For a heating cycle of 200°C x 24h, for the first 10 cycles, in the worst case:

$$S_{H2} \propto \frac{1}{n}$$

- When the activation cycle is carried out at temperatures lower than 250°C, pumping speed can be partially recovered by increasing the heating temperature.

- The loss of performance recorded along the first 10 cycles does not depend on the thickness of the film, for thickness higher than 0.25 μm.

About 1 Kg of Ti-Zr-V will be spread over the LHC to coat about 1200 vacuum chambers of roughly 6 Km of long straight section beam pipe.

Most important vacuum chambers are in the proximity and in the centre of the 4 gigantic experiments.

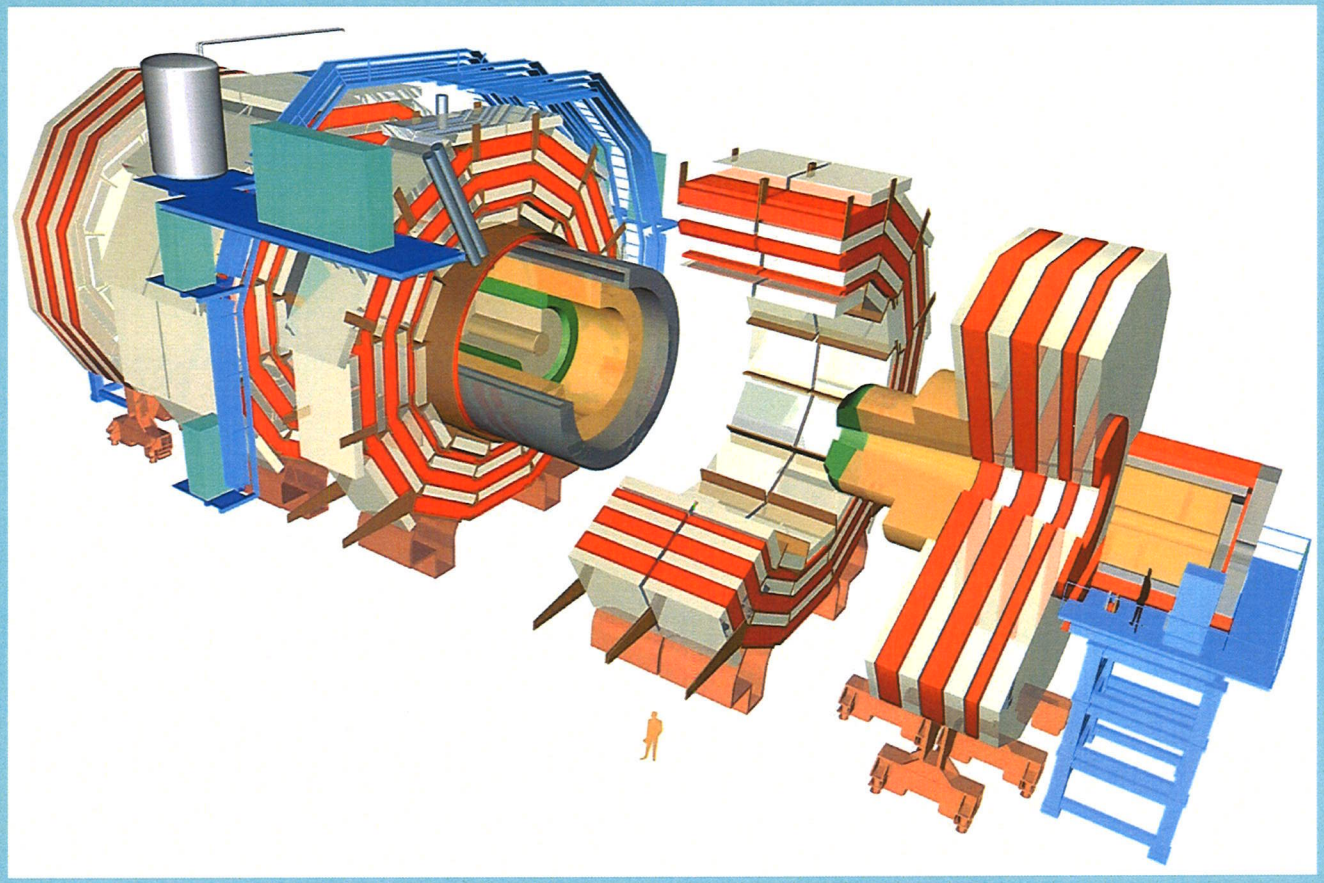

A dedicated coating facility is available at CERN since 2004:

- ✓ 3 independent magnetron sputtering systems
- ✓ maximum length: 7.5 m; maximum diameter: 60 cm
- ✓ maximum production rate: 20 chambers per week.

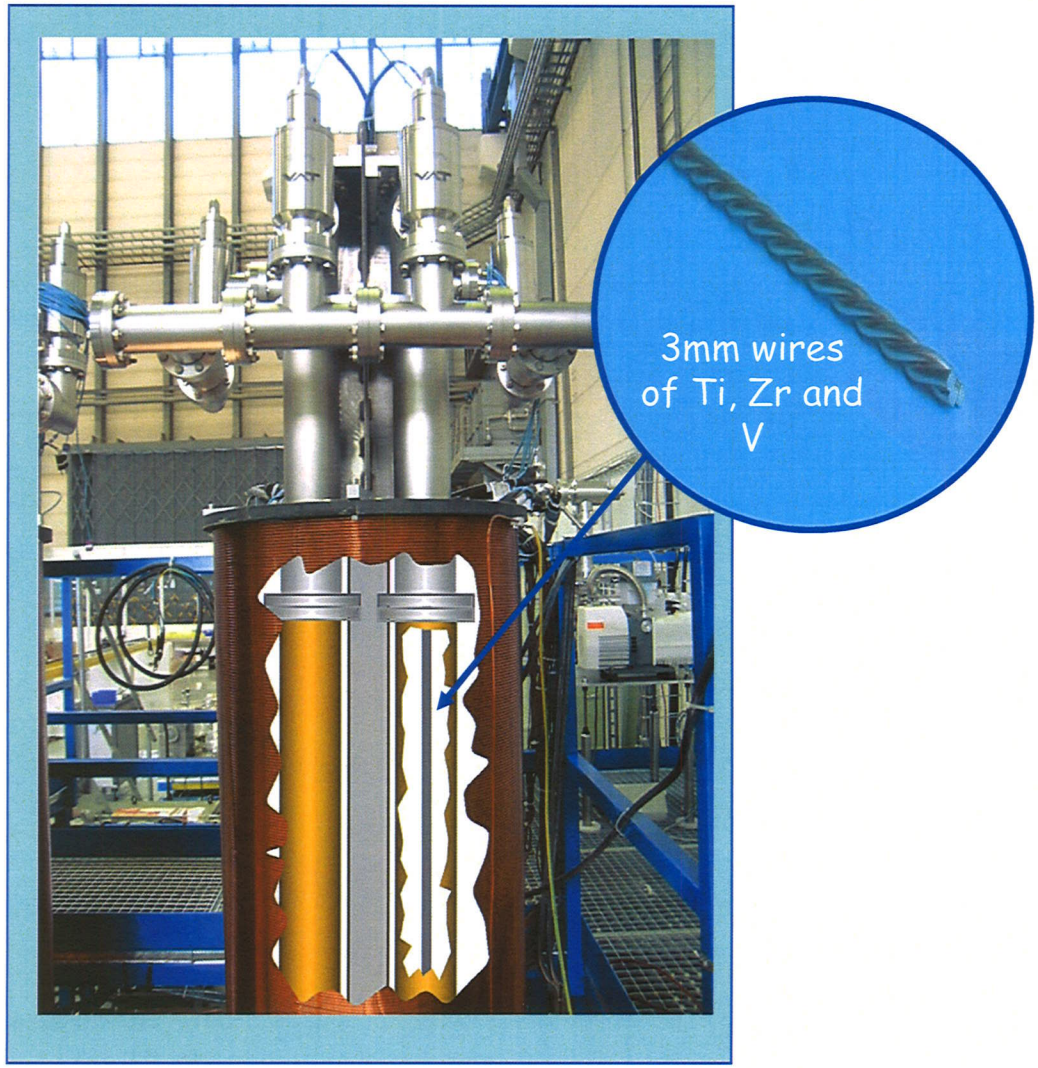
3mm wires
of Ti, Zr and
V

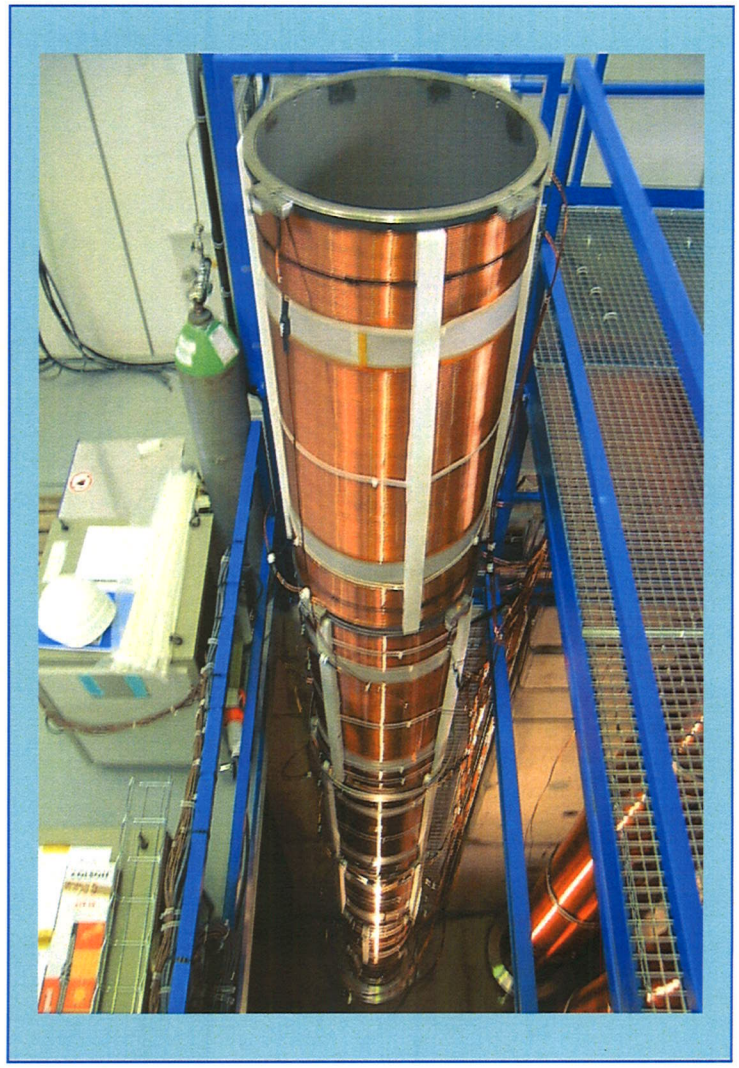

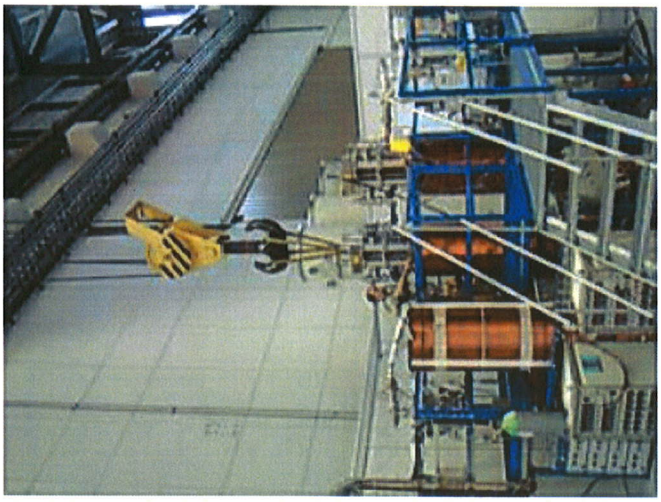

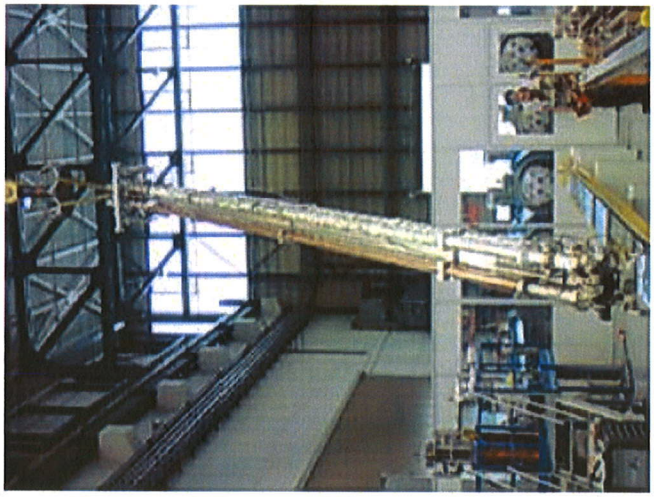

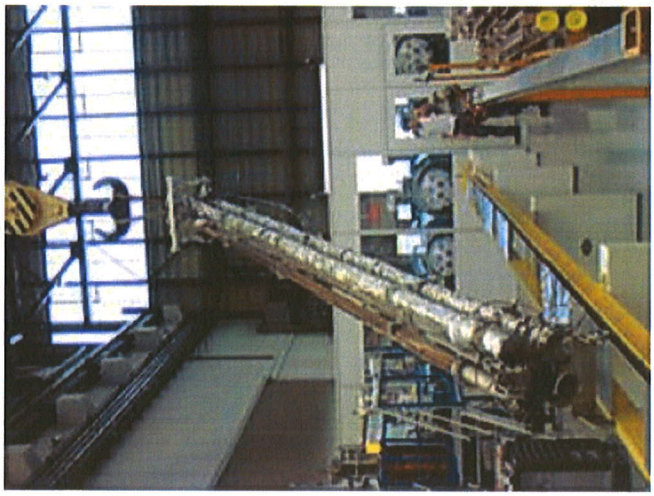

3.3.3 CRYOPUMPING

Pressures and gas density at low temperature

$T_1 < T_2$

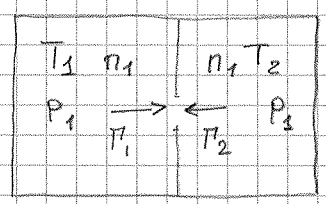

unit surface area opening between the 2 volumes

$$\Gamma_1 = \frac{1}{4} n_1 v_1 \; ; \quad \Gamma_2 = \frac{1}{4} n_2 v_2$$

In equilibrium: $n_1 v_1 = n_2 v_2$

$$P_1 = n_1 k_B T_1 \qquad P_2 = n_2 k_B T_2 \Rightarrow \frac{P_1}{k_B T_1} \cdot v_1 = \frac{P_2}{k_B T_2} v_2$$

$$v \propto \sqrt{T} \Rightarrow \frac{n_1}{n_2} = \frac{v_2}{v_1} = \sqrt{\frac{T_2}{T_1}}$$

$$\Rightarrow \frac{P_1}{\sqrt{T_1}} = \frac{P_2}{\sqrt{T_2}} \Rightarrow \frac{P_1}{P_2} = \sqrt{\frac{T_1}{T_2}}$$

In the colder volume the gas density is higher, but the pressure is lower.

$\sqrt{\frac{T_1}{T_2}}$ = thermomolecular transpiration factor

Saturated vapour pressure

For a given gas and surface temperature, by progressively increasing the surface coverage a saturation equilibrium between gas adsorption and desorption is established. The corresponding gas pressure is the saturated gas pressure.

T

gas adsorbed

gas phase

desorption : $A \frac{N_s}{\tau_0} \cdot e^{-\frac{E_v}{k_B T}}$

adsorption : $\frac{1}{4} A n \cdot v_{th} \cdot \alpha$

Most of the gases have a saturated gas pressure lower than 10^{-11} Torr at 20 K except for Ne, H_2 and He.

At the He boiling temperature (4,3 K), the vapour pressure of H_2 is in the the 10^{-7} Torr range. At 3 K the H_2 vapour pressure is in the 10^{-11} Torr range. At the superfluid He critical temperature, $P_{H_2} < 10^{-12}$ Torr.

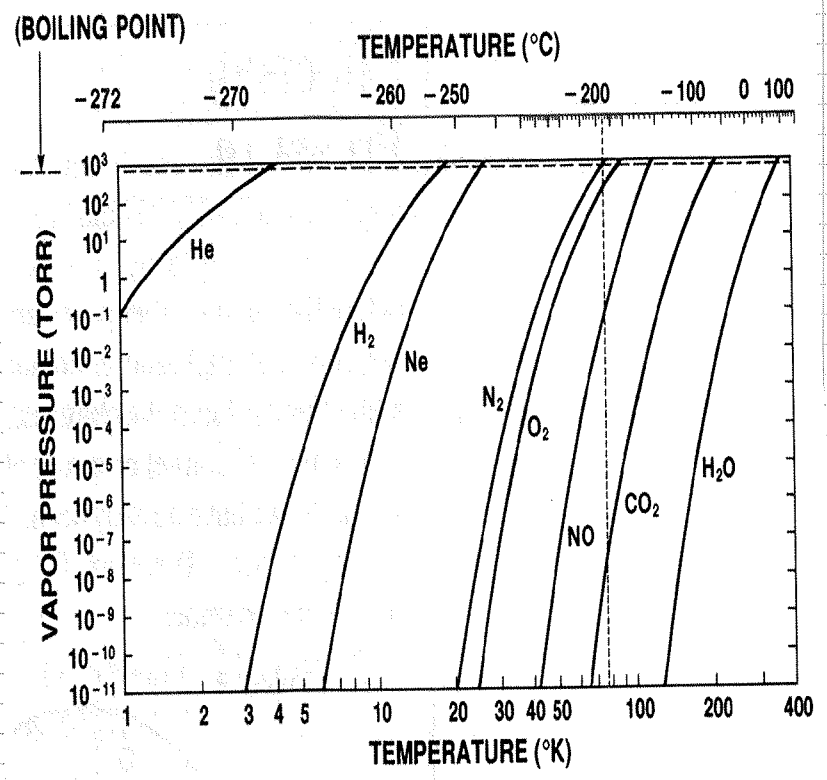

VAPOR PRESSURES OF COMMON GASES

E_v Heat of vaporisation [kcal/mol] @ Boiling temperatures [K]

He	0.020	4,2
H_2	0,215	20,3
Ne	0.431	27,1
N_2	1,333	77,3
CO	1,444	82
Ar	1.558	87,2
CH_4	1.995	111,6
H_2O	9,7	373

$$1 \frac{eV}{molecule} = 23 \frac{kcal}{mol}$$

The <u>CONDENSATION CRYOPUMPS</u> are based on gas condensation on a cold surface. Once a condensation layer is formed, these pumps cannot achieve a pressure lower than the satured gas pressure:

$$P = \frac{Q}{S} + P_{sat}$$

Lower pressures than P_{sat} are obtained for submonolayer coverage. This is possible because the attractive van der Waals forces are stronger between the gas molecules and the substrate then between similar gas molecules in the condensed phase.

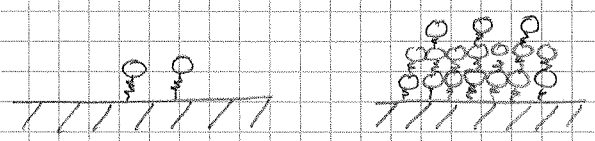

HIGHER BINDING ENERGY

For example:

He on porous glass at low coverage

$E_{ads} \simeq 0,68$ kcal/mol

$E_v = 0,02$ kcal/mol

H_2:

$E_{ads} \simeq 1,97$ kcal/mol

$E_v = 0,215$ kcal/mol

The important consequence is that H_2 can be significantly cryosorbed at 20 K and He at 4,2 K, up to a monolayer coverage.

Submonolayer quantities of all gases may be effectively cryosorbed at their own boiling temberature; at 77 K all gases except He, H_2 and Ne.

The pumps based on physisorption at low coverage are called <u>CRYOSORPTION PUMPS</u>. To increase the adsorption area, porous materials are used (charcoal and zeolites). Huge surface area can be obtained; for charcoal $\sim 1000\ m^2$ per gram are typically achieved. About $10^{-6}\ \frac{Torr\,l}{cm^2}$ of He can be adsorbed before the pressure rises above 10^{-10} Torr.

Most of the commercial cryopumps used in particle accelerators rely on cryosorption. The condensation cryopumping is in general a bonus of the superconducting magnet cooling.

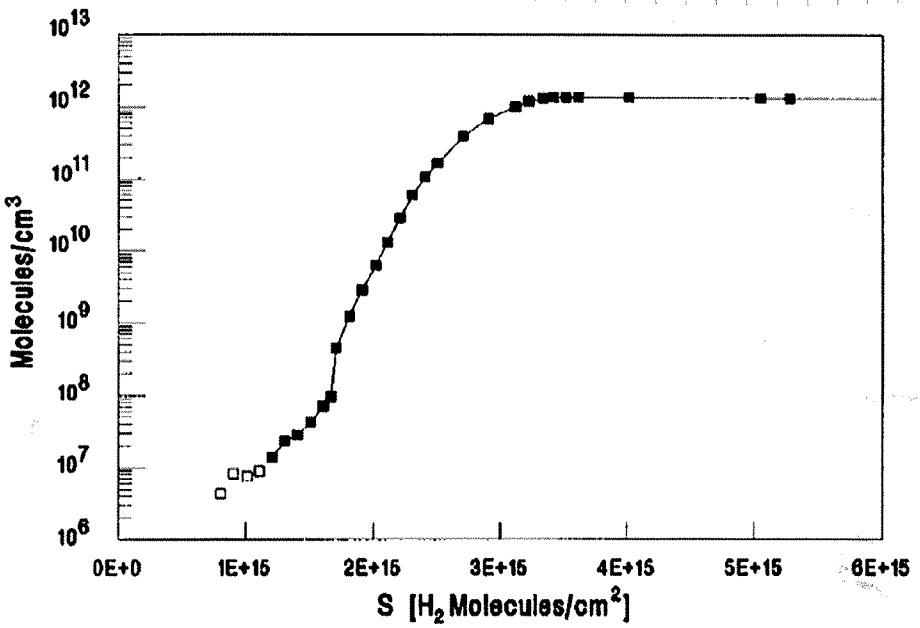

FIG. 2. Isotherm for H_2 on Cu plated stainless steel at 4.2 K plotted as a function of the surface density of H_2. The nonfilled markers represent measured points on the isotherm that are less than 10% above the background pressure of the instruments.

The cryogenic pumps that are commercially available take advantage of both cryosorption and cryocondensation. Cooling is usually achieved by a two stage refrigerator providing about 80 K on the first stage and 10 K on the second. A part of the coldest surface is coated with a porous material to provide a large pumping speed for H_2.

If a large load of gas heavier then H_2 is pumped on the porous material, the H_2 pumping is strongly reduced. For this reason the heavier gases are captured on 10-20 K smooth surfaces before arriving on the porous one. (see picture)

Cryogenic pumps can provide very large pumping speed ($>10^4$ l/s). They need regeneration to release the adsorbed gas after long period of pumping. This implies the need for a valve to separate them from the rest of the system and the help of a turbomolecular pump to remove the desorbed gas. Their cost is relatively high.

He gas refrigerators are used to cool cryosorption pumps.

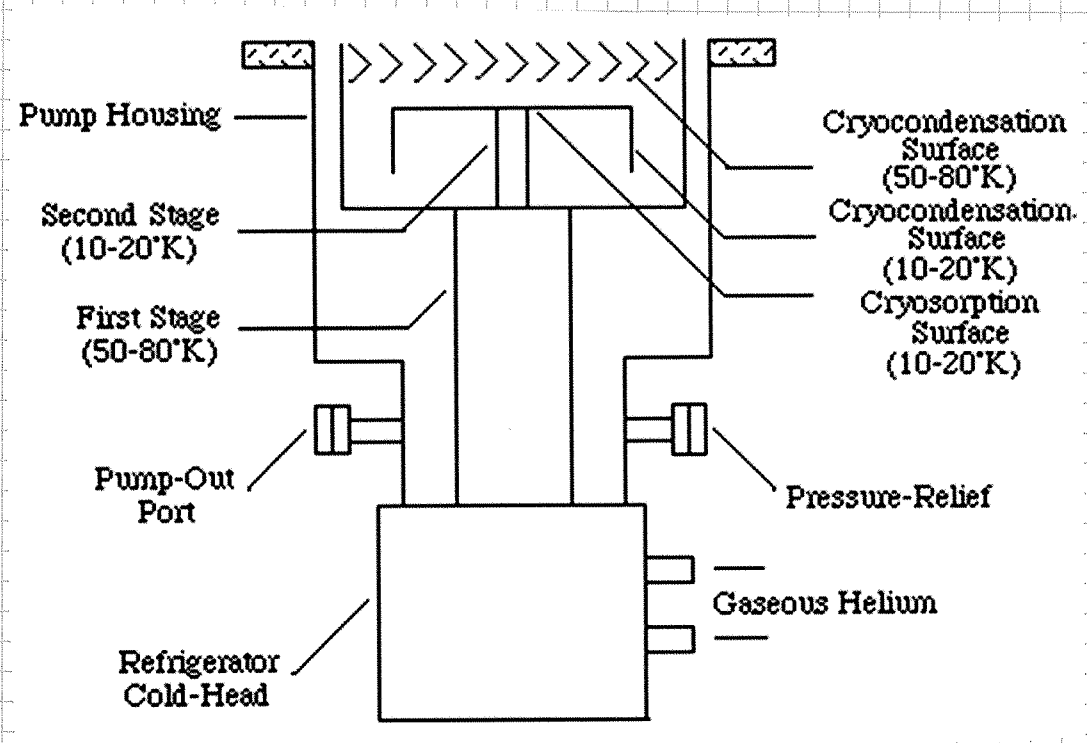
Pump Housing
Second Stage
(10-20°K)
First Stage
(50-80°K)
Pump-Out
Port
Refrigerator
Cold-Head
Cryocondensation
Surface
(50-80°K)
Cryocondensation
Surface
(10-20°K)
Cryosorption
Surface
(10-20°K)
Pressure-Relief
Gaseous Helium

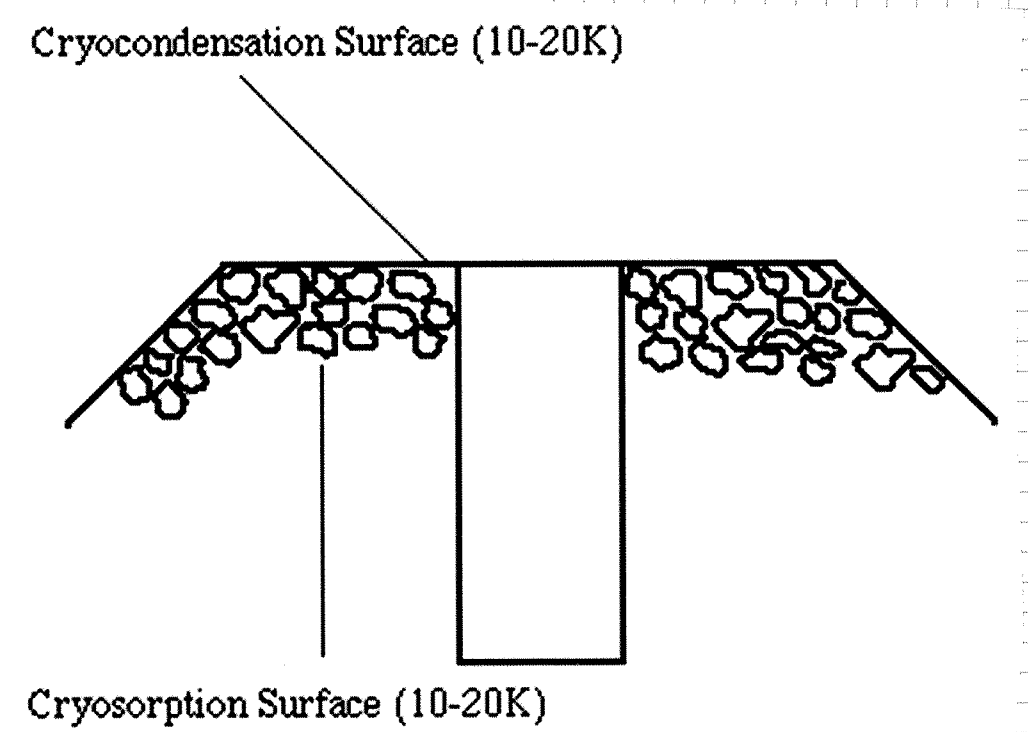
Cryocondensation Surface (10-20K)
Cryosorption Surface (10-20K)

3.3.4 CRYOPUMPING IN THE LHC

The vacuum chamber in contact with the arc magnets ("cold bore") is at about 1.9 K. At this temperature all gases have saturated vapour pressures lower than 10^{-12} Torr.

The heat load due to the beam is due to:

$$\sim 1\,W/m \begin{cases} \text{synchrotron radiation : } 0{,}2\ W/m \text{ per beam} \\ \text{energy loss by nuclear scattering : } 30\ mW/m \text{ per beam} \\ \text{image current } 0{,}2\ W/m \text{ per beam} \\ \text{electron cloud} \end{cases}$$

At 1,9 K a huge power is needed to transfer this thermal load at room temperature (about 1 KW per W).

To intercept the thermal load, a beam screen kept at 5 - 20 K is interposed between the beam and the cold bore.

The beam screen has pumping holes that allow the transfer of molecules to the cold bore surface.

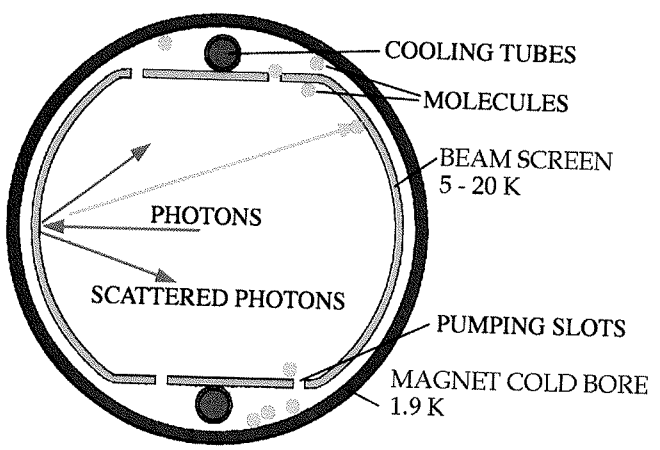

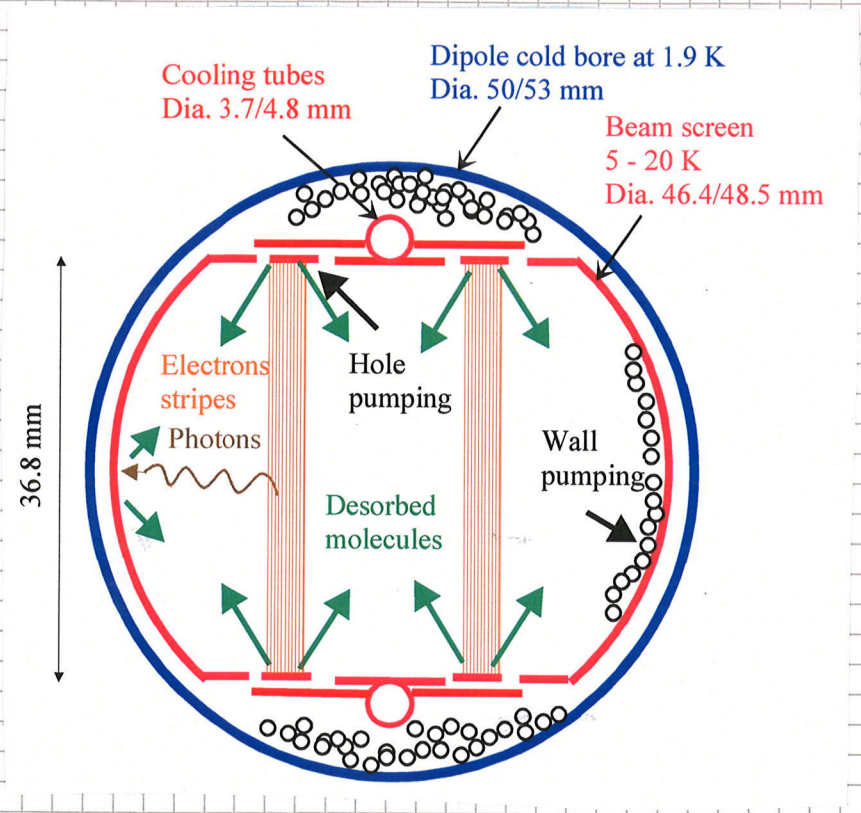
Cooling tubes
Dia. 3.7/4.8 mm
Dipole cold bore at 1.9 K
Dia. 50/53 mm
Beam screen
5 - 20 K
Dia. 46.4/48.5 mm
36.8 mm
Electrons
stripes
Photons
Hole
pumping
Desorbed
molecules
Wall
pumping

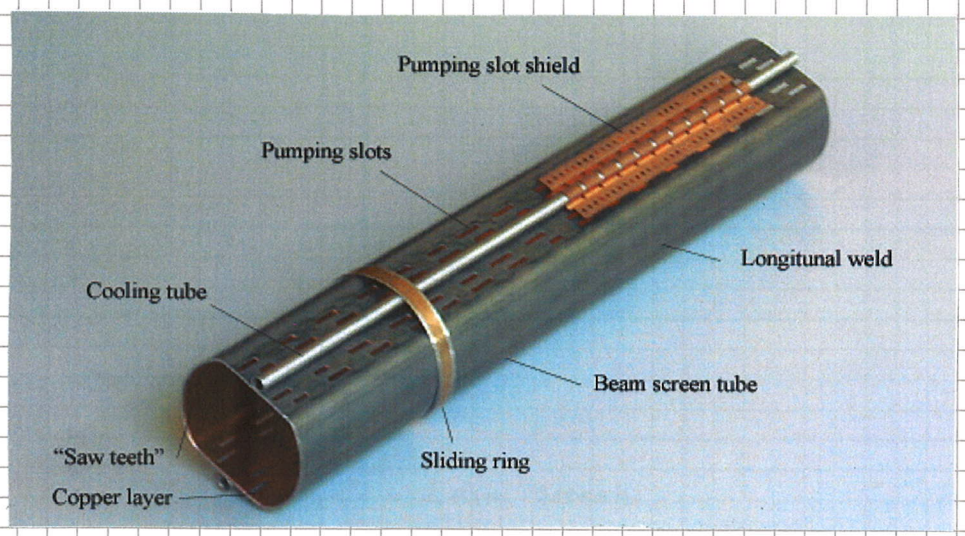
Pumping slot shield
Pumping slots
Longitunal weld
Cooling tube
Beam screen tube
"Saw teeth"
Sliding ring
Copper layer

In a few magnets the cold bores are cooled only at 4.3 K and, as a consequence, the H_2 pumping cannot rely on cryocondensation.

Cryosorbers made of woven carbon fibers (developed by BINP) are inserted between the beem screen and cold bore. At 6 K, 10^{18} H_2 molecules/geometric cm^2 are adsorbed with vapour pressure lower than 10^{-8} Torr.

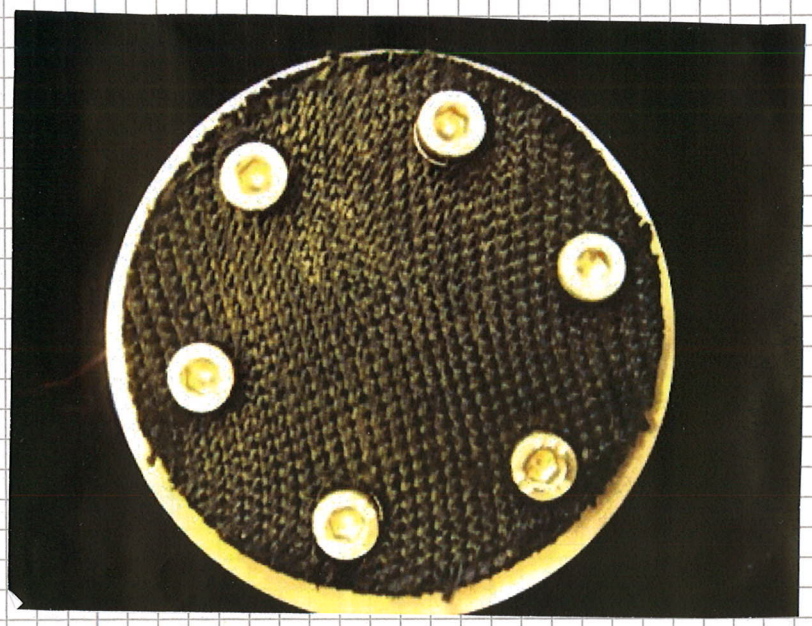

X 25

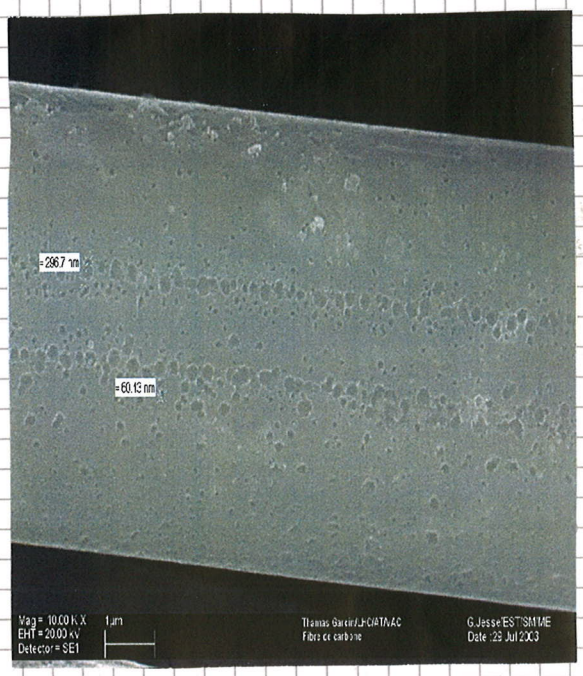

x 10 000

UNIT 4 :

ULTRA HIGH VACUUM INSTRUMENTATION

- In vacuum technology pressures are measured either directly (force acting on surfaces) or indirectly.

  The force measurement is at best limited to 10^{-7} N/cm^2. This gives a lower limit to the pressure measurement: $10^{-4} \div 10^{-5}$ Torr. In general in particle accelerators, the pressure is much lower. The direct methods are never used for the beam pipes.

- The indirect pressure measurements are obtained:

  1) by considering the thermal conductivity dependence on gas pressure (Thermal conductivity vacuum gauges).

  2) by ionizing the gas and detecting the density of ions (ionization gauges).

- In the first group of gauges, a filament is heated by ohmic effect. The current, voltage or temperature are monitored.

Filament radius: r_1

length L

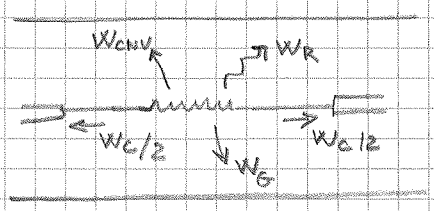

There are 4 different thermal transport phenomena:

1) Thermal conduction at the end of the filament:

$$\frac{1}{2} W_c = \pi r_1^2 K_{wire} \cdot \frac{dT}{dt}$$

2) Thermal irradiation

$$W_R = \varepsilon_1 (2\pi r_1 L) \sigma (T_1^4 - T_2^4) \quad \text{Stefan-Boltzmann}$$

3) Gas convention for $P > 10$ Torr; do not depend on pressure.

4) Thermal conduction in the gas.

$$W_G = F \cdot P$$

where F is a function of the gas characteristics and, in first approximation, independent of pressure

Comparing the 4 heat transport mechanisms, it comes out that:

- for low pressure (low 10^{-3} Torr) the thermal transport is dominated by pressure independent processes (radiation + solid conduction)
- for high pressure (> 10 Torr) the gas convection dominates the thermal balance ⇒ pressure independent

Therefore the thermal conductivity gauge gives significant reading in the range:

$$\sim 10^{-3} < P < \sim 10 \text{ Torr}$$

The signal from the filament can be obtained in 2 different ways:

1) Measuring the resistance or dissipated power. The temperature of the filament is maintained constant and the required heating power is measured. Reversely the heating current is kept constant and the resistivity variation is measured.

⇒ PIRANI GAUGES

The filament is part of a Wheatstone bridge, which increases sensitivity.

2) The temperature of the filament is measured by a thermocouple

⇒ THERMOCOUPLE GAUGES

Thermal conductivity gauges are used in particle accelerators to measure the first part of the pumpdown process and the pressure on mechanical pumps.

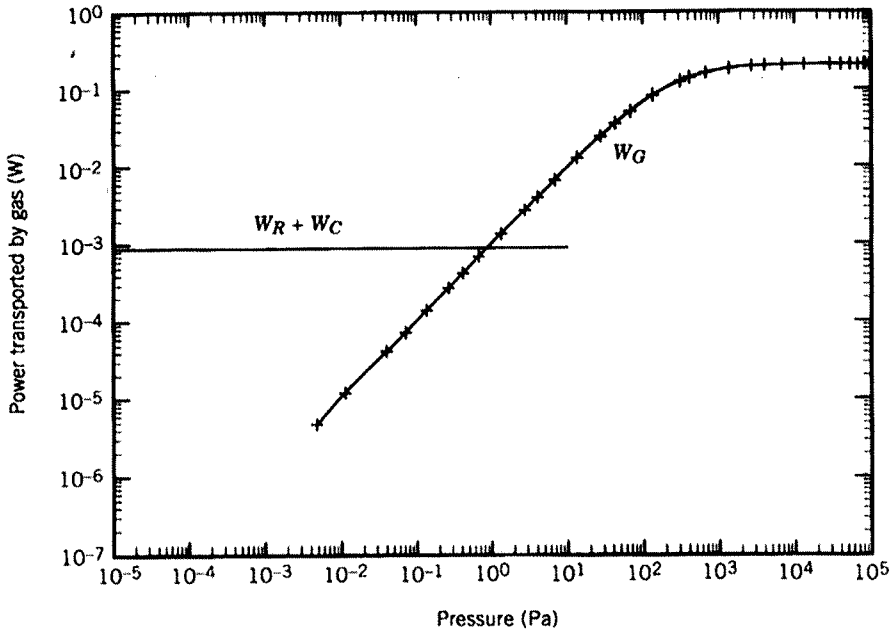
Power transported by gas (W)
Pressure (Pa)
$W_R + W_C$
W_G
10^0
10^{-1}
10^{-2}
10^{-3}
10^{-4}
10^{-5}
10^{-6}
10^{-7}
10^{-5}
10^{-4}
10^{-3}
10^{-2}
10^{-1}
10^0
10^1
10^2
10^3
10^4
10^5

4.1 IONIZATION GAUGES

The pressure is proportional to the gas density n:

$$PV = N k_B T \rightarrow P = n k_B T$$

The simplest way to measure n at low pressure is ionize the gas molecules by electron impact and collect the ions.

Electrons are emitted by a hot filament (thermoionic current) or extracted from a Penning discharge. The first family of gauges is called hot cathode gauges, the second cold cathode (or Penning) gauges.

The ionization process is characterized by the ionization cross section, which depends on electron energy and nature of the gas.

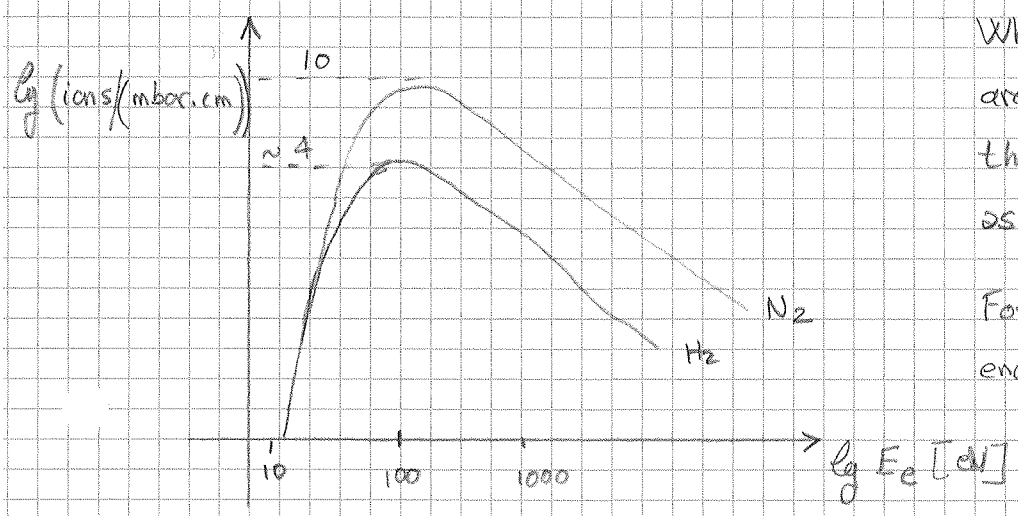

When in a vacuum system there are more than a single gas, the pressure reading is given as N_2 equivalent.

For a fixed value of electron energy, the ratio of the cross sections is constant and is independent of the gauge geometry.

4.1.1 COLD CATHODE GAUGES

The working mechanism is similar to the one of sputter ion pumps.
A magnetic field force electron to move onto spiral paths leading to higher ionization probability. An electric field accelerates electrons and pushes the ions on a collector.

$$\begin{cases} \text{magnetic field} \sim 0{,}1 \div 0{,}2 \text{ T} \\ \text{voltage} \sim 3000 \text{ V} \end{cases}$$

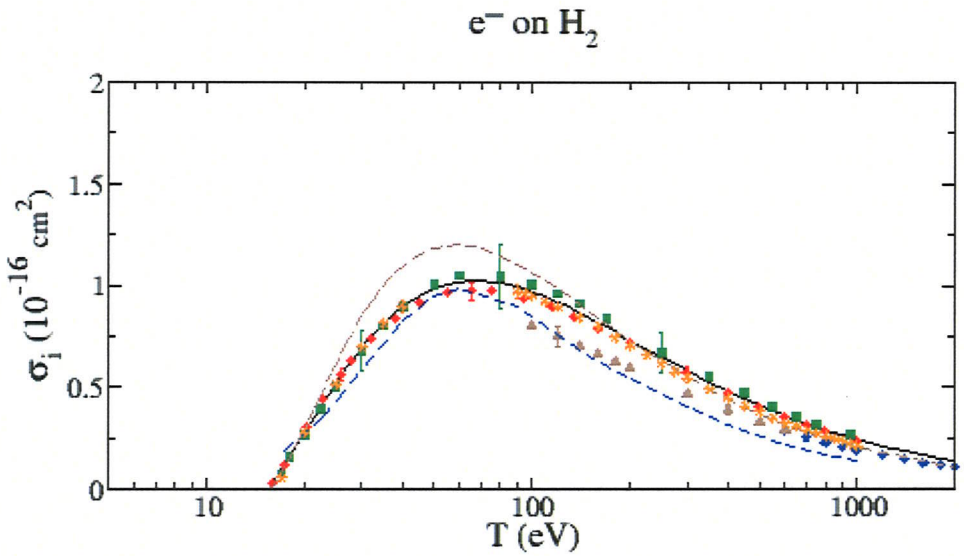
e⁻ on H2
σi (10-16 cm2)
T (eV)
0
0.5
1
1.5
2
10
100
1000

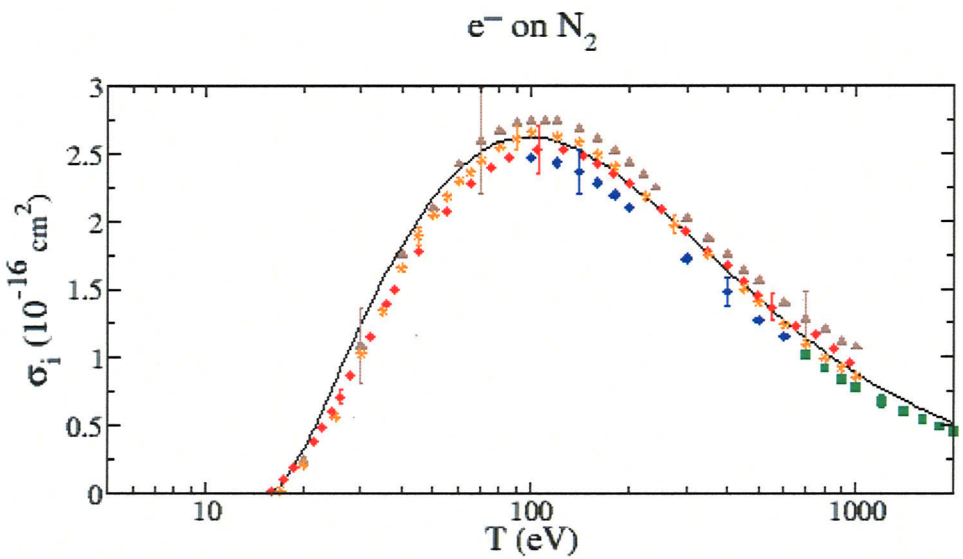
e⁻ on N2
σi (10-16 cm2)
T (eV)
0
0.5
1
1.5
2
2.5
3
10
100
1000

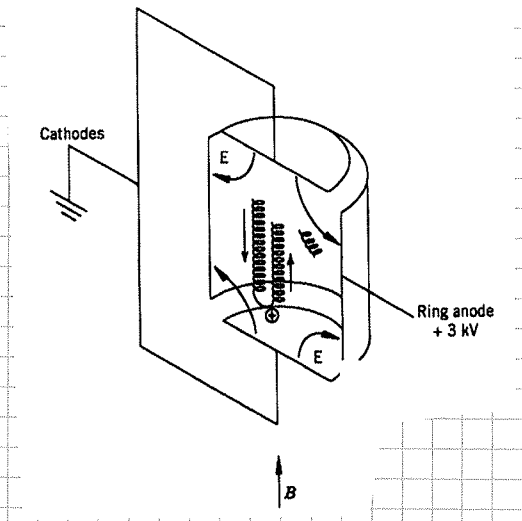

Secondary electrons produced by ions and electron impingement nourish the discharge.

The ion current is a measurement of pressure;

$$P \propto I_+^m \qquad 1 \leq m \leq 1{,}4 \quad \text{(depends on gauge design)}$$

The gauge configuration used nowadays is the inverted magnetron one.

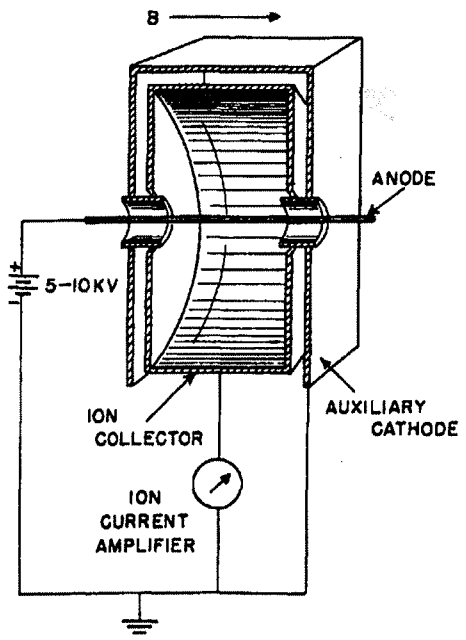

Inverted magnetron gauges are used for pressure measurement in the range $10^{-4} \div 10^{-10}$ Torr.
Most of the gauges in particle accelerators are inverted magnetron gauges. They are extensively employed for interlock purpose for the protection of delicate components (for example Kickers and RF cavities).

4.1.2 HOT CATHODE GAUGES (BAYARD-ALPERT GAUGE)

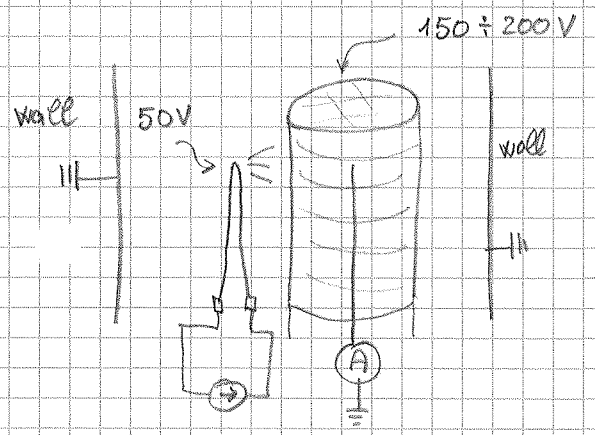

The electrons are extracted from a filament by thermoionic effect and accelerated toward a very transparent grid by an electric field.

The electrons cross the grid and, once outside it, they are decelerated and return in the grid.
They continue to move back and forth until they collide with a molecule or impinge on the grid.

The ion are collected by a very thin wire placed at the centre of the grid.

- The collected current is given by:

$$I^+ = \sigma \cdot L \cdot n \cdot I^-$$

gas molecule density

electron emission current

ionization cross section

the average path length of the electrons in the grid

$$I^+ = \sigma L \cdot \frac{P}{K_B T} \cdot I^- = \Sigma \cdot P \cdot I^-$$

gas nature

$$\Sigma = \text{gauge sensitivity} = \frac{1}{K_B T} \cdot \sigma \cdot L$$

gauge geometry

$$\left.\begin{array}{l} I^- \sim 10^{-3}\,A \\ \Sigma \sim 10\ \text{Torr}^{-1} \end{array}\right\} \Rightarrow \text{For } 10^{-11}\ \text{Torr} \quad I^+ = 10^{-13}\,A \ !$$

Typical values

$$\left.\begin{array}{l} I^- = 4\times10^{-3} \\ \Sigma = 45\ \text{Torr}^{-1} \end{array}\right\} \text{For } 10^{-11}\ \text{Torr} \quad I^+ = 1{,}8\times10^{-12}\,A$$

(Best Bayard-Alpert gauges)

In addition to gas ions, other sources of collector current are measured.

$$I^+ = \Sigma P I_e^- + I_R^- \longleftarrow \text{residual current pressure independent}$$

I_R → a) photo electron current extracted by soft x-ray.

I_R → b) electron stimulated desorption of positive ion.

a) electrons impinging on the grid produce bremsstrahlung radiation; the photons strike the central collector; photoelectron are extracted → equivalent to collected positive charges. (x-ray limit)

b) electrons impinging on the grid extract positive ions by electron stimulated desorption; the energetic ESD ion in direct view of the collector are counted.

The x-ray limit can be reduced by retracting the collector outside the grid. The ions are pushed outside the grid toward the collector by electrostatic plates: extractor gauge and Helmer gauge.

Bayard-Alpert gauges of optimized design attain x-ray limit in the low 10^{-12} Torr range. Extractor and Helmer gauges lower the limit down to 10^{-14} Torr.

Modified Helmer gauges produced at CERN measured 2×10^{-14} Torr.

- The accuracy of hot cathode gauge is much better than that of cold cathode. In addition they are stable and do not undergo sudden instability.

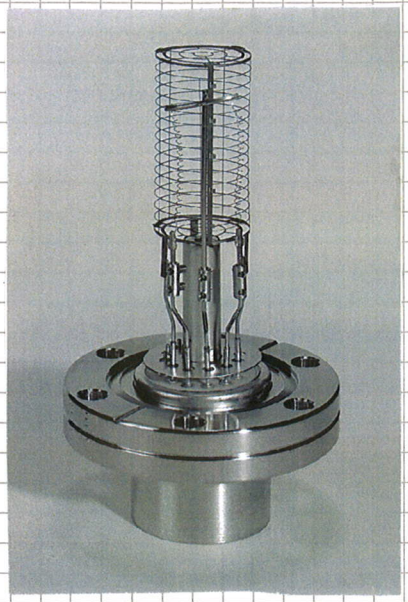

Svt

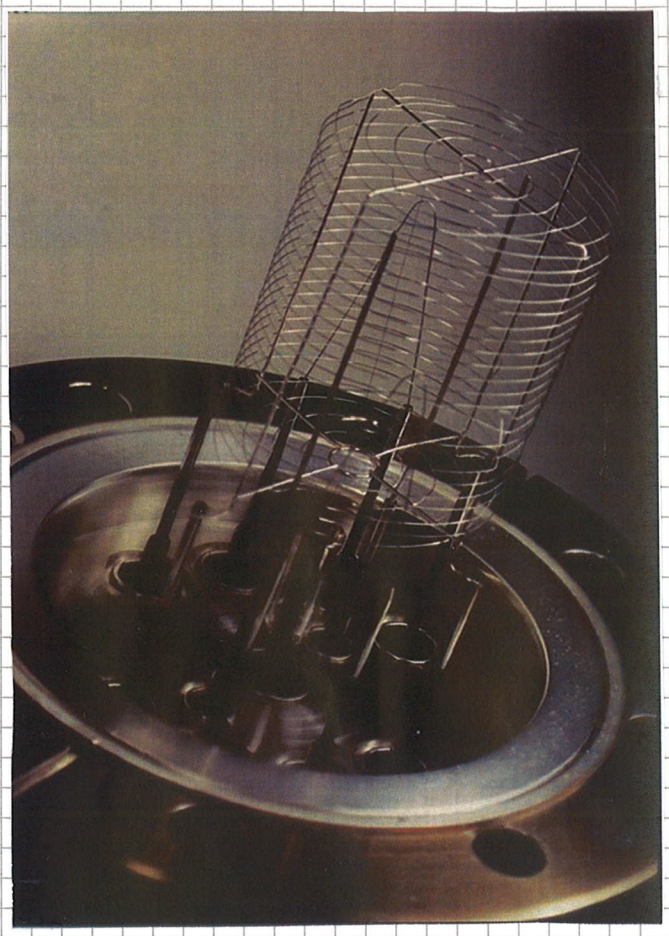

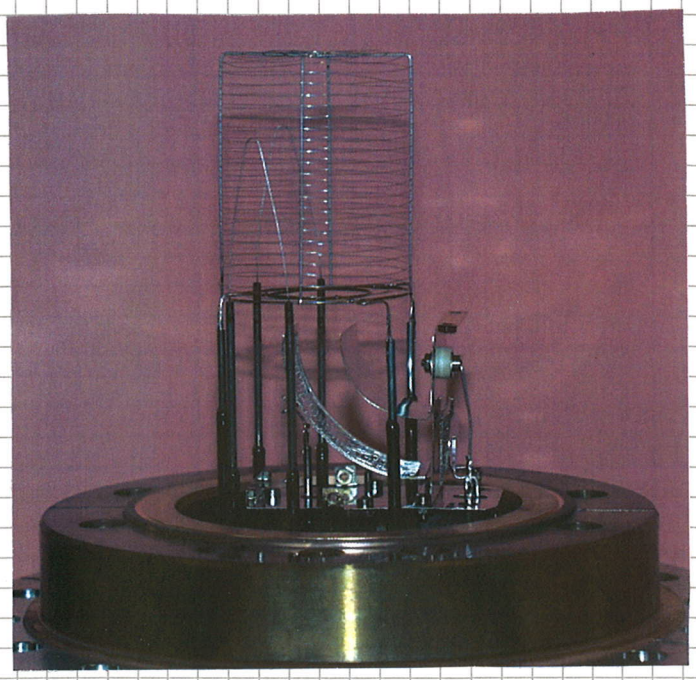

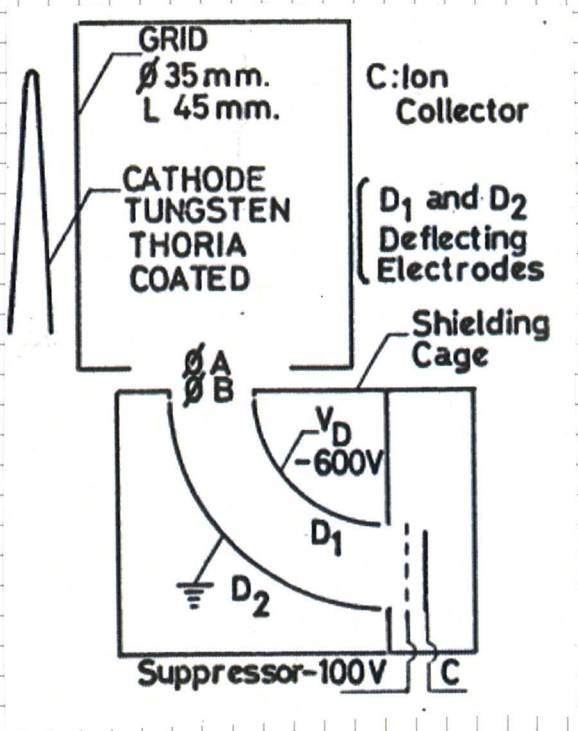
GRID
Ø 35 mm.
L 45 mm.
C: Ion Collector
CATHODE
TUNGSTEN
THORIA
COATED
D1 and D2
Deflecting
Electrodes
Shielding
Cage
ØA
ØB
VD
-600V
D1
D2
Suppressor-100V
C

4.2 RESIDUAL GAS ANALYSERS

- It is important to know the nature of the residual gas in vacuum system. Residual gas analysers ionize all gas molecules and select them by a radiofrequency filter. Only the molecules with the selected mass get out from the filter and are detected.

- The electron bombardment causes fragmentation of the molecules in addition to ionization. The molecular dissociation is not an unwanted complication; the fragmentation pattern (cracking pattern) facilitates the identification of the gas nature.

- The ionization is produced, as in hot cathode gauges, in a grid. The ions are extracted by polarized plates and injected into the filter with a defined energy.

- The filter is a quadrupole mass filter invented by W. Paul. It consists of a set of four cylindrical electrodes.

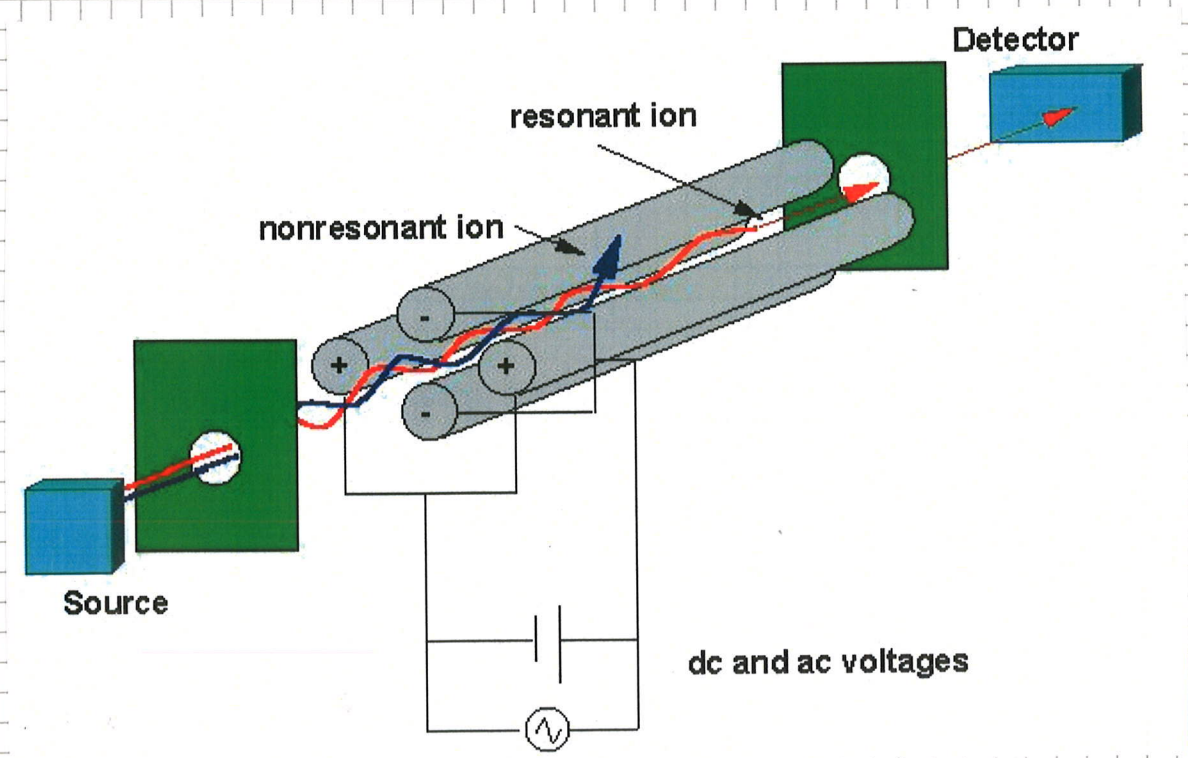

Flight paths of positive ions

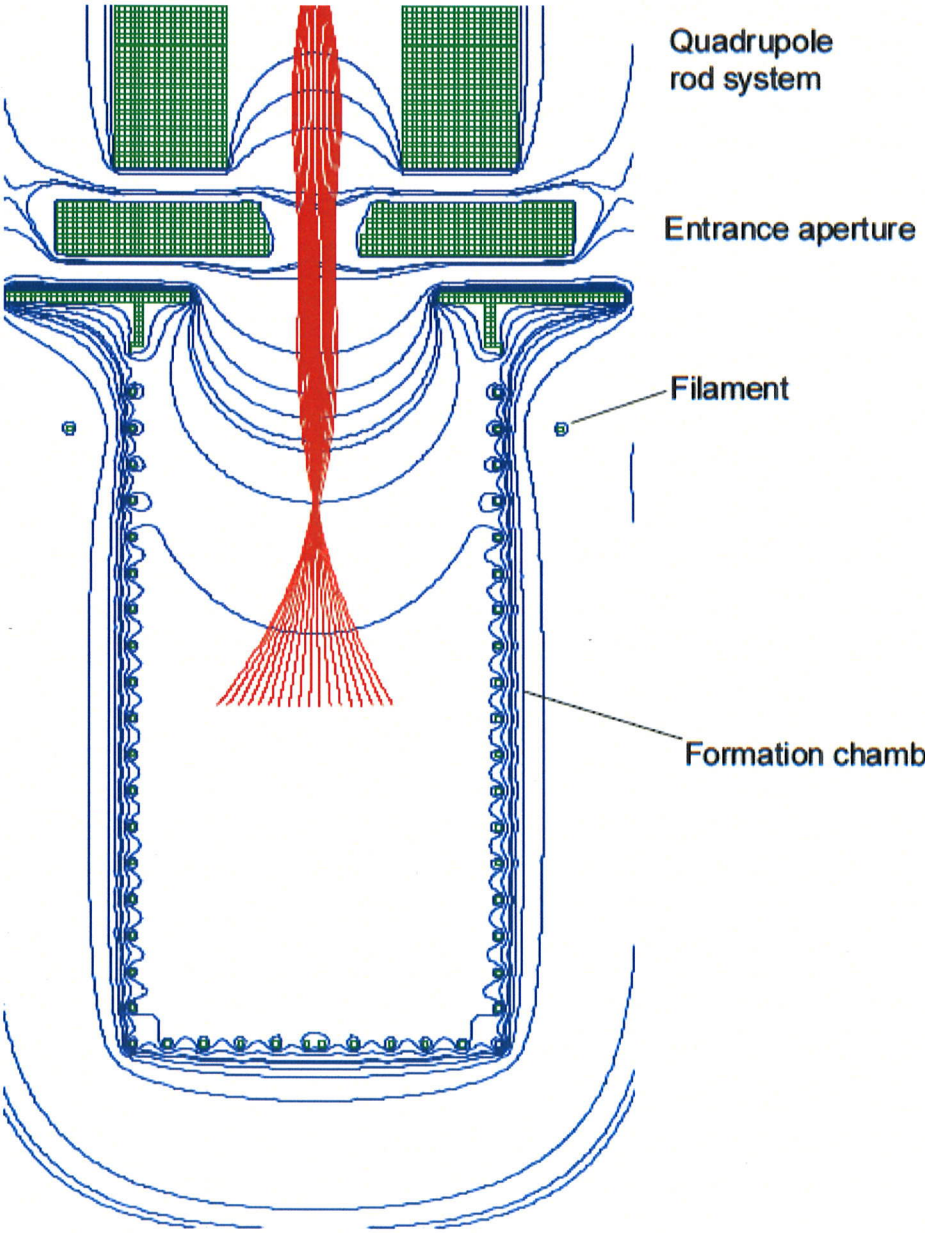

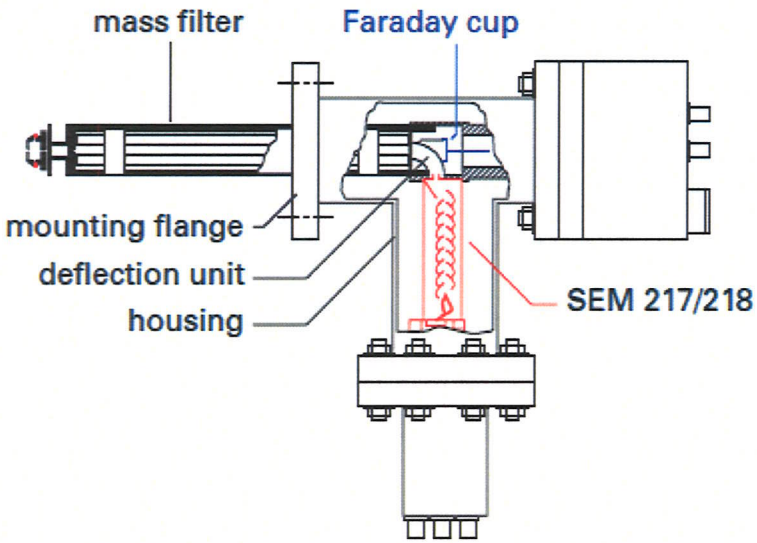
mass filter
Faraday cup
mounting flange
deflection unit
housing
SEM 217/218

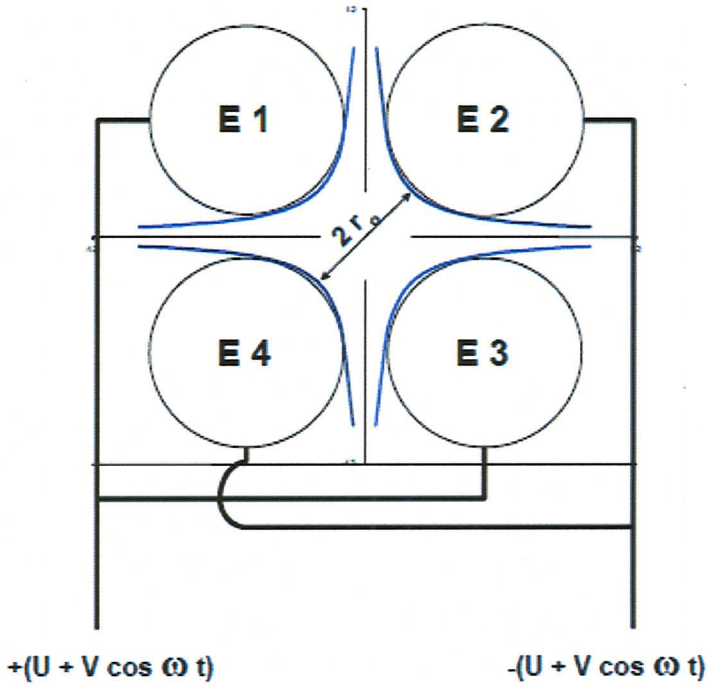
E 1
E 2
E 4
E 3
2 r₀
+(U + V cos ω t)
-(U + V cos ω t)

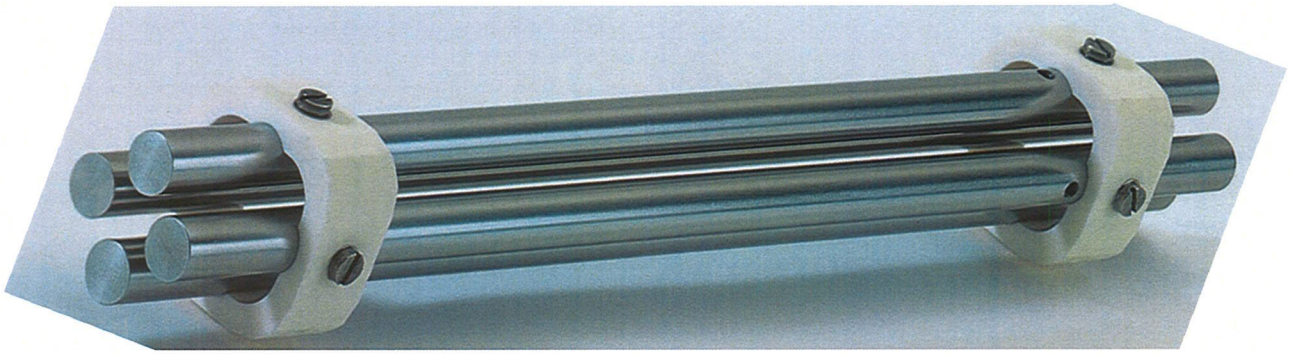

The filter action is obtained superposing a DC to a time periodic potential.

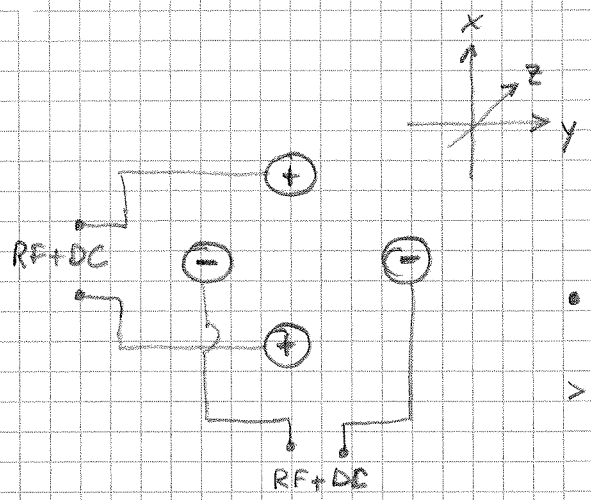

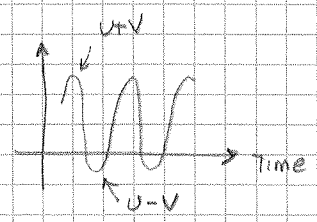

- In the x-z plane:
  - > the positive DC potential focus the ions on the central axis
  - > when the RF field is superposed, for a short time, the two electrodes become negatively biased
  - > during this time, light ions can promptly react and be defocused and lost
  - > heavy ions do not have time to react and continue their trajectory close to the axis.

⇒ In the x-z plane the quadrupole is a high-pass filter.

- In the y-z plane:
  - > the negative DC potential defocuses all ions from the central axis
  - > when the RF field is superposed, for a short time the two electrodes become positively biased
  - > light ions react rapidly and are refocused and possibly they do not strike on the electrods
  - > heavy ions do not have time to react and are lost

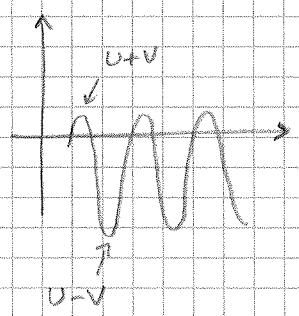

⇒ In y-z plane the quadrupole is a low-pass filter.

Superposing the two effects a band-pass filter is obtained.

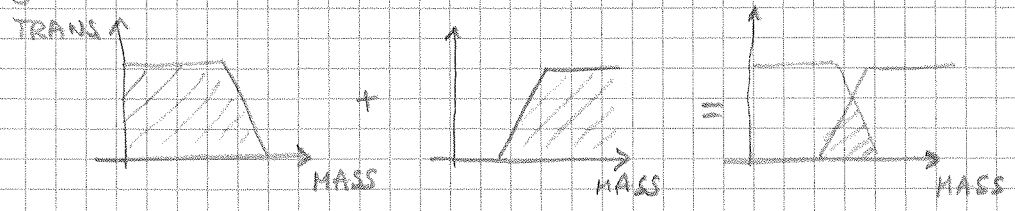

Selected ion mass

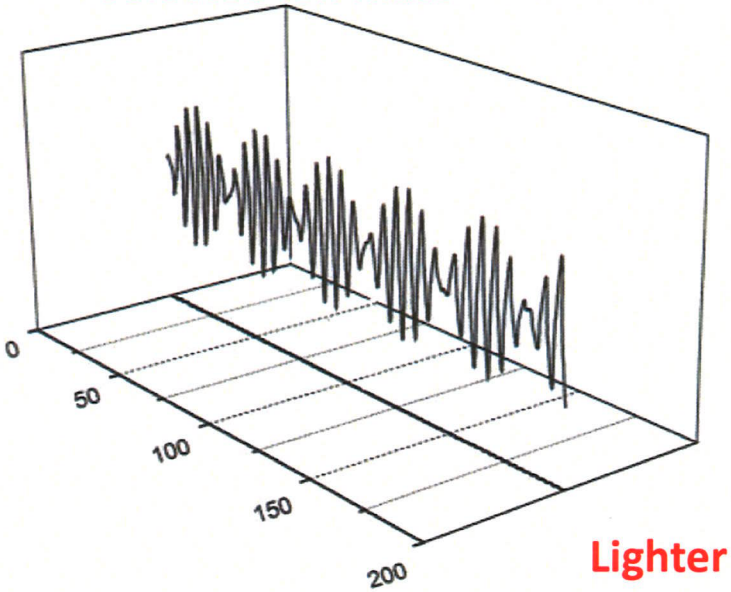

Heavier than selected

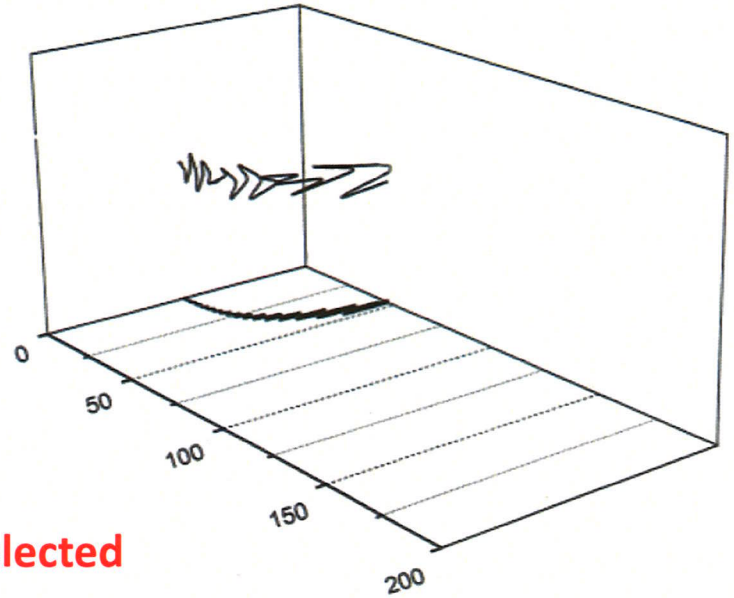

Lighter than selected

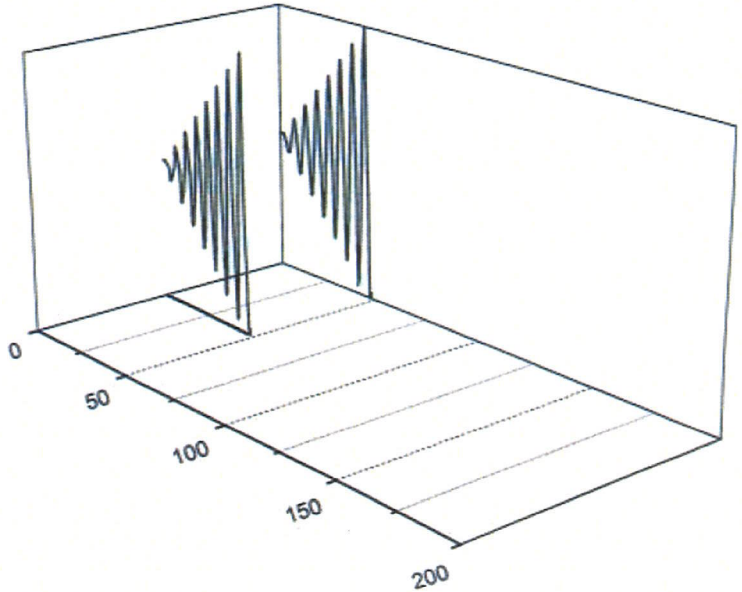

DC polarities

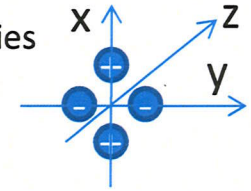

The ions escaped from the filter are detected by Faraday cup or secondary electron multipliers (SEM).

Typical spectra:

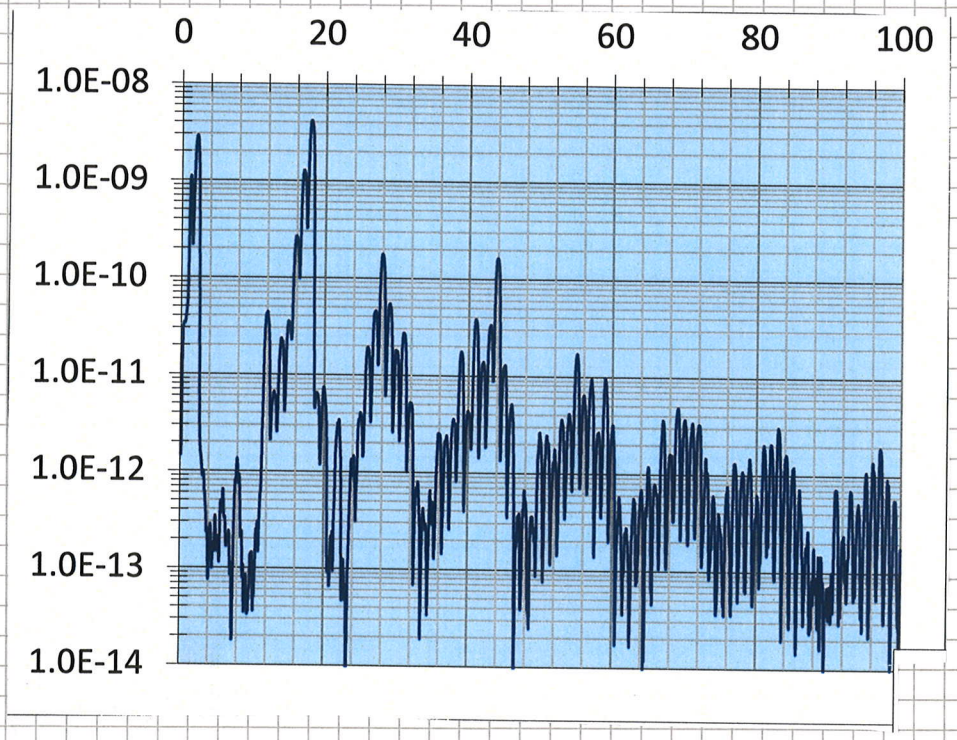

Unbaked system (Faraday cup)

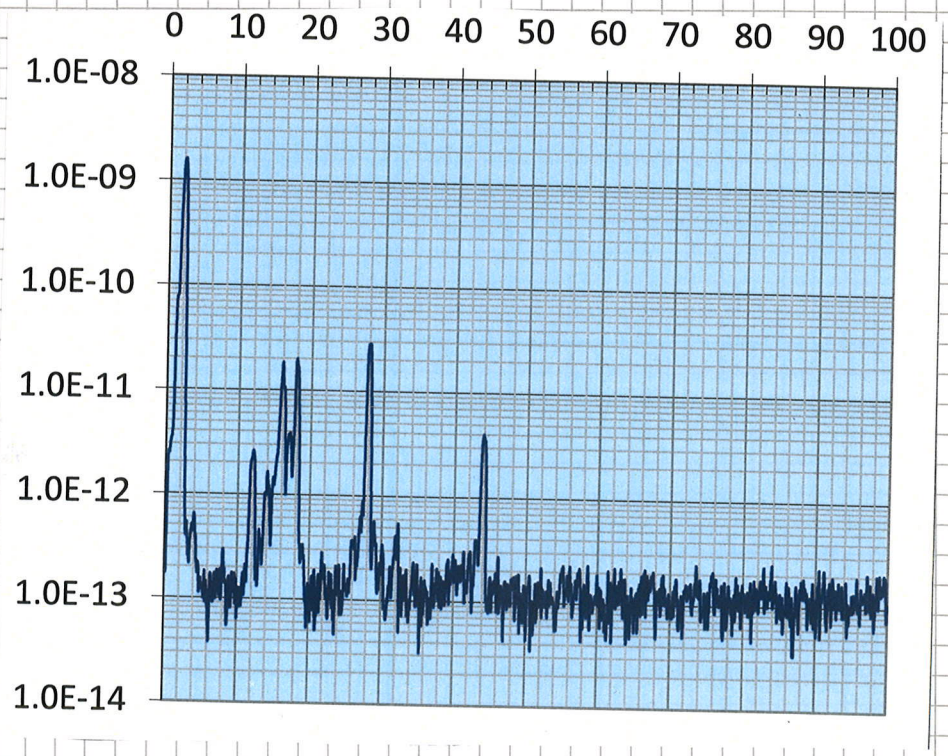

Baked system (secondary electron multiplier)